Instructions for preparation of manuscripts

It is recommended that the following guidelines be followed by the authors of the manuscripts:

- Original papers dealing with the principles of mineral processing and papers on technological aspects of mineral processing will be published in the journal which appears once a year
- The manuscript should be sent to the Editor for reviewing before February 15 each year
- The manuscript should be written in English. For publishing in other languages an approval of the editor is necessary
- Contributors whose first language is not the language of the manuscript are urged to have their manuscript competently edited prior to submission.
- The manuscript should not exceed 10 pages
- Two copies of the final manuscript along with an electronic version should be submitted for publication before April 15
- There is a 80 USD fee for printing the paper. No fee is required for the authors participating in the Annual Symposium on Physicochemical Problems on Mineral Processing
- Manuscripts and all correspondence regarding the symposium and journal should be sent to the editor.

Physicochemical Problems of Mineral Processing 43 (2009)

Pawel Nowak guest editor
Institute of Catalysis and
Surface Chemistry
Polish Academy of Sciences, Kraków

CONTENTS

T. Chmielewski*, J. Wódka*, Ł. Iwachów*

AMMONIA PRESSURE LEACHING FOR LUBIN SHALE MIDDLINGS

Ammonia pressure leaching has been investigated as an alternative for hydrometallurgical processing of Lubin middlings – a shale-enriched flotation by-product. The effect of primary parameters: temperature, oxygen partial pressure, ammonia and ammonium sulfate concentration and stirring rate on leaching recovery of Cu, Ag, Zn, Ni, and Co were examined.

key words: hydrometalurgia, ammonia leachng, black shales

INTRODUCTION

Ammonia has been widely applied as an effective leaching agent in numerous hydrometallurgical processes for many years. Ammonia can be effectively used for leaching of base metals (Cu, Ni, Co, Zn) as well as for precious metals (Ag, Au) because of formation of soluble, very strong ammonia complexes. Moreover, ammonia has been considered as an attractive leaching agent due to its low toxicity, low costs and ease of regeneration by evaporation from alkaline solutions. An important advantage of ammonia environment in hydrometallurgy is its selectivity in terms of solubilization of desired metals and precipitation of undesirable iron in one unit operation (Meng and Han, 1996).

Ammonia leaching can be used in non-oxidative, oxidative and reductive leaching. It was first applied and developed for recovery of copper from its metallic and oxide raw materials. Copper forms well soluble and very stable complexes ($[Cu(NH_3)_4]^{2+}$) and can be leached at ambient conditions due to the excellent solubility of ammonia in water.

---

*   Wroclaw University of Technology, Faculty of Chemistry, Division of Chemical Metallurgy
    Wybrzeże Wyspiańskiego 27, 50-370 Wrocław, Poland, tomasz.chmielewski@pwr.wroc.pl

In industrial scale ammonia leaching with oxygen as oxidant was applied since 1954 for treatment of copper, nickel and cobalt sulfide ores and concentrates at Fort Saskatchewan by Sherritt Gordon (Forward, 1953). The Arbiter ammonia leaching process for sulfide flotation concentrates was developed in 1970's in Anaconda (Kuhn et al., 1974). The process used ammonia leaching at 34.5 kPa with oxygen as oxidant. Copper in PLS was purified by means of solvent extraction and electrowon to marketable cathodes. The Arbiter ammonia process was also considered as an alternative for hydrometallurgical processing of Polish copper concentrates (KGHM Polish Copper).

Escondida (Chile) applied oxygenated ammonia solutions for partial leaching of copper from chalcocite concentrates at atmospheric pressure (Duyvetseyn and Sabacky, 1995). Solid residue after leaching, containing CuS, was subsequently floated to produce concentrate for smelter. It was successfully applied for several years to elevate the plant capacity at Escondida. The plant was closed after smelter expansion.

Decreasing copper recovery and concentrates grade observed at KGHM concentrators (particularly at Lubin) is a result of increasing concentration of shale fraction in Polish copper ores. Black shale is a lithological fraction exhibiting remarkably elevated concentration of base (Cu, Ni, Co, Zn) and precious metals (Ag, Au, PGE) with regard to dolomitic and sandstone fractions. Simultaneously, the growing presence of shale material is a primary reason for observed technical problems in flotation plans. Separation of black shale from the flotation circuit and application of hydrometallurgy for its processing was an idea presented by authors as a result of three years (2004–2007) laboratory investigations performed within the frame of BIOSHALE research project (d'Hugues et al., 2007, d'Hugues et al., 2008, Groudev et al., 2007, Chmielewski et al., 2007).

Selection of black shale feed and experimental determination of conditions for effective recovering of copper and other valuable metals (Fe, Ni, Co, Pb, Au, PGM…) from shale containing materials (ore, middlings, shale concentrates) was the general task at the starting point of the BIOSHALE project. The research program was initially focused on the geological shale samples collected for preliminary laboratory examinations (chemical and mineralogical analyses, non-oxidative, atmospheric and acid pressure leaching). After the extended period of experimental work, the shale middlings – tailings from the 1st cleaning flotation at Lubin Concentrator (ZWR Lubin) - were finally selected and accepted by a technical and engineering staff at KGHM as an only shale containing solid for hydrometallurgical laboratory tests and for future full scale alternative processing. Simultaneously, this material was unanimously recognized as the most troublesome solid in existing flotation circuit at Lubin Concentrator due to the high content of shale fraction (organic matter) and sulfide minerals fine dissemination. It is fully considered as a shale concentrate, which can be separated from the flotation circuit for hydrometallurgical treatment. Initial samples were collected of numerous shale ore fractions from various LGOM (Poland) deposits.

Chemical analyses exhibited varying metal content in the shale. For further laboratory studies the process alternatives were selected including chemical pretreatment with H_2SO_4 for flotation, non-oxidative leaching, atmospheric leaching and pressure leaching investigations as BIOSHALE project WP4 tasks. The laboratory tests undoubtedly confirmed that the assumptions made in the first stage of the work program were correct.

Acidic leaching of shale middlings appeared to be very effective from mineralogical and technical point of view. Favorable mineralogical composition of Lubin middlings (dominating content of copper in the form of chalcocite and bornite) and easy access to sulfuric acid, being, in fact, a waste material from copper smelters, makes this approach very attractive for future technological alterations(Chmielewski, 2007, Konopaca et al., 2007, Wódka et al., 2007).

One of the main reason, that black shale fraction became a serious problem in flotation of Polish copper ores is a very fine mineralization of metal-bearing sulfides and their dissemination in hydrophilic carbonate and organic matter. It is impossible to liberate these minerals only by means of mechanical grinding. Consequently, a great amount of metal values remain in flotation tailings and leads to hardly accepted metals loses. Very complex and expensive alteration in flotation and grinding circuits appeared to be ineffective in terms of declining flotation indexes. Both the recovery and concentrate grade have been decreasing remarkably, particularly at Lubin Concentrator.

An additional unfavorable effect has been lately observed during the flash smelting at Głogów II smelter. The growing content of shale fraction (Table 1) and, consequently, increase in organic carbon content - exceeding 9 % for Lubin and Polkowice - in the concentrate smelter feed, results in a notable diminishing efficiency of the process (Kubacz and Skorupska, 2007). Therefore, separation of shale fraction from the flotation circuits (e.g. Lubin middlings) and its individual, hydrometallurgical processing, postulated within the frame of BIOSHALE project, can be accepted as a key alternative for existing technologies. Such alteration can result in the following advantages:

- Integration of new technology with existing processes.
- Simplification of existing flotation circuits and enhancement of flotation efficiency.
- Increase of metals recovery in total (flotation concentrate + hydrometallurgy) – remarkable decrease of metals loses and environmental impact.
- Stabilization of organic carbon content in concentrates on the proper level, accepted for flash smelting process.
- Effective utilization of an excess of sulfuric acid – a byproduct or waste from smelting.

It seems rather to be obvious that due to observed apparent decline of copper ores quality and upgradeability, particularly from Lubin and Polkowice deposits (Table 1),

present beneficiation technologies are not able to guarantee the acceptable metals recovery and concentrate grade without significant technology alteration and urgent instruction of new alternative concepts. Ammonia leaching can be considered as an alternative process. This appeared to be urgent for Polish copper industry.

Table 1. Content of shale fraction in Polish copper ores mined from various LGOM deposits (Kubacz and Skorupska, 2007)

Mine	Year		
	2002	**2004**	**2006**
Lubin	18.8	15.0	27.0
Polkowice-Sieroszowice	11.3	13.3	11.2
Rudna	2.2	3.9	4.0

The objectives of this paper was to evaluate the effect of key parameters (oxygen pressure, temperature, ammonia concentration, ammonium sulfate concentration, solid to liquid ratio and stirring rate) on the recovery of Cu, Ni, Co, Zn and Ag during ammonia pressure leaching of Lubin shale middlings - tailings from 1st cleaning at Lubin Concentrator.

Ammonia pressure leaching of Lubin shale middlings was selected as an alternative to acidic - atmospheric and pressure leaching. Ammonia leaching was expected to be applied without a need of carbonates acidic decomposition, as it was necessary for leaching in acidic media. Major advantage of ammonia solutions is confirmed leachability of most metals which are being recovered from shale enriched Lubin middlings (Cu, Co, Ni, Zn, Ag, Au…).

EXPERIMENTAL

LUBIN MIDDLINGS CHARACTERIZATION

Shale middlings from Lubin Concentrator were collected and characterized in details in D.4.2. Deliverables within BIOSHALE European project, on the basis of 1st sampling campaign in 2006 and 2nd sampling campaign in 2007. Middlings from 2nd sampling campaign were used as a feed for ammonia leaching. It is well seen from Table 2, that chemical composition of material examined in 2007 was very similar to those used in previous investigations. Copper content was about 2.60 %, organic carbon was 6.30 % - lower than in 2006 campaign. The content of accompanying metals was observed to be almost identical, except of zinc. The comparison of chemical analyses of Lubin middlings samples from 2006 and 2007 evidently shows, that examined feed is fairly stable in terms of its chemical composition.

Table 2. Chemical characterization of Lubin shale middlings (1st and 2nd sampling campaigns – 2006 and 2007).

CONTENT					
	Cu, %	**Fe, %**	**Ni, g/Mg**	**Co, g/Mg**	*Pb, %*	**As, %**
1st campaign	2,72	1,76	374	572	1,51	0,090
2nd campaign	2,60	1,89	328	613	-	0,085
CONTENT					
	Ag, g/Mg	**Zn, g/Mg**	**S_c, %**	**Sso_4, %**	**C_{total}, %**	**C_{org}, %**
1st campaign	190	1 200	2,95	1,45	14,30	8,96
2nd campaign	168	740	2,62	2,47	10,4	6,30

Figure 1 exhibits the mineralogical composition of Lubin middlings and compares with composition of Lubin final concentrate currently produced as a feed for smelting. This analysis was made by BRGM laboratories and became a very important justification in discussion on considered technology alterations. The mineralogical composition of concentrate appeared to be very similar to the composition of the ore. Chalcocite (Cu_2S) and bornite (Cu_5FeS_4), easiest to leach copper sulfides, are dominating in the material. The content of chalcopyrite ($CuFeS_2$), most refractory copper sulfide, is only about 20.6 %.

In contrary to concentrate, mineralogical composition of shale middlings appeared to be extremely favorable for hydrometallurgical treatment. Chalcocite was reported to be dominating (90.5 %) with some content of bornite (9 %). Chalcopyrite is a negligible component in this by-product. Such a mineralogical composition can be considered as an ideal for hydrometallurgical or biometallurgical treatment. The observed mineralogical composition of shale middlings exhibits evidently, that beneficial mineralogical segregation of minerals takes place during flotation process at Lubin Concentrator.
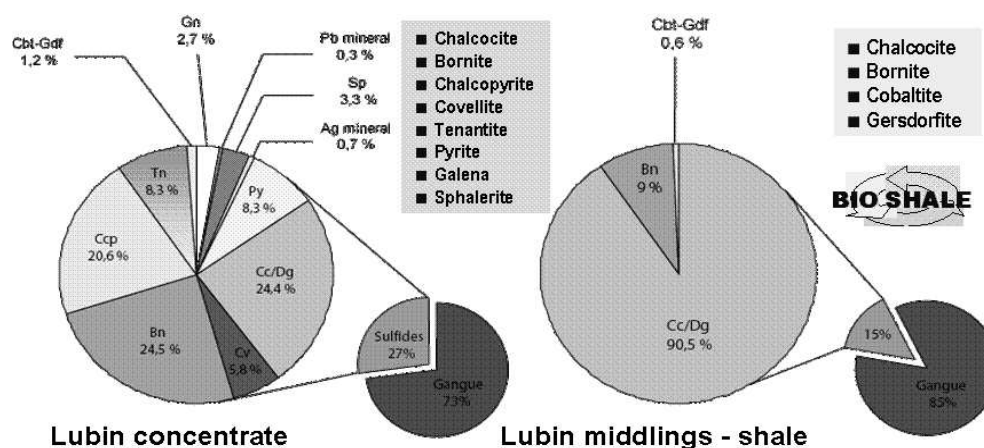
Fig. 1. Mineralogical composition of Lubin final concentrate and Lubin shale middlings (BRGM data).

Metals value breakdown for 1 ton of Lubin shale middlings, presented in Table 3, indicates that the value of copper (217,3 US$) is even somewhat lower than the value of accompanying metals (Ag, Ni, Co, Zn, Pb) (250,9 US$), taking into account metals prices from 21 February 2008.

Table 3. Metals value in 1 ton of Lubin shale middlings (metal prices from 21 February 2008)

Metal	Content	Metal price, US$ (21 February 2008)	Value, US$
Cu	2,7 %	8 050 US$/Mg	217,3
Ni	373 g/Mg	27 900 US$/Mg	10,4
Co	569 g/Mg	50 US$/lb	62,3
Pb	1,52 %	3 170 US$/Mg	48,2
Ag	180 g/Mg	17,5 US$/oz	127,2
Zn	1200 g/Mg	2 350 US$/Mg	2,8

Value of Cu – 217,3 US$, Value of accompanying metals – 250,9 US$

It is very obvious that shale fraction has to be processed not only as a copper-bearing raw material but mainly as a polymetallic one. Separation of this fraction from flotation circuit and its processing for recovering of Cu and other metals is therefore fully justified.
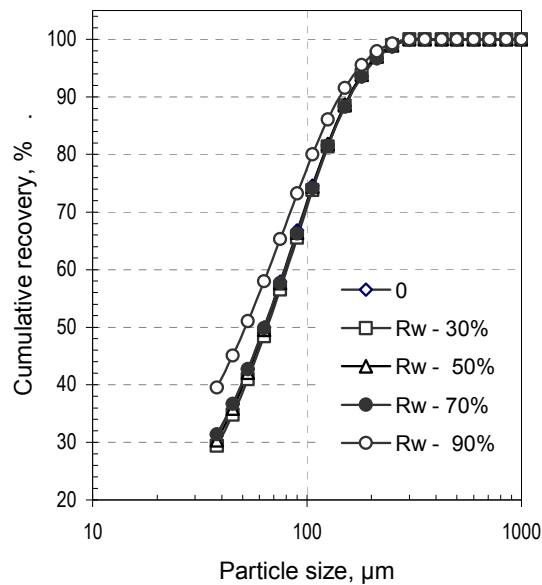
Fig. 2. Particle size analyses of Lubin middlings raw and subjected to the non-oxidative acidic leaching at various degree of carbonate decomposition (within 30 – 90 %).

Particle size analyses for Lubin middlings (Figure 2.) indicate that applied material was rather coarse from the point of view of hydrometallurgy. Parameter d_{80} exceeded 100 μm even after non-oxidative leaching with H_2SO_4. Additional microscopic SEM (Figure 3) observations lead to the conclusion that most coarse particles are formed by shale material, which can not be decomposed during chemical treatment, even in the presence of oxygen (Figure 3D). Therefore, separation of particle fraction above 70–80 μm and their additional regrinding seem to be very desirable to facilitate further leaching. During ammonia leaching Lubin middlings were applied using neither chemical pretreatment nor mechanical grinding. This was in order to compare the ammonia leaching results with previous atmospheric and pressure leaching, where same feed was applied.
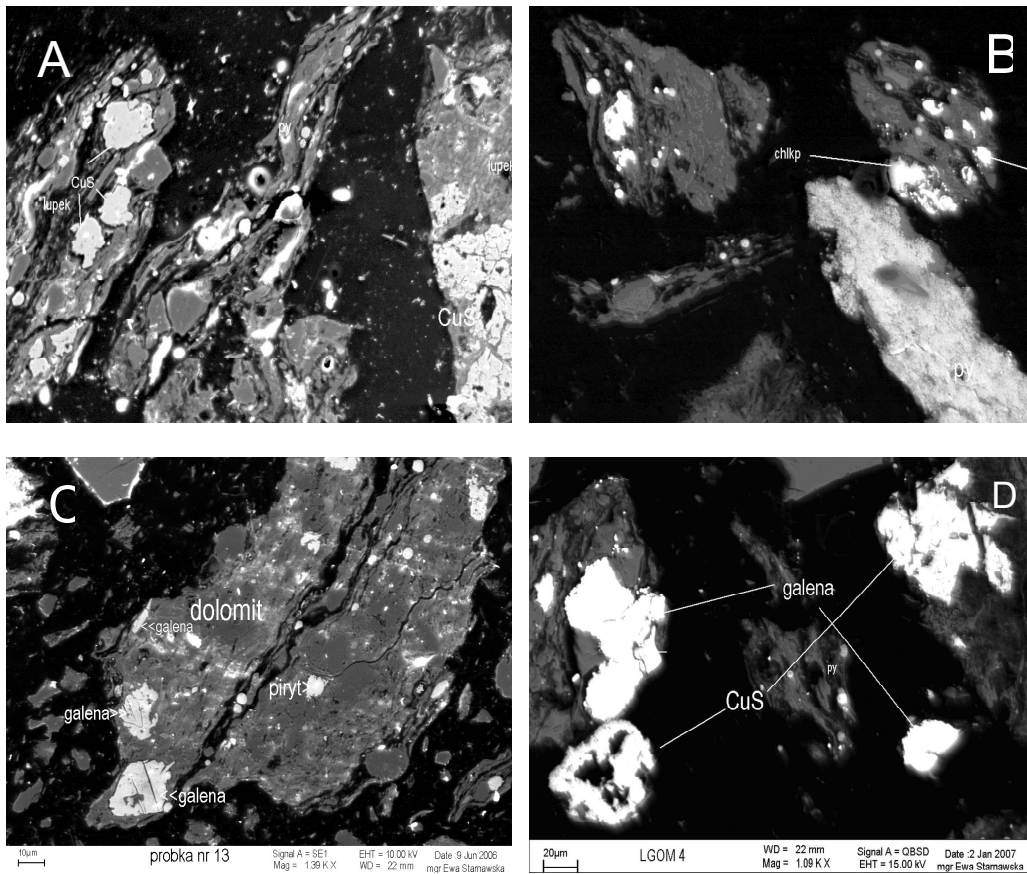
Fig. 3. SEM mineralogical analyses of Lubin shale middlings before leaching (A,B,C) and after atmospheric leaching in acidic consitions (D).

AMMONIA LEACHING PROCEDURE

All ammonia leaching experiments were performed in 1 liter Parr autoclave. Leaching solution was composed of ammonia, ammonium sulfate and oxygen under pressure as an oxidizing agent ($NH_3 + NH_4^+ + O_2$).

Ammonia solutions as a leaching medium for Lubin middlings can be considered as an excellent alternative for acidic oxidative solutions. The reason for that are very high stability constants of ammonia complexes for silver, gold, cobalt, copper, nickel and zinc (Table 4).
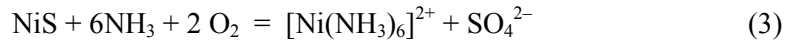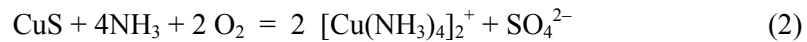
Aqueous ammonia + ammonia salt solutions as complexing medium is an effective and selective leaching agent for copper, silver, nickel, cobalt and zinc. Leaching of sulfide minerals takes usually place in the presence of oxygen under pressure within 1–20 atm. and at temperatures within 110 – 200 ºC. Solubilized metals are in the solution in the form of stable ammonia complexes, while sulfidic sulfur is oxidized to sulfate(VI) ion. No formation of elemental sulfur is observed during the process. This is an important advantage of the process.

Table 4. Stability constants of ammonia complexes (data for metals present in Lubin middlings).

Metal	Chemical formula	Stability constant
Ag^+	$[Ag(NH_3)_2]^+$	$1{,}7 \cdot 10^7$
Au^+	$[Au(NH_3)_2]^+$	$1 \cdot 10^{27}$
Co^{2+}	$[Co(NH_3)_6]^{2+}$	$7{,}7 \cdot 10^4$
Co^{3+}	$[Co(NH_3)_6]^{3+}$	$5{,}0 \cdot 10^{33}$
Cu^+	$[Cu(NH_3)_2]^+$	$3{,}8 \cdot 10^{10}$
Cu^{2+}	$[Cu(NH_3)_4]^{2+}$	$4{,}8 \cdot 10^{12}$
Ni^{2+}	$[Ni(NH_3)_6]^{2+}$	$1{,}26 \cdot 10^9$
Zn^{2+}	$[Zn(NH_3)_4]^{2+}$	$3{,}98 \cdot 10^9$

The following reaction takes place for copper, nickel and cobalt sulfides:

$$2Cu_2S + 12NH_3 + 4NH_4^+ + 5\ O_2 = 4[Cu(NH_3)_4]_2^+ + 2SO_4^{2-} + 2H_2O \qquad (1)$$

$$CuS + 4NH_3 + 2\ O_2 = 2\ [Cu(NH_3)_4]_2^+ + SO_4^{2-} \qquad (2)$$

$$NiS + 6NH_3 + 2\ O_2 = [Ni(NH_3)_6]^{2+} + SO_4^{2-} \qquad (3)$$

$$2CoS + 10NH_3 + 2NH_4^+\ 9/2\ O_2 = 2[Co(NH_3)_6]^{3+} + 2SO_4^{2-} + 2H_2O \qquad (4)$$

Particularly substantial advantage of ammonia leaching for solids containing copper-iron and iron minerals (chalcopyrite, bornite, pyrite, pyrrhotite) is that iron present in the solid can not be dissolved in alkaline ammonia solution. Fe is oxidized to insoluble iron(III) oxide and precipitates from the solution. The following reaction can be observed for pyrrhotite:

$$4FeS + 6NH_3 + 4\,H_2O + 9O_2 \;=\; 2Fe_2O_3\downarrow + 2HSO_4^- + 2SO_4^{2-} + 6NH_4^+ \qquad (5)$$
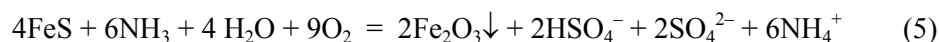
Therefore, selective separation of copper and iron takes place in one leaching operation.

Table 5 exhibits the range of parameters applied during the ammonia leaching investigations of Lubin middlings presented in this paper.

Table 5. Ammonia leaching parameters for Lubin middlings.

Temperature, °C	Ammonia Conc., M	Oxygen partial pressure, atm	$(NH_4)_2SO_4$ conc., g/dm^3	s/dm^3	Stirring rate, rpm
120–180	1.5–3.0	5.0–12.5	50–100	1:10	200–500

Aqueous ammonia + ammonia salt solution is an effective and selective complexing leaching agent for copper, silver, nickel, cobalt and zinc. Leaching of metal sulfide minerals contained in the Lubin shale middlings (Table 2) takes place in the stirred reactor under oxygen pressure at vigorous stirring rate in order to saturate the solution with oxygen. Effect of ammonia concentration was initially examined for copper leaching from the middlings (Figure 4). It is well seen that within the investigated ammonia concentration range leaching of copper is very efficient and can be, in terms of metals recovery, compared with acidic pressure leaching. Copper recovery was about 90 % after 90 minutes of leaching. Further increase in copper recovery was not observed as a result of copper minerals encapsulation in the shale fraction.

RESULTS AND DISCUSSION

Leaching recovery of nickel and zinc was found to be lower than it was observed for copper. About 60–70 % of nickel and slightly above 70 % of zinc was leached out. Dissemination of Ni and Zn in shale organic and carbonate matter can explain the observed results and hindering the leaching process.

Stirring rate appeared to be a key parameter for ammonia leaching of copper from Lubin middlings (Figure 6). We found that highest reaction rate for applied reactor can be observed when stirring rate was kept within the range of 400–500 rpm. Similarly to Figure 4, maximum leaching recovery was about 90 %.

Silver was observed to leach in ammonia solution (Figure 7) and the highest leaching rate was observed for stirring rate 400 and 500 rpm. Apparently lower leaching rate was observed when stirring rate was in the range of 200 – 3000 rpm. Silver leaching recovery was in the range of 50 – 60 %. Dissemination of silver in coarse particles of shale was the main reason for such a recovery, which can be improved by additional grinding of middlings coarse fraction. Zinc leaching was observed to be most

effective when stirring was 500 rpm. Maximum leaching recovery was in the range of 70 – 80 %.
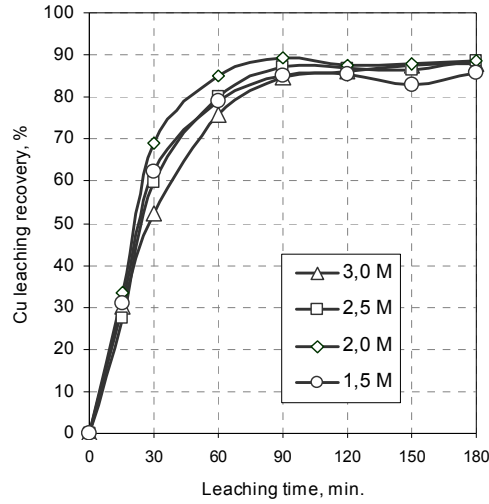
Fig. 4. Effect of ammonia concentration on Cu leaching from Lubin middlings
temp. $140^{o}C$, s/dm^3 = 1:10, pO_2 = 7.5 atm, $(NH_4)_2SO_4$ concentration - 50 g/dm^3, stirring rate - 400 rpm.
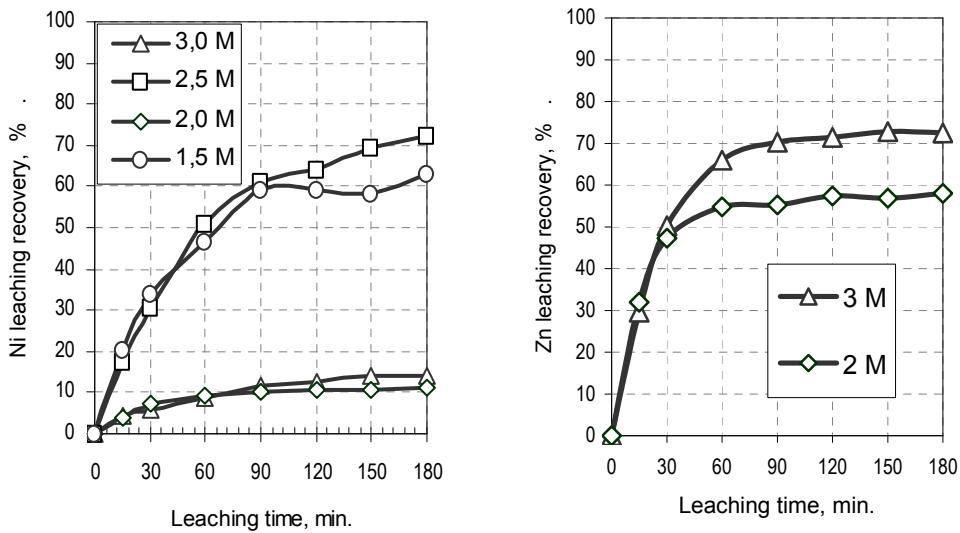
Fig. 5. Effect of ammonia concentration on Ni and Zn leaching from Lubin middlings
temp. $140^{o}C$, s/dm^3 = 1:10, pO_2 = 7.5 atm, $(NH_4)_2SO_4$ concentration - 50 g/dm^3, stirring rate - 400 rpm.
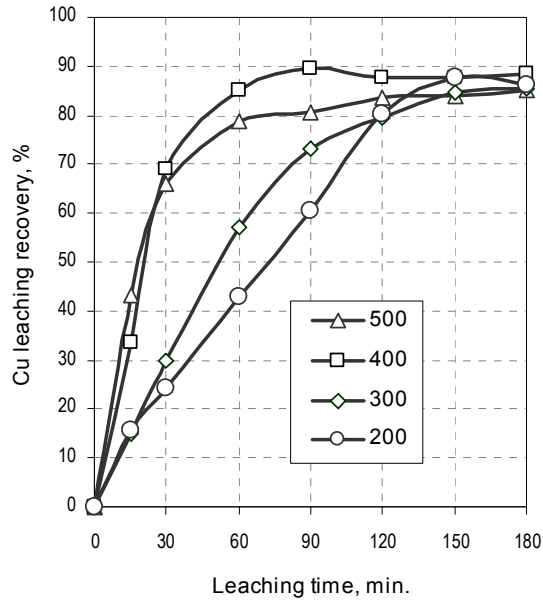
Fig. 6. Effect of stirring rate (in rpm) on Cu leaching rate
temp. = 140°C, s/dm^3 = 1:10, pO$_2$ = 7.5 atm, (NH$_4$)$_2$SO$_4$ = 50 g/dm^3, NH$_3$ = 2 M

Fig. 7. Effect of stirring rate (in rpm) on Ag and Zn leaching from Lubin middlings
temp. = 140 ^{o}C, s/dm^3 = 1:10, pO$_2$ = 7.5 atm, (NH$_4$)$_2$SO$_4$ = 50 g/dm^3, NH$_3$ = 2 M.

T. Chmielewski, J. Wódka, Ł. Iwachów
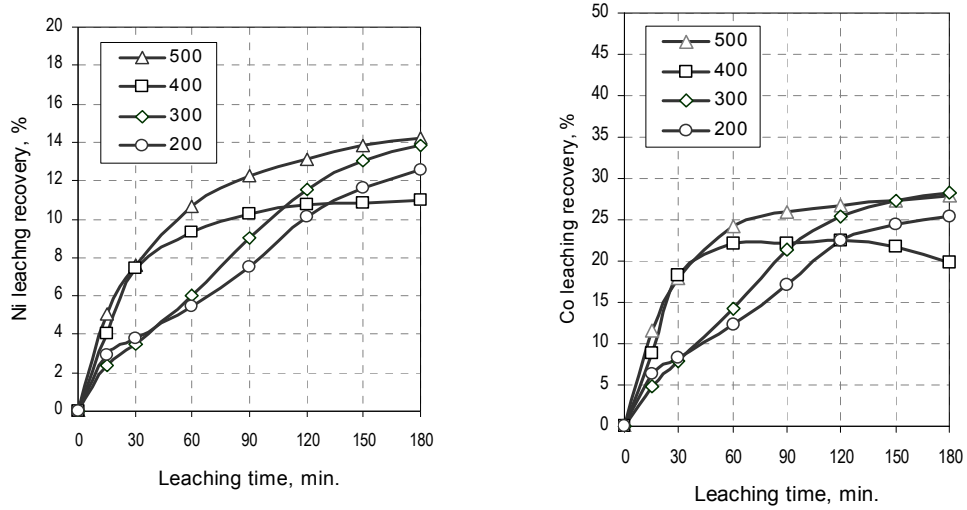
Fig. 8. Effect of stirring rate (in rpm) on Ni and Co leaching from Lubin middlings
temp. = 140°C, s/dm^3 = 1:10, pO$_2$ = 7.5 atm, (NH$_4$)$_2$SO$_4$ = 50 g/dm^3, NH$_3$ = 2 M..
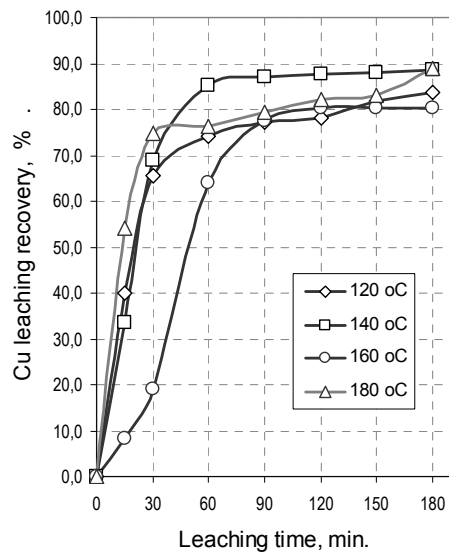
Fig. 9. Effect of temperature on Cu ammonia leaching from Lubin middlings
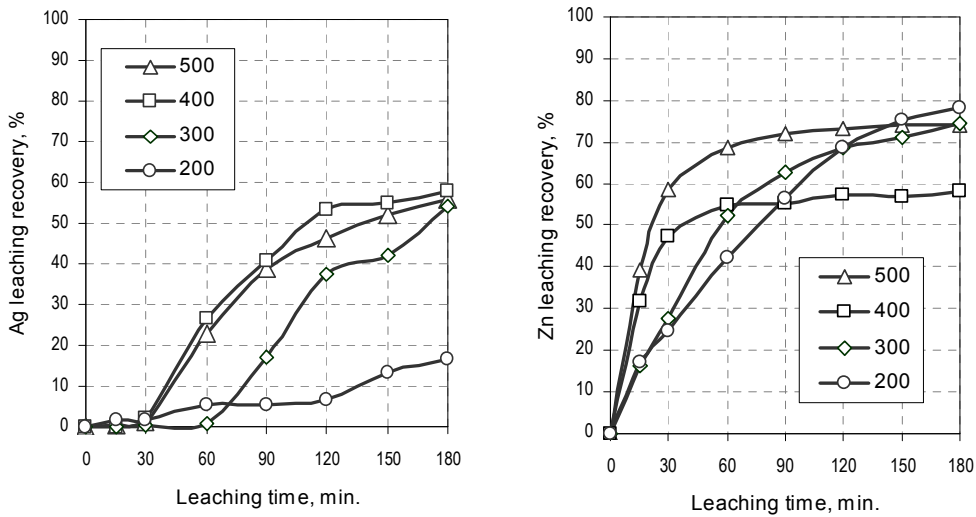s/dm^3 = 1:10, pO$_2$ = 7.5 atm, (NH$_4$)$_2$SO$_4$ = 50 g/dm^3, NH$_3$ = 2 M, stirring rate - 400 rpm.

From previous mineralogical investigations we fond that nickel was disseminated mainly in iron oxide phases (goethite). This was the reason of low leaching recovery observed both during acidic and ammonia leaching.

Temperature is a key parameter for ammonia leaching of copper from Lubin middlings. Leaching examinations carried out within the temperature range of 120–180 ^{o}C evidently shown, that ammonia leaching temperature for copper can not exceed 180 ^{o}C. Decrease in ammonia and oxygen dissolution seems to be the limiting factor at these leaching conditions. Observed results of copper leaching were, however, very satisfactory.

In contrast to copper, leaching of zinc was very effective and exhibited the highest level at 180 ^{o}C and recovery of zinc to the solution was about 95 %. Cobalt exhibited the highest recovery at temperatures below 160 ^{o}C. We suspect that reason for that was instability of ammonia complexes of Co at higher temperatures and precipitation of its hydroxyl compounds.

In all ammonia leaching experiments recovery of arsenic did not exceed 3 % and iron was completely insoluble at the experimental conditions.

Examination of the effect of oxygen pressure (Figure 11) shown that the highest leaching rate and highest leaching recovery were observed for the experiments performed at 12.5 atm of oxygen. Surprisingly, almost 100 % of Cu was leached out. It was evidently higher with regard to previous experiments carried out at 5 atm of oxygen pressure.
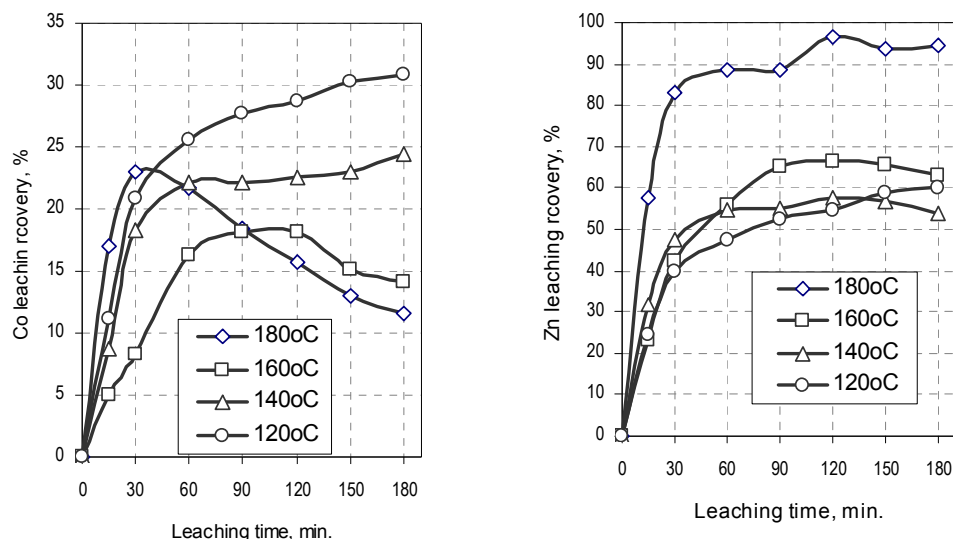
Fig. 10. Effect of temperature on Co, and Zn leaching
s/dm^3 = 1:10, pO$_2$ = 7.5 atm, (NH$_4$)$_2$SO$_4$ = 50 g/dm^3, NH$_3$ = 2 M, stirring rate - 400 rpm.
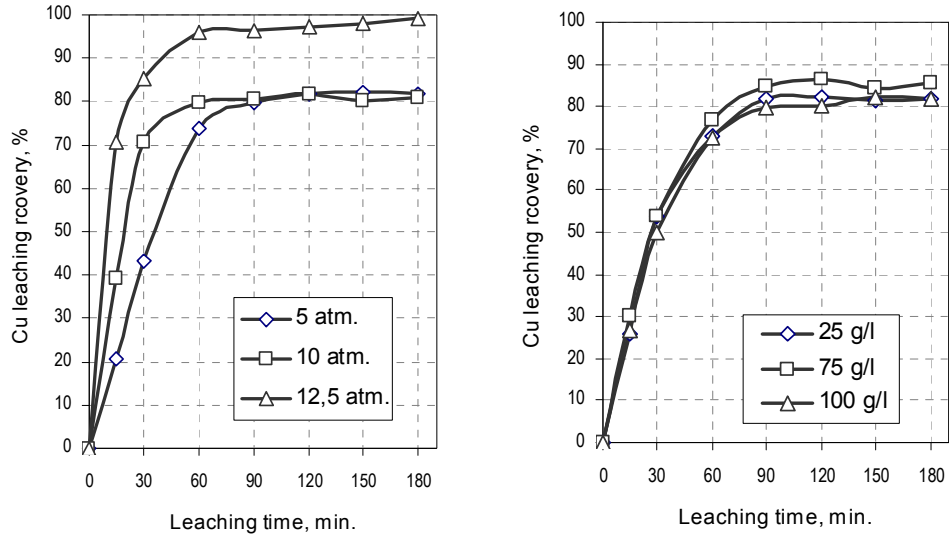
Fig. 11. Effect of oxygen pressure and ammonia sulfate concentration (in grams per liter) on ammonia Cu leaching from Lubin middlings.
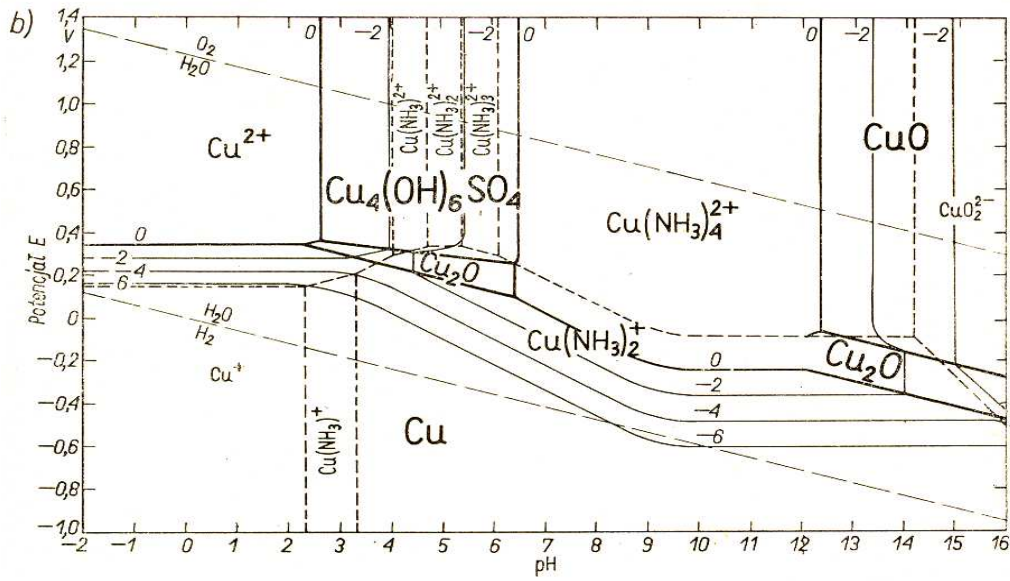
Fig. 12. Eh-pH diagram for Cu–H_2O–NH_3–SO_4^{2-} system at 25 ^{o}C.

Another parameter examined during leaching test was concentration of ammonium sulfate –$(NH_4)_2SO_4$ (Figure 11). Recorded cooper concentration – leaching time plots indicated, that optimum concentration of ammonium salt was 50 g/dm^3. The concentration of ammonium ions together with ammonia form a buffer solution and control the solution pH at the level where stability of copper tetraamina complexes is the highest (Figure 12). This corresponds to the range of 8–11. If the pH of ammonia – ammonium solution is either to low or exceeds the optimum level of pH, stability of copper complexes decreases.

CONCLUSSIONS

Ammonia pressure leaching of Lubin shale middlings experiments appeared to be an efficient alternative for acidic atmospheric or pressure leaching. The following conclusions can be formulated after the detailed investigations of main process parameters:

- Ammonia pressure leaching in oxygenated NH_3 + $(NH_4)_2SO_4$ solution is an effective process for Lubin middlings, allowing the recovery of Cu, Ag, Ni, Co and Zn. Fe and As remain in the solid.
- Temperature, ammonia concentration, ammonium sulfate concentration, oxygen pressure and stirring rate are the key leaching parameters. The optimum range of parameters for recovery of metals are: ammonia concentration: above 1.5 M, ammonium sulfate concentration: 50 g/dm^3, oxygen pressure: 12.5 atm., temperature: 120 – 160 ^{o}C, stirring rate: 400 – 500 rpm for the applied reactor,
- Above 95 % of Cu, 30 % Co, 70 % Ni, 95 % Zn and 60 % Ag can be recovered during 90–120 minutes leaching. Leaching rate and leaching recovery can be remarkably enhanced if coarse particles of shale will be separated for additional size reduction below 70 – 80 μm.
- Fe and As remain in the solid residue during ammonia pressure leaching.

REFERNCES

MENG X., HAN K.N., *The principle and application of ammonia leaching of metals – a review*, Min. Process. Extr.Metall.Review, 16 (1996) 23–61.

FORWARD F.A., *Ammonia pressure leach process for recovering copper, nickel and cobalt from Sherritt Gordon nickel sulfide concentrate*, Can. Min. Metall. Bull., 499 (1953) 677 – 684.

KUHN M.C., ARBITER N., KLING H., *Anaconda's Arbiter Process for copper, CIM Bulletin*, Fecruary 1974, pp.62–73.

DUYVETSEYN W.P.C., SABACKY B.J., *Ammonia leaching process for Escondida copper concentrates*, Trans. Inst. Min. Met., 104 (1995) C125 – C140.

D'HUGUES P., NORRIS P.R., JOHNSON B., GROTOWSKI A., CHMIELEWSKI T., ŁUSZCZKIEWICZ A., SADOWSKI Z., SKŁODOWSKA A., FARBISZEWSKA T, *Presentation of the FP6 European Project Bioshale. Exploitation of black shale ores using biotechnologies - Polish case studies*, Physicochemical Problems of Mineral Processing, 41 (2007) 373–386.

D'HUGUES P., NORRIS P.R., HALLBERG K.B., SÁNCHEZ F., LANGWALDT J., GROTOWSKI A., CHMIELEWSKI T., T. GROUDEV T., Bioshale consortium, Bioshale FP6 European project: *Exploiting black shale ores using biotechnologies?,* Minerals Engineering 21 (2008) 111–120.

GROUDEV S., SPASOVA I., NICOLOVA M., CHMIELEWSKI T., LUSZCZKIEWICZ A., *Recovery of copper by flotation of microcially pretreated black shales, Proceedings: Bio- and Hydrometallurgy'07*, Falmuth, UK, 1–2 May 2007 (published in the form of CD).

CHMIELEWSKI T., ŁUSZCZKIEWICZ A., KONOPACKA Ż., *Separation and concept of processing of black shale copper ore from Lubin Mine*, 7th International Conference on Non-ferrous Ore Processing, May 21–23,Wojcieszyce, Poland, KGHM Cuprum, Wrocław 2007, 171–184.

CHMIELEWSKI T., *Non-oxidative leaching of black shale copper ore from Lubin Mine*, Physicochemical Problems of Mineral Processing, 41 (2007) 323–348.

KONOPACKA Ż., ŁUSZCZKIEWICZ A., CHMIELEWSKI T.: *Effect of non-oxidative leaching on flotation efficiency of Lubin Concentrator Middlings.* Physicochem. Probl. Miner. Process. 41 (2007) 275–289.

CHMIELEWSKI T., *Atmospheric leaching of shale by-product from Lubin concentrator*, Physicochemical Problems of Mineral Processing, 41 (2007) 337–348.

WÓDKA J., CHMIELEWSKI T., ZIÓŁKOWSKI B*., Pressure leaching of shale ore in oxygenated sulfuric acid,* Physicochemical Problems of Mineral Processing, 41 (2007) 349–364.

KUBACZ N., SKORUPSKA B. 2007. *Estimation of influence of organic carbon on concentration and smelting processes.* Conf. Proc. VIII International Conference On Non-ferrous Ore Processing, ICNOP'07, 21–23 May, Wojcieszyce, Poland, KGHM, IMN, 157–166 (in Polish).

Chmielewski T., Wódka J., Iwachów Ł., *Ciśnieniowe ługowanie amoniakalne łupkowego półproduktu flotacji z ZWR Lubin*, Physicochemical Problems of Mineral Processing, 43 (2009), *5–20* (w jęz. ang)

Badano proces ciśnieniowego ługowania amoniakalnego półproduktu flotacji z ZWR Lubin, wzbogaconego we frakcję łupkową. Ługowanie amoniakalne analizowano jako alternatywny sposób hydrometalurgicznego przetwarzania tego półproduktu. Badano wpływ najważniejszych parametrów: temperatury, ciśnienia parcjalnego tlenu, stężenia amoniaku i siarczanu amonowego oraz szybkości mieszania na szybkość ługowania Cu, Ag, Zn, Ni i Co.

słowa kluczowe: hydrometalurgia, ługowanie amoniakalne, czarne łupki

P. Górska*, A. Zaleska*, A. Suska*, J. Hupka*

PHOTOCATALYTIC ACTIVITY AND SURFACE PROPERTIES OF CARBON-DOPED TITANIUM DIOXIDE

Carbon-doped TiO_2 was prepared by hydrolysis of titanium (IV) isopropoxide and calcination at 350ºC for 2h in air. Phenol (0.21 mM) was successfully degraded in the aqueous suspension of the powder, under visible light ($\lambda > 400$ nm). Characteristics of obtained photocatalyst by BET method and UV-Vis diffuse reflectance spectroscopy showed about 127 m^2/g of specific surface area, absorption of light in the visible region and 3.35 eV of band gap energy. Photocatalytic activity and selected properties of five samples prepared independently were investigated.

key words: photocatalysis, carbon-doped TiO_2, visible light

INTRODUCTION

To achieve Vis light-activated TiO_2 many doping procedures using metal or non-metal heteroatoms were proposed. Single element or multi element doping with such non-metalic elements like carbon (Lettmann, 2001; Sakthivel, 2003; Tseng, 2006; Górska, 2008), nitrogen (Irie, 2003; Sakthivel, 2004; Kuroda, 2005; Zaleska 2007), sulphur (Umebayashi, 2003; Ohno, 2004), fluorine (Hattori 1998, Yamaki, 2002), iodine (Hong, 2005), chlorine (Long, 2007), phosphorus (Shi, 2006) and boron (Bettinelli, 2007; Zaleska 2008) can successfully modify TiO_2 properties and shift its photoactivity towards the visible region.

---

* Department of Chemical Technology, Gdansk University of Technology, ul. G. Narutowicza 11/12, 80-952 Gdansk, Poland, azal@chem.pg.gda.pl

Carbon could improve the photoactivity of TiO_2, stabilize anatase structure and increase adsorption of organic molecules on the photocatalyst surface (Tsumura, 2002; Janus, 2006; Ren, 2007; Górska, 2008). Tseng et al. studied oxidation of NO_x using their own carbon-doped catalysts, which were illuminated with UV and Vis light (Tseng, 2006). The catalysts were prepared by the sol-gel process using titanium alkoxide in ethanol solution with nitric acid as a catalyst, followed by calcination at 150 to 600ºC. Experimental results showed about 70% removal of NO_x in a continuous flow type reaction system with a modified catalyst. They stated that the presence of carbonaceous species and mixed crystalline phase in TiO_2 powder enhances absorption of visible light by the photocatalyst. A significant influence of the alkyl groups was observed by Lettmann et al. (Lettmann, 2001). TiO_2 catalysts were prepared by modified sol-gel process using different alkoxide precursors, in the absence of any dopant. Powders containing carbonaceous species revealed photocatalytic activity for 4-chlorophenol decomposition in visible light. Sakthivel and Kisch also observed 4-chlorophenol degradation in the presence of carbon-doped photocatalyst and diffused indoor daylight (Sakthivel, 2003). In this case, powders were prepared by hydrolysis of titanium tetrachloride with tetrabutylammonium hydroxide as a carbon precursor. Ren et al. reported higher rate of rhodamine B degradation for carbon-doped TiO_2 prepared by an impregnation of amorphous TiO_2 in aqueous solution of glucose in comparison to photocatalyst prepared by Sakthivel and Kisch, which was used as reference material (Ren, 2007).

Recently, TiO_2 powders were obtained by hydrolysis of TIP, in the absence of any dopant, and calcinated at temperatures ranging from 350 to 750ºC (Górska, 2008). The experimental data clearly indicated a correlation between light absorption by powders and their photocatalytic performance in phenol degradation. Absorbance over the entire VIS region and the highest phenol degradation efficiency under visible light ($\lambda > 400$ nm) was observed for the sample calcinated at 350ºC. X-ray photoelectron spectroscopy confirmed presence of carbonaceous species at the TiO_2 surface. According to the literature, incorporation of carbonaceous species (C–C) occurs in highly condensed and coke-like structure, so it could play the role of a sensitizer to induce the visible light absorption and response (Lettmann, 2001; Tseng, 2006).

In this work we consider the reproducibility of carbon-doped TiO_2 effectiveness and selected properties. The photocatalyst was prepared by TIP hydrolysis and calcinations at 350°C. The photocatalytic activity in Vis light and selected properties of C–TiO_2 samples prepared in five independent runs were investigated. UV-Vis diffuse reflectance spectroscopy and BET methods were used to characterize the samples. Additionally, TiO_2 samples obtained by the same preparation procedure, but calcinated at temperatures lower than 350ºC (i.e. 250 and 300ºC), were studied.

METHODS

PREPARATION OF PHOTOCATALYST

Carbon-doped TiO_2 photocatalysts were obtained, according to procedures described earlier (Górska, 2006; Zaleska, 2007). Titanium (IV) isopropoxide (97%, Sigma-Aldrich Co., Germany) was hydrolyzed with distilled water only. Nitric acid was not used in the preparation procedure to avoid surface rutile, which is formed under such conditions (Tseng, 2006). After hydrolysis, the suspension was kept at 80ºC for 12h. The precipitate was filtered, rinsed with ethanol, dried at 80ºC for 12h and calcinated at 350ºC for 2h in air. The obtained carbon-doped TiO_2 was in the form of brown powder. The photocatalyst was prepared five times in separate batches, in order to investigate reproducibility of catalyst' properties.

MEASUREMENT OF PHOTOCATALYTIC ACTIVITY

The photocatalytic activity of TiO_2 samples was estimated by measuring the decomposition rate of phenol in 0.21 mM aqueous solution under visible light. Phenol was selected as the model contaminant. Recently, phenol was proposed as one of four substrates in a multi photoactivity test (Choi, 2007). Phenol is present in wastewater from oil refining, pharmaceutical synthesis, electroplating, papermaking, coking and iron-smelting.

The experimental set-up for photocatalytic activity tests was described elsewhere (Górska, 2008). 1000 W Xenon lamp (6271H, Oriel) was used as the irradiation source. The optical path included water filter and glass filters (GG400, Schott AG) to cut off IR and UV irradiation, respectively. The temperature during the experiments was maintained at 10 ºC. 25 ml of aqueous suspension containing 125 mg of a photocatalyst and phenol were stirred magnetically and aerated (5 l/h) prior and during the irradiation. Aliquots of about 1.0 ml of the suspension were collected during irradiation and filtered through syringe filters (Ø=0.2 μm) to remove fine particles of the photocatalyst. The phenol concentration was estimated by the colorimetric method after derivatization with diazo-p-nitroaniline, using UV-Vis spectrophotometer (DU-7, Beckman).

Photocatalytic degradation runs were preceded with blind tests in the absence of a photocatalyst or illumination. Commercial TiO_2 P-25 (Degussa) was used as reference material.

CHARACTERISTICS

Gemini V Analyzer (Micromeritics Instrument Co.) was used for measurements of BET surface area, by physical adsorption and desorption of nitrogen. The UV-Vis/DR spectra were recorded using UV-Vis spectrometer (Jasco, V-530) equipped with integrating sphere accessory for diffuse reflectance. The band gap energy (E_g) was calculated from the first derivative of UV-Vis absorption, according to the Planck's equation. More details referring to these experimental procedures one can find in our previous papers (Zaleska, 2007, 2008; Górska, 2008).

RESULTS AND DISCUSSION

PHOTOCATALYTIC ACTIVITY

No degradation of phenol was observed in the absence of a photocatalyst or illumination. Phenol degradation efficiency results in Vis light for TiO_2 powders prepared by TIP hydrolysis, and for TiO_2 P-25 (Degussa) are presented in Figure 1.
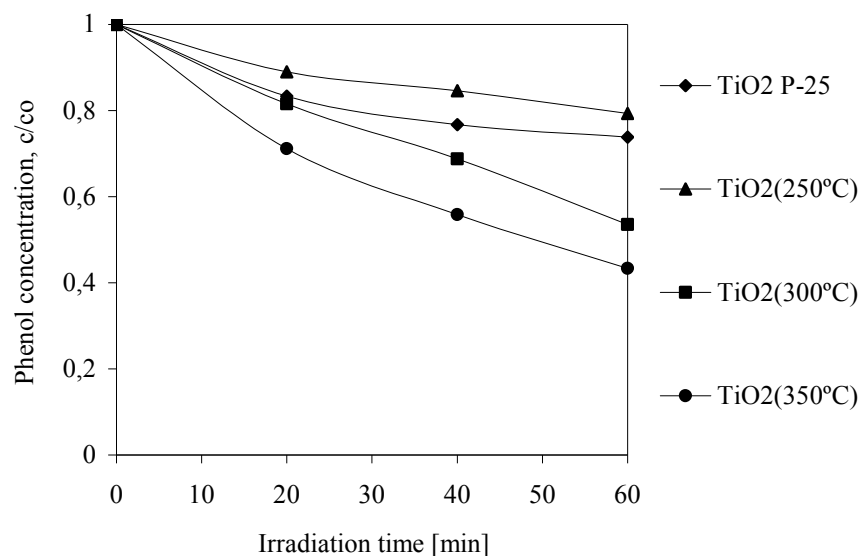
Fig. 1. Kinetics of photocatalytic degradation of phenol
in the irradiated suspension of prepared TiO_2 samples and TiO_2 P25
Experimental conditions: C_o=0.21 mM, m (TiO_2)=125 mg, T=10°C, Q_{air}=5 dm^3/h, λ>400 nm

The most efficient phenol degradation took place in irradiated suspension of sample calcinated at 350ºC i.e. TiO_2 (350ºC). After 60 min of irradiation, almost 60% of phenol was degraded. Sakthivel et al. observed 70% of TOC reduction (4-chlorophenol, c_o=0.25 mM) in carbon-doped TiO_2 suspension, irradiated with light having a wavelength equal to 455 nm (Sakthivel, 2003). The photocatalyst was prepared by $TiCl_4$ hydrolysis with tetrabutylammonium hydroxide and calcinated at 400ºC for 1 h. The authors reported that increasing the calcination temperature leads to a loss of photoactivity in the presence of visible light, which is in good agreement with our results published previously (Górska, 2008). At the same time of irradiation, Lettmann et al. reported 30% of 4-chlorophenol (c_o=0.25 mM) degradation after 100 min of irradiation (λ>400), in the presence of a catalyst obtained by TIP hydrolysis, followed by calcination at 250ºC for 3 h (Lettmann, 2001). In our case, irradiation of TiO_2 calcinated at 250ºC, resulted in the lowest contaminant degradation efficiency (20%), see Figure 1. Similarly, irradiation of reference suspension (TiO_2 P-25) resulted in 25% contaminant decomposition. Low degradation efficiency in this case was due to a poor photocatalytic activity of pure TiO_2 in the visible light (Fujishima and Zhang, 2006). TiO_2 powder calcinated at 300ºC also revealed lower photoactivity than TiO_2 (350ºC).

Phenol degradation efficiency results for five independently prepared TiO_2 (350ºC) catalyst samples are shown in Figure 2.
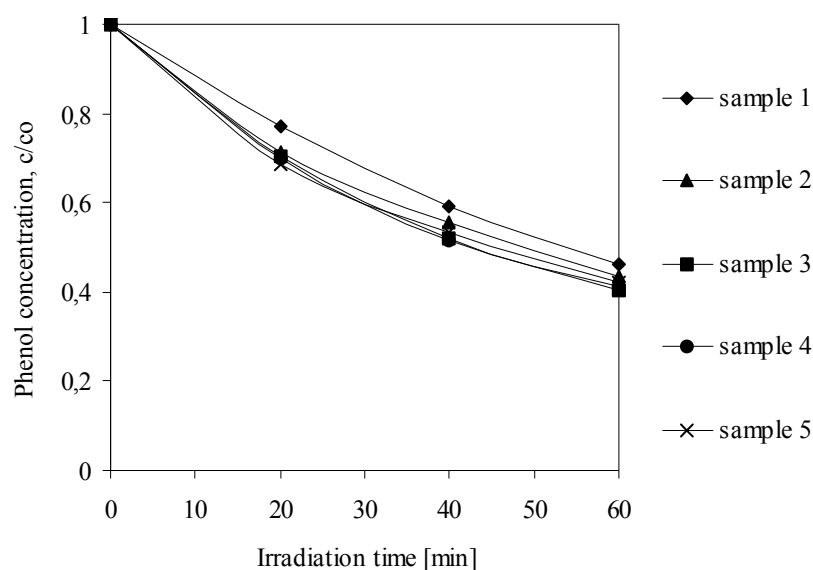
Fig. 2. Kinetics of photocatalytic degradation of phenol
in irradiated suspensions of TiO_2 calcinated at 350ºC
Experimental conditions: C_o=0.21 mM, m (TiO_2)=125 mg, T=10°C, Q_{air}=5 dm^3/h, λ>400 nm

Data in Figure 2 indicates that all TiO_2 (350°C) samples behaved similarly. Basing on these data, we calculated average values of phenol degradation efficiency after 20, 40 and 60 min of irradiation, including confidence limit, see Table 1.

Table 1. Phenol degradation efficiency for TiO_2(350°C) catalyst

Irradia-tion time [min]	Phenol degradation efficiency for TiO_2 (350°C), E [%]					$\overline{X} \pm \Delta X$
	Sample 1	Sample 2	Sample 3	Sample 4	Sample 5	
20	28.9	23.0	29.7	30.1	31.2	28±4.0
40	44.2	40.8	47.8	48.6	46.8	46±3.9
60	56.6	54.0	59.8	58.7	57.8	57±2.8

The confidence level for these calculations was 95% and the statistical factor "t" (Student's t-distribusion) was 2.78 for four degrees of freedom.

CHARACTERISTICS

Values of specific surface area of five separately prepared TiO_2 (350°C) catalysts and an average S_{BET} with the confidence limit are presented in Table 2.

Table 2. Specific surface area of TiO_2 (350°C) catalyst

Specific surface area of TiO_2 (350°C), S_{BET} [m^2/g]					$\overline{X} \pm \Delta X$
Sample 1	Sample 2	Sample 3	Sample 4	Sample 5	
127.4	127.3	127.0	127.1	126.8	127±0.3

The confidence level for these calculations was 95% and the statistical factor "t" (Student's t-distribusion) was 2.78 for four degrees of freedom.

All TiO_2 samples prepared by TIP hydrolysis and calcinated at 350°C had high specific surface area of about 127 m^2/g. An average S_{BET} value was more than two times greater than BET specific surface area of commercial TiO_2 P-25 (50 m^2/g). Large surface area may contribute to enhanced activity of TiO_2, but cannot be responsible for the highest phenol degradation efficiency in visible light, since samples with larger specific surface area, i.e. TiO_2(250°C) (136 m^2/g) and TiO_2(300°C) (131 m^2/g) revealed lower photoactivity, see Figure 1. On the other hand, large surface area is usually associated with numerous crystalline defects, which promote recombination of electrons and positively charged holes, leading to lower activity under UV irradiation (Carp, 2004).

UV-Vis absorption spectra of TiO_2 (350°C) samples and TiO_2 P-25 (Degussa) are presented in Figure 3. Pure TiO_2 P-25 showed clear absorption edge at around 350 nm and insignificant absorption in visible region above 400 nm. Visible light was absorbed by all TiO_2 (350°C) powders. In this case, absorption edge was not as sharp as the edge of reference material.

The band-gap energy values (E_g) were determined using the first derivative of UV-Vis absorption spectra. Usually, E_g values reported in the literature for anatase are around 3.2 eV, whilst 3.0 eV for pure rutile phase (Hoffmann, 1995; Ohno, 2004). The band-gap energy of pure TiO_2 P-25 was 3.15 eV, since this reference material is composed of two different TiO_2 crystalline phases, i.e. anatase (70%) and rutile (30%) (Macyk, 2003). Each investigated TiO_2 (350°C) sample had the band gap energy equal to 3.35 eV.
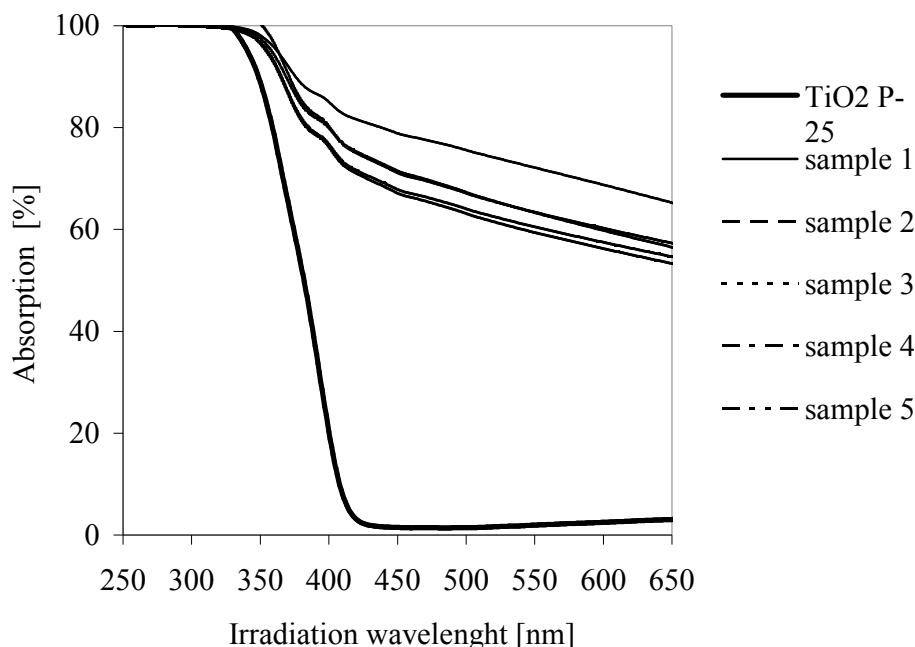
Fig. 3. UV-Vis absorption spectra of TiO_2 (350°C) samples and TiO_2 P25

The experimental results showed lack of band-gap narrowing, which was postulated by many researchers as main consequence of TiO_2 doping (Asahi, 2001; Sakthivel, 2003). The E_g value of our photocatalyst was wider than for pure bulk anatase. According to Saupe et al., this phenomenon is due to a combination of quantum size effects, caused by the crystallite size, and the dopant atoms in the structure (Saupe, 2005).

CONCLUSIONS

The experimental data confirm that the proposed preparation procedure provided reproducible effectiveness and studied properties of the photocatalyst. Five separately prepared TiO_2 (350°C) samples revealed comparable photoactivity under visible light, absorption properties and specific surface area.

According to a comparison between phenol degradation efficiencies of our carbon-doped TiO_2 and commercial TiO_2 P-25 (Degussa), see Table 3, we stated that our photocatalyst is more suitable for water purification under visible light. The experimental data confirm our earlier observations (Zaleska, 2007; 2008; Górska, 2008), that lack of band gap narrowing with increase of the absorption intensity still can lead to effective degradation of organic compounds. Enhanced visible light-activity of TiO_2 (350°C) catalyst resulted rather from the presence of carbon, mainly in the form of C–C species, as well as from high surface area, see Table 3. Content of C–C species in TiO_2 calcinated at 350°C exceeds content in others samples, see our previous publication (Górska, 2008).

Table 3. Comparison of experimental results of TiO_2 (350°C) sample and TiO_2 P-25

Sample name	Phenol degradation efficiency after 60 min [%]	Specific surface area BET [m^2/g]	Band gap energy [eV]	Content of C–C species [at.%]
TiO_2 P_25	26.2	50	3.15	-
TiO_2 (350°C)	57.4[*]	127[*]	3.3[*]	10.3[**]

   *   an average value, calculated from data obtained for five separately prepared samples
   * *   previously published result

Carbon-doped TiO_2 exhibited similar visible light activity with respect to some photocatalysts prepared in our previous investigations (Zaleska, 2007; 2008) using dopant precursors (boric acid triethyl ester, thiourea, thioacetamide). Moreover, the proposed procedure is simple, reproducible, obtained photocatalyst does not contain intentionally introduced elements, therefore, is more acceptable for industrial applications and subsequent disposal/reuse.

ACKNOWLEDGMENTS

REFERENCES

ASAHI, R., MORIKAWA, T., OHWAKI, T., AOKI, K., TAGA, Y., (2001) *Visible-light photocatalysis in nitrogen-doped titanium oxides* .Science 293, 269–271.

BETTINELLI, M., DALLACASA, V., FALCOMER, D., FORNASIERO, P., GOMBAC, V., MONTINI, T., ROMANO, L., SPEGHINI, A., (2007) *Photocatalytic activity of TiO_2 doped with boron and vanadium*. J. Hazard. Mater. 146, 529–534.

CARP, O., HUISMAN, C.L., RELLER, A., (2004) *Photoinduced reactivity of titanium dioxide.* Progress in solid state chemistry 32, 33–177.

CHOI, W., RYU, J., (2007) *Multi-aspects of photocatalytic activities of TiO_2: Sustrate-specificy and implication for the activity tesr standardization.* Proceedings of Second International Conference on Semiconductor Photochemistry, July 2–25 2007, Aberdeen, Scotland.

FUJISHIMA, A., ZHANG, X., (2006) *Titanium dioxide photocatalysis: present situation and future approaches*. C.R. Chemie 9, 750–760.

GÓRSKA, P., ZALESKA, A., KOWALSKA, E., HUPKA, J., (2006) *Visible light-enhanced degradation of phenol in the presence of modified TiO_2*. Pol. J. Chem. Tech. 8, 102–105.

GÓRSKA, P., ZALESKA, A., KLIMCZUK, T., SOBCZAK, J.W., SKWAREK, E., HUPKA, J., (2008) *TiO_2 photoactivity in Vis and UV light: the influence of calcination temperature and surface properties.* Appl. Catal. B 84, 440–447.

HATTORI, A., YAMAMOTO, M., TADA, H., ITO, S., (1998) *A promoting effect of NH_4F addition on the photocatalytic activity of sol-gel TiO_2 films*. Chem. Lett. 27, 707–708.

HERRMANN, J.M., (1999) *Heterogeneous photocatalysis: fundamentals and application to the removal of various types of aqueous pollutants*. Catal. Today 53, 115–129.

HOFFMANN, M.R., MARTIN, S.T., CHOI, W., BAHNEMANN, D.W., (1995*) Environmental applications of semiconductor photocatalysis*. Chem. Rev. 95, 69–96.

HONG, X.T., WANG, Z.P., CAI, W.M., LU, F., ZHANG, J., YANG, Y.Z., MA, N., LIU, Y.J., (2005) *Visible-Light-Activated Nanoparticle Photocatalyst of Iodine-Doped Titanium Dioxide*. Chem. Matter. 17, 1548–1552.

IRIE, H., WATANABE, Y., HASHIMOTO, K., (2003) *Nitrogen-concentration dependence on photocatalytic activity of TiO_2–xNx powders*. J Phys Chem B 107, 5483–5486.

M. JANUS, M. INAGAKI, B. TRYBA, M. TOYODA, A.W. MORAWSKI, *Carbon-modified TiO_2 photocatalyst by ethanol carbonisation*, Appl. Catal. B 63 (2006) 272–276.

KURODA, Y., MORI, T., YAGI, K., MAKIHATA, N., KAWAHARA, Y., NAGAO, M., KITTAKA, S., (2005) *Preparation of visible-light-responsive TiO_2-xNx photocatalyst by a sol-gel method: analysis of the active center on TiO_2 that reacts with NH_3*. Langmuir 21, 8026–8034.

LETTMANN, C., HILDEBRAND, K., KISCH, H., MACYK, W., MAIER, W.F., (2001) *Visible light photodegradation of 4-chlorophenol with a coke-containing titanium dioxide photocatalyst*. Appl. Catal. B 32, 215–227.

LONG, M., CAI, W., CHEN, H., XU, J., (2007) *Preparation, characterization and photocatalytic activity of visible light driven chlorine-doped TiO_2.* Front. Chem. China 2(3), 278–282.

MACYK, W., KISCH, H., (2003) *Photosensitization of Crystalline and amorphous Titanium Dioxide by Platinum(iv) Chloride Surface Complexes*. Chem. Eur. J. 7, 1862–1875.

OHNO, T., AKIYOSHI, M., UMEBAYASHI, T., ASAI, K., MITSUI, T., MATSUMURA, M., (2004) *Preparation of S-doped TiO_2 photocatalysts and their photocatalytic activities under visible light*. Appl. Catal. A 265, 115–121.

REN, W., AI, Z., JIA, F., ZHANG, L., FAN, X., ZOU, Z., (2007) *Low temperature preparation and visible light photocatalytic activity of mesoporous carbon-doped crystalline TiO_2.,*Appl. Catal. B 69, 138–144.

SAKTHIVEL, S., KISCH, H., (2003) *Daylight photocatalysts by carbon-modified titanium dioxide.* Angew. Chem. Int. Ed. 42, 4908–4911.

SAKTHIVEL, S., JANCZAREK, M., KISCH, H., (2004) *Visible light activity and photo-electrochemical properties of nitrogen-doped TiO₂*. J. Phys. Chem. B 108, 19384–19387.

SAUPE, G.B., ZHAO T.U., BANG, J., DESU, N.R., CARBALLO, G.A., ORDONEM, R., BUBPHAMALA T., (2005) *Evaluation of a new porous titanium-niobium mixed oxide for photocatalytic water decontamination.* Microchemical Journal 81, 156–162.

SHI, Q., YANG, D., JIANG, Z., LI, J., (2006) *Visible-light photocatalytic regeneration of NADH using P-doped TiO₂ nanoparticles*. J. Mol. Catal. B 43, 44–48.

TSENG, Y., KUO, C., HUANG, C., LI, Y., CHOU, P., CHENG, C., WONG, M., (2006) *Visible-light-responsive nano-TiO₂ with mixed crystal lattice and its photocatalytic activity*. Nanotechnology 17, 2490–2497.

TSUMURA, t., KOJITANI, N., IZUMI, I., IWASHITA, N., TOYODA, M., INAGAKI, M., (2002) *Carbon coating of anatase-type TiO₂ and photoactivity*. J. Mater. Chem. 12, 1391–1396.

UMEBAYASHI, T., YAMAKI, T., TANAKA, S., ASAI, K., (2003) *Visible Light-Induced Degradation of Methylene Blue on S-doped TiO₂*. Chem. Lett. 32, 330–331

XU, t., SONG, c., LIU, Y., HAN, G., (2006) *Band structures of TiO2 doped with N, C and B*. Zhejijang Univ. Sci. B 7, 299–303.

YAMAKI, T., SUMITA, T., YAMAMOTO, S., (2002) *Formation of TiO₂-xFx compounds in fluorine-implanted TiO₂*. J.Mater.Scien.Lett. 21, 33–35.

ZALESKA, A., GÓRSKA, P., SOBCZAK, J.W., HUPKA, J., (2007) *Thioacetamide and thiourea impact on visible light activity of TiO₂*. Appl. Catal. B 76, 1–8.

ZALESKA, A., SOBCZAK, J.W., GRABOWSKA, E., HUPKA, J., (2008) *Preparation and photocatalytic activity of boron-modified TiO₂ under UV and visible light*. Appl. Catal. B 78, 92–100.

GÓRSKA P., ZALESKA A., SUSKA A., HUPKA J., *Aktywność fotokatalityczna i właściwości powierzchniowe tlenku tytanu(iv) domieszkowanego węglem*

TiO₂ domieszkowany węglem otrzymano poprzez hydrolizę izopropanolanu tytanu(IV) i kalcynację w 350 ºC w atmosferze powietrza przez 2h. Przeprowadzone badania wykazały, że fenol (0.21 mM) jest efektywnie degradowany w fazie wodnej, w obecności otrzymanego fotokatalizatora oraz światła z zakresu widzialnego (λ>400 nm). Pole powierzchni właściwej otrzymanego C–TiO₂ wynosiło około 127 m²/g, fotokatalizator absorbuje światło z zakresu widzialnego a przerwa energetyczna E_g wynosi 3,35 eV. W pracy przebadano aktywność oraz wybrane właściwości dla pięciu niezależnie otrzymanych próbek.

słowa kluczowe: fotokataliza, TiO₂-domieszkowany węglem, światło widzialne

E. Grządka*, S. Chibowski*,

INFLUENCE OF A KIND OF ELECTROLYTE AND ITS IONIC STRENGTH ON THE ADSORPTION AND ZETA POTENTIAL OF THE SYSTEM: POLYACRYLIC ACID/MnO$_2$/ELECTROLYTE SOLUTION

The influence of a kind of electrolyte (NaCl, KCl, CaCl$_2$ and MgCl$_2$), its ionic strength (0.01; 0.1; 1) and pH of a solution (3; 6; 9) on the adsorption of polyacrylic acid (PAA 2 000 and 60 000) on the surface of manganese dioxide (MnO$_2$) was measured. PAA adsorption was the highest in the presence of calcium chloride. Adsorption of polyacrylic acid increased also with ionic strength but decreased with the increase of pH of the solution. These results are consistent with theoretical findings concerning adsorption of anionic polyelectrolytes on surface of metal oxides. The influence of a kind of electrolyte and its ionic strength on the zeta potential in the presence of PAA was also measured. It was proved, that the zeta potential of MnO$_2$ is highest in the presence of calcium chloride as a background electrolyte. Moreover the zeta potential increased with ionic strength of all measured systems.

key words: polyacrylic acid, manganese dioxide polymer adsorption, polymer conformation, zeta potential

INTRODUCTION

Adsorption of high molecular weight substances arouses an increasing interest over the past few years. It is the results of the fact that the adsorption of polymer is completely different from the adsorption of small particles and ions. Polymer chains may form lots of different conformations in both the bulk phase and the interface,

---

* M. Curie-Skłodowska University, Faculty of Chemistry, Department of Radiochemistry and Colloid Chemistry, M. Skłodowska-Curie Square 3, 20-031 Lublin, Poland, egrzadka@wp.pl

while the ions and the small particles have invariable and defined shape (Cohen Stuart et al. 1991). The practical aspect of the polymer adsorption on solid surfaces is related to two processes: stabilisation and flocculation that are applied in many different branches of industry (Fleer et al. 1993, Fleer et al. 1993, Pan et al. 2001). The addition of low-molecular weight polymers to a dispersion causes sterical stabilisation of the dispersed system. This process is applied in production of: drugs, cosmetics, paints, varnishes and also in production of paper. On the other hand, the addition of high molecular weight polymers to a dispersion causes flocculation, widely used in treatment of industrial wastes occurring as water suspensions. Measurements of polymers' adsorption on the solid surfaces are determined by many different factors. Among them the most important ones are: the character of interactions between an adsorbent and an adsorbate, a type of used electrolyte, ionic strength and pH of the solution, polydispersity of the used polymer and the presence of impurities.

Manganese dioxide has been chosen as an adsorbent. It occurs in nature as a mineral called battery manganese or pyrolusite. Manganese dioxide forms a few polymorphic modifications (α, β, γ) but none of them has a stoichiometric composition (Kolditz 1994). Under standard conditions MnO_2 is insoluble and has amphoteric properties. Moreover MnO_2 has a also well-defined interface MnO_2/polyelectrolyte solution is stable in broad pH range. This dioxide finds applications in production of matches, in glass-making industry to decolourization of glass and as a depolarizer in voltaic cells (Trzebiatowski 1979).

Polyacrylic acid has been used as a polyelectrolyte in all measurements. This polymer has been chosen because of the wide spectrum of its applications (Szlezyngier 1998). It is used as: a supplement to surfactants, a compound used in production of paper, an inhibitor of fur formation, a concentrator in cosmetics and a component of drugs.

The aim of this paper is to define the influence of a type of used electrolyte, its ionic strength and pH of the solution on polyacrylic acid (PAA) adsorption on MnO_2 surface. Another important information about electrokinetic properties of manganese dioxide in the presence of PAA has been obtained by measurements of zeta potential in the presence and absence of polymer.

MATERIALS AND METHODS

MnO_2 produced by POCh-Gliwice was used as an adsorbent in all measurements. The specific surface area of manganese dioxide, calculated using the BET method was $38 \ m^2 \ g^{-1}$ and the average diameter of this oxide particles was equal to 280 nm. MnO_2 average pores diameter, also calculated using the BET method, was equal to 4.6 nm. Before the measurements MnO_2 was washed with doubly distilled water until the conductivity of the supernatant was smaller than $2 \ \mu S \ cm^{-1}$.

NaCl, KCl, MgCl$_2$ and CaCl$_2$ were used as background electrolytes. Concentrations of these electrolytes were chosen so as to provide a desired ionic strength (0.01; 0.1; 1). Polyacrylic acid (molecular weights: 2 000 and 60 000) produced by Aldrich was used as a polyelectrolyte.

The adsorption of PAA (Γ [mg m^{-2}]) in the concentration range from 30 ppm to 200 ppm on the MnO$_2$ surface was carried out using the static method (Chibowski et al. 1999) presented below. Into the Erlenmeyer flasks, which contained 10 ml of the polymer solution (chosen concentration of the polymer, electrolyte and pH) 0.2 g of MnO$_2$ was added. These suspensions were shaken for 24 hours. Then manganese dioxide was centrifuged and 5 ml of the clear solutions were taken for further analysis. The adsorption was calculated from the difference between PAA concentration before and after the adsorption. The base of analysis was the reaction between polyacrylic acid and hyamine, proposed by Crumette and Hummel (Crummett et al. 1963). The opacity increas after hyamine addition to the solution was measured turbidimetrically using a spectrophotometer (Specord M42, Carl Zeiss) using a special computer programme M500. The wavelength used was 500 nm.

The zeta potential measurements were made using a zetameter (Zetasizer 3 000, Malvern Instruments). The samples were prepared by ultrasonification of 0.05 g MnO$_2$ with 500 ml of solution and carefully defined: electrolyte (NaCl; KCl; MgCl$_2$; CaCl$_2$), ionic strength (0.01; 0.1; 1), polymer concentration (0.01 ppm; 0.1 ppm; 1 ppm) and pH. The zeta potential was measured in the presence and absence of polymers (PAA 2 000; PAA 60 000).

RESULTS AND DISCUSSION

Figure 1 presents the polyacrylic acid (PAA 60 000) adsorption isotherms on the surface of MnO$_2$ in the presence of four different electrolytes (CaCl$_2$, MgCl$_2$, KCl, NaCl) characterized by the same ionic strength (0.1), at pH 6.

Background electrolyte has the great influence on the adsorption of polyacrylic acid. As it can be seen, adsorption of PAA is higher when divalent cation chlorides are used as background electrolytes in comparison to PAA adsorption in the presence of NaCl and KCl. This phenomenon is a consequence of the creation of bidental complexes between Ca^{2+} or Mg^{2+} ions and dissociated carboxylic groups (Vermöhlen et al. 2000). These complexes may be created between two different polyelectrolyte chains or between carboxylic groups from the same macromolecule. It results in a spatial polymer conformation rich in loops and tails structures. Because of the fact, that the number of the adsorption sites on the surface of the metal oxide is constant, formation of such a conformation, built in the direction of bulk solution, causes the increase of polymer adsorption (Chibowski 1988).
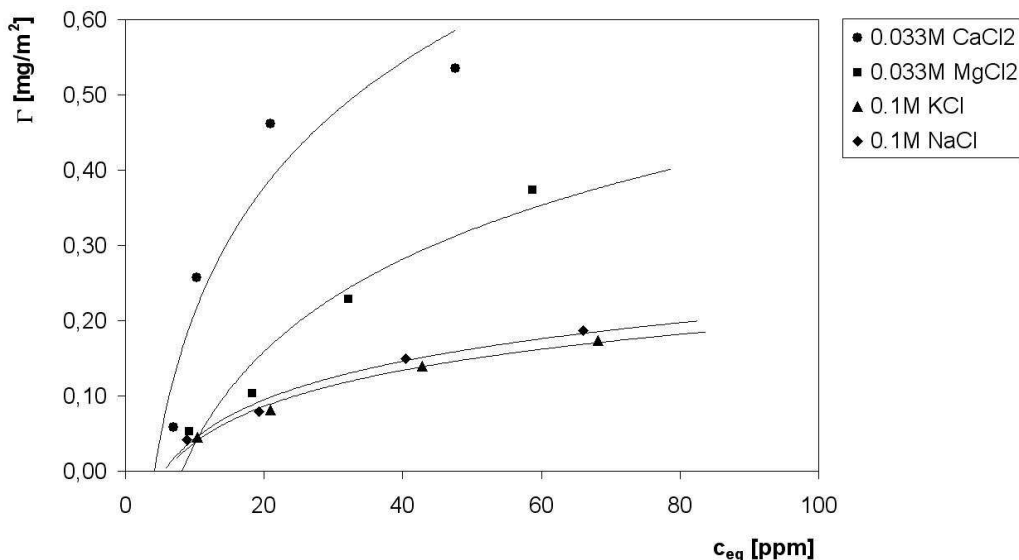
Fig. 1. Adsorption isotherms of PAA 60000 in the presence of different electrolytes, pH=6

Moreover, PAA adsorption in the presence of $CaCl_2$ as a background electrolyte is higher than in the presence of $MgCl_2$. This is a consequence of differences in desorption energy of calcium and magnesium ions. It is known that calcium cations desorb poorly from the surface of metal oxide, what is the evidence of strong interaction between them and the oxide surface groups. On the other hand, magnesium cations can desorb from the surface quite easily. Therefore, a better contact between PAA macromolecules and oxide surface is observed in the presence of $CaCl_2$, what increases the polymer adsorption. The presented isotherms shows also the similarity between PAA adsorption in the presence of monovalent metal chlorides. This situation may be explained by similarities in sodium and potassium ions activity and their equal charge.

Figure 2 presents the dependency between PAA adsorption and electrolyte ionic strength. As one can notice, the increase of ionic strength increases the PAA adsorption. This is a consequence of a few effects: changes in dissociation degree of carboxylic groups in PAA chain, conformational changes of polyacrylic acid on the surface of the metal oxide and changes of a kind and number of adsorbent surface groups (Tekin et al 2006). At pH values higher than pH_{pzc} of MnO_2 (~4.5) the screening effect of repulsion forces between negatively charged oxide surface and dissociated PAA chains (pK_a of polyacrylic acid=4.5 (J.E. Gebhardt et al. 1983)) has the most important influence on the increase of PAA adsorption with the increase of salt concentration. As it is known from our previous results the increase of electrolyte concentration as well as the increase of pH both increase the dissociation of polyacrylic acid (Grządka et al. 2008) and result in the appearance

of larger number of dissociated carboxylic groups in the measured system together with the increase of metal cation concentration.
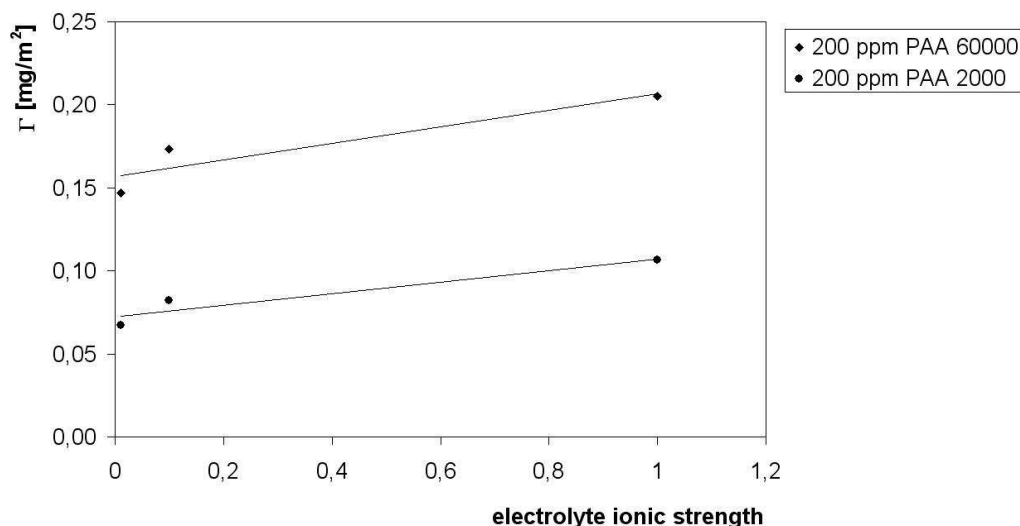
Fig. 2. Dependency between PAA adsorption and KCl ionic strength, pH=6

These cations are able to screen the repulsion between the negatively charged surface Its consequence is the increase of PAA adsorption on MnO_2 with the increase of electrolyte concentration. Moreover, in solution of high electrolyte concentration polymer chains are much more flexible (Adachi et al. 2002), what favors spacious polymer conformation, rich in loops and tails structures. Creation of such a conformation on the metal oxide surface leads to the increase of the polymer adsorption.

Figure 3 points out that PAA adsorption decreases with the increase of pH. As was mentioned above, PAA macromolecules at pH lower than 4.5 consist mostly of nondissociated carboxylic groups, but with further increase of pH the number of $-COO^-$ groups increases. The decrease of polyacrylic acid adsorption with the increase of pH results from the above-mentioned increase of negative charge in PAA chain. If the repulsion between adsorbent and adsorbate intensifies, interactions between polymer and surface of the solid are reduced. At low pH values the most possible adsorption mechanism is electrostatic attraction and nonelectrostatic, specific interaction between carboxylic groups and surface metal oxide groups, mostly hydrogen bond type (Solberg et al. 2003). At pH values higher than pH_{pzc} the most important mechanism responsible for PAA adsorption is the formation of complexes between polymer segments and adsorbent surface groups.
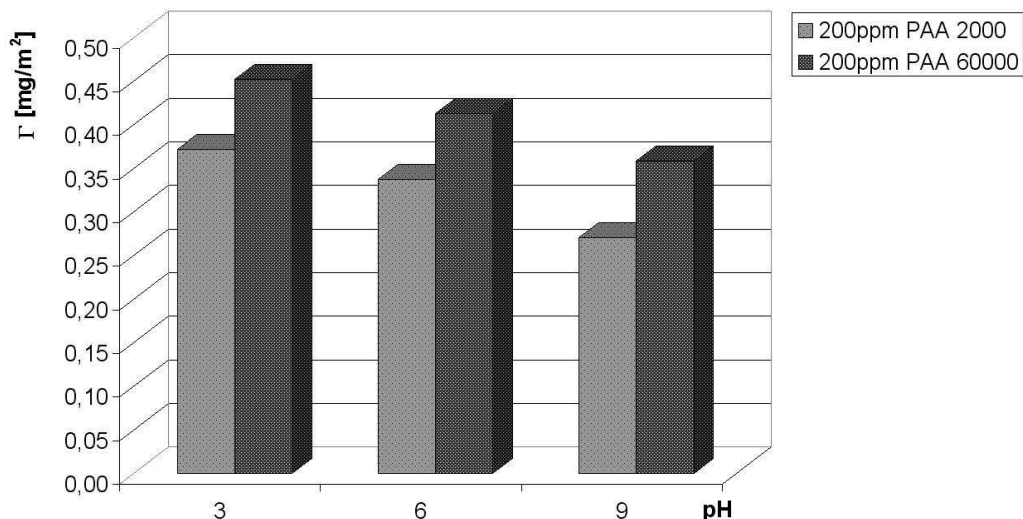
Fig. 3. Dependency between PAA adsorption and pH of the solution
in the presence of 0.333M MgCl₂

Figures 4–6 show the dependencies of the zeta potential of MnO₂ on the concentration of polymer, on the type of electrolyte and on electrolyte ionic strength. There are three effects responsible for the changes in values of the zeta potential in the presence of polymer. The first one is the presence of the charge of the dissociated polymer groups in the by-surface layer of the solid. The second one the shift of the slipping plane caused by the polymer adsorption on the metal oxide surface and the last one is the change of position of counterions in the Stern layer, which follows the polymer adsorption process. The first and the second effects cause the decrease of the zeta potential, but the third one causes the increase of this value. It must be underlined that these three effects occur simultaneously. The increase or the decrease of the zeta potential depend only on their quantitative contribution.

As it might be seen from Figure 4 the zeta potential of manganese oxide in the presence of polyacrylic acid is lower in the whole pH range than in the absence of polymer. That results from the presence of dissociated carboxylic groups in olymer chain mainly in the by-surface layer of MnO₂. Moreover, with the increase of pH the PAA dissociation increases. This situation causes not only the decrease of the zeta potential but also the conformational changes in PAA chains are observed (Das et al. 2001). Created conformation causes the shift of the slipping plane towards the bulk solutions, what leads to the decrease of the zeta potential value. The increase of polymer molecular weight and polyelectrolyte concentration both cause that the zeta potential of MnO₂ decreases. Such a behavior is reasonable because the increase of polymer molecular weight and the increase of polymer concentration both

cause two effects: the increase of total negative charge in polymer chain and the increase of the adsorption layer thickness. That causes the shift of the slipping plane in the bulk solutions and the decrease of the zeta potential values is observed.
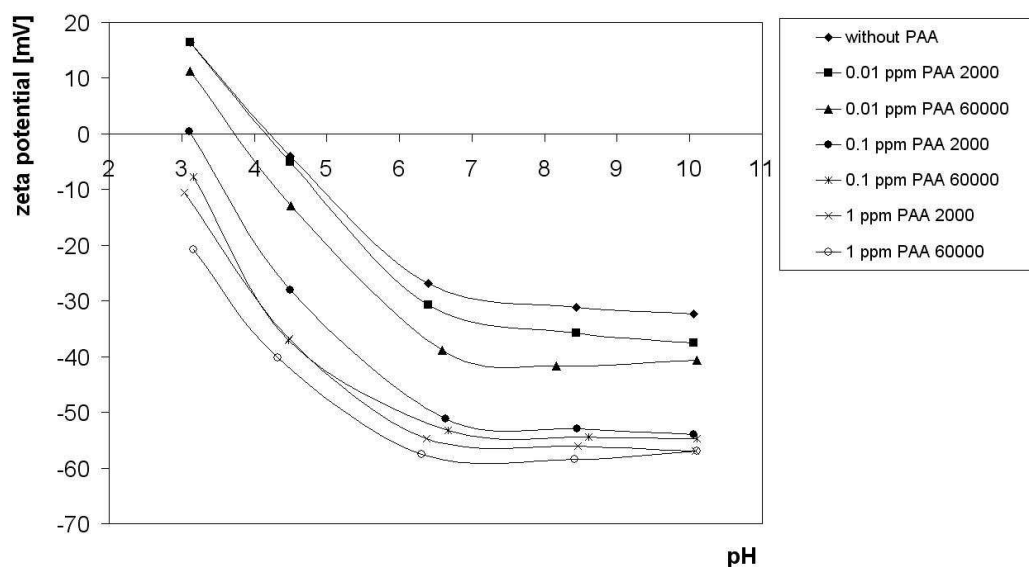
Fig. 4. Manganese dioxide zeta potential as a function of pH
in the presence of 0.01M NaCl and PAA

Some conclusions on the influence of kind of electrolyte on the zeta potential of MnO_2 might be drown from Figure 5. As one can see, when monovalent metal chlorides are used as electrolytes the zeta potential of MnO_2 curves have the similar run and the similar zeta potential values are obtained. This phenomenon is a consequence of the similar character of NaCl and KCl and their equal charge. On the other hand, when $CaCl_2$ is used as a background electrolyte, higher zeta potential values are obtained in comparison to the zeta potential values decreased in the presence of $MgCl_2$. Moreover, in the presence of divalent metal chlorides the obtained zeta potential data are more divergent than rather compact values obtained for the systems: MnO_2/PAA/monovalent metal chlorides. It is due to the above mentioned difference between the desorption energies of calcium and magnesium from the metal oxide surface. A competitive adsorption between electrolyte ions and polymer segments may occur in the systems containing calcium cations, but the same process is rare in the systems where magnesium cations are present. That competitive adsorption causes the blockade of the adsorption sites and results in the increase of the zeta potential of MnO_2 in the presence of $CaCl_2$.

Moreover, higher zeta potential values are obtained in the presence of divalent metal chlorides in comparison to zeta potential values in the presence of monovalent

chlorides and the smaller differences in the zeta potential of MnO_2 in the presence of polymer and without it in the presence of monovalent metal chlorides are observed. This fact is rather surprising because not only the adsorption of PAA but also the thickness of polyacrylic acid adsorption layer on MnO_2 in the presence of different electrolytes show that polyelectrolyte conformation is spacious in the presence of divalent metal chlorides. For that reason the decrease in elektrokinetic potential was expected in the presence of divalent metal chlorides mainly because of a bigger shift of the slipping plane. The only one explanation of the measured zeta potential increase is more effective screening of negative charge along polymer chains by divalent cations. Furthermore, these cations can interact with metal oxide surface groups and with polymer segments creating bidental complexes type: R–COO–Me–COO–R. This phenomenon is responsible for the second reversal of charge of MnO_2 in the presence of divalent chlorides. This effect is clearly visible at high pH values. Another reason for that is the overcharging of the electric double layer simultaneous with a formation of $–SO^-Ca^{2+}$ groups.
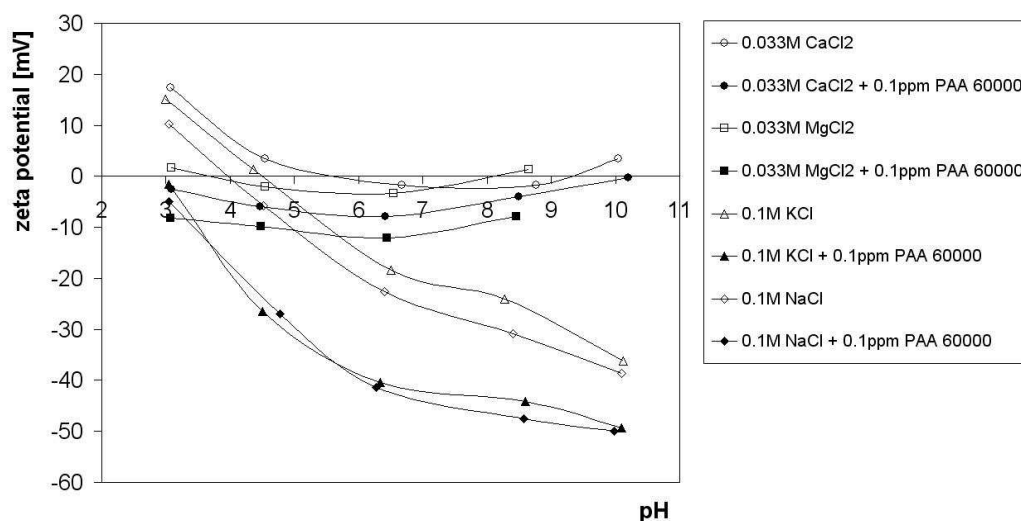
Fig. 5. Manganese dioxide zeta potential as a function of pH
in the presence of different electrolytes and PAA 60000

The data presented on Figure 6 allows the analysis of the influence of ionic strength on MnO_2 zeta potential. As one can notice, increase of the zeta potential accompanies the increase of salt concentration. This results from the screening effect of negative charge between dissociated PAA carboxylic groups and metal oxide surface by the growing number of background electrolyte cations. Moreover, there are visible differences between the zeta potential curves in the presence of 0.333M $MgCl_2$

in comparison to the zeta potential curves in the presence of less concentrated electrolytes. These differences result from differences between adsorption of cations and anions (Kosmulski et al. 2007).
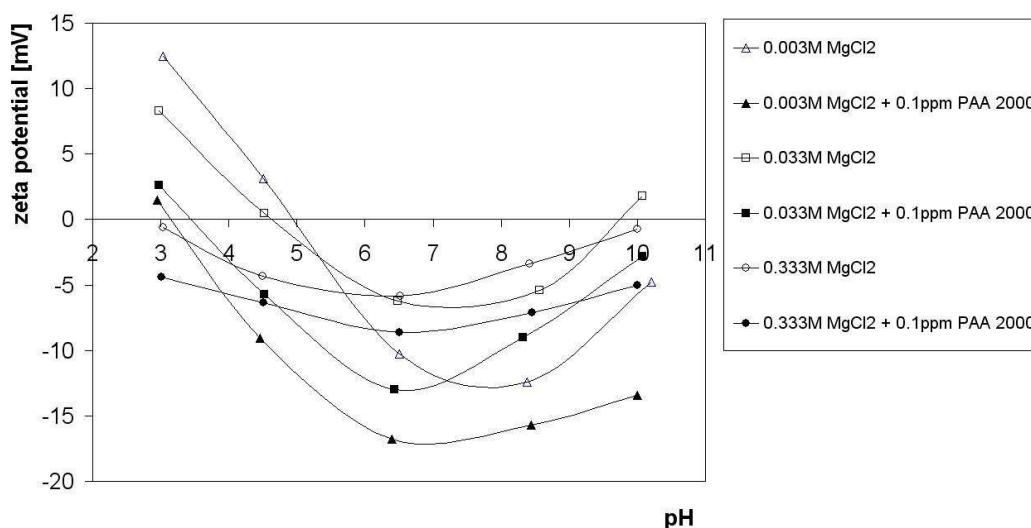
Fig. 6. Manganese dioxide zeta potential as a function of pH for various concentration of KCl
in the presence or absence of PAA 2000

CONCLUSIONS

- The highest polyacrylic acid adsorption is observed in the presence of $CaCl_2$.
- PAA adsorption on MnO_2 surface is higher for divalent than for monovalent metal chlorides as background electrolytes.
- There are no large differences between the polyacrylic acid adsorption in the presence of NaCl and KCl.
- With the increase of ionic strength the increase of PAA adsorption is observed.
- The presence of divalent cations in the system: PAA/MnO_2/electrolyte solution results in the increase of the zeta potential of MnO_2.
- The increase of electrolyte ionic strength causes the increase of the zeta potential.

REFERENCES

ADACHI Y., MATSUMOTO T., COHEN STUART M.A., (2002), *Effects of hydrodynamic mixing intensity coupled with ionic strength on the initial stage dynamics of bridging flocculation of polystyrene latex particles with polyelectrolyte*, Coll. Surf. A, 207, 253.

CHIBOWSKI S., (1988), *Effect of the ionic composition of the solution on the polyvinyl alcohol adsorption on the surface of Al_2O_3*, Mater. Chem. Phys., 20, 65.

CHIBOWSKI S., KRUPA M., (1999), *Study of the influence of poly(acrylic acid) and polyacrylamide on the electrochemical properties of the ZrO_2/solution interface*, Adsorption Sci. Technol., 17, 813.

COHEN STUART M.A., FLEER G.J., LYKEMA J., NARDE W., SCHEUTJENS J.M.H.M., (1991), *Adsorption of ions, polyelectrolytes and proteins,* Adv. Coll. Inter. Sci. 34 477.

CRUMMETT W.B., HUMMEL R.A., (1963), *The determination of traces of polyacrylamides in w*ater, J. Am. Water Works Assoc., 55, 209.

DAS K.K., SOMASUNDARAN P., (2001), *Ultra-low dosage flocculation of alumina using polyacrylic acid*, Coll. Surf. A, 182, 25.

FLEER G.J., COHEN STUART M.A., SCHEUTJENS J.M.H.M., COSGROVE T., VINCENT B., (1993), Polymers at Interfaces, Chapman & Hall, London.

FLEER G.J., SCHEUTJENS J.M.H.M. in: DOBIAS B. (Ed.), (1993), *Coagulation and Flocculation*; Theory and Applications, Chapter 5, Marcel Dekker, New York.

GEBHARDT J.E., FURSTENAU D.W., (1983), *Adsorption of polyacrylic acid at oxide/water interfaces*, Coll. and Surf.A, 7, 221.

GRZĄDKA E., CHIBOWSKI S., (2008), *Influence of a kind of electrolyte and its ionic strength on the conformation changes of polyacrylic acid during its coming from the bulk solution to the surface of MnO_2,* Physicochemical Problems of Mineral Processing, 42, 47.

KOLDITZ L. (ed.), (1994), Chemia nieorganiczna, PWN, Warszawa.

KOSMULSKI M., DAHLSTEN P., PRÓCHNIAK P., ROSENHOLM J.B., (2007), *Electrokinetics at high ionic strengths*: Alumina, Coll. Surf. A, 301, 425.

TEKIN N., DINCER A., DEMIRBAS Ö., ALKAN M., (2006), *Adsorption of cationic polyacrylamide onto sepiolite*, J. Hazardous Materials B., 134, 211.

PAN Z., CAMPELL A., SOMASUNDARAN P., (2001), *Polyacrylic acid adsorption and conformation in concentrated alumina suspensions,* Coll. and Surf. A, 191, 71.

SOLBERG D., WAGBERG L., (2003), *Adsorption and flocculation behavior of cationic polyacrylamide and colloidal silica,* Coll. Surf. A, 219, 161.

SZLEZYNGIER W., (1998), Tworzywa Sztuczne, WOF, Rzeszów.

TRZEBIATOWSKI W., (1979), Chemia nieorganiczna, PWN, Warszawa.

VERMÖHLEN K., LEWANDOWSKI H., NARRES H-D., SCHWUGER M.J., (2000), *Adsorption of polyelectrolytes onto oxides - the influence of ionic strength, molar mass, and Ca^{2+} ions*, Coll. Surf. A, 163, 45.

Grządka E., Chibowski S., *Wpływ rodzaju elektrolitu i jego siły jonowej na adsorpcję i właściwości elektrokinetyczne układu: kwas poliakrylowy/MnO_2/roztwór elektrolitu.,* Physicochemical Problems of Mineral Processing, 43 (2009), 31–42 (w jęz. ang)

Badano wpływ rodzaju elektrolitu (NaCl, KCl, $CaCl_2$ i $MgCl_2$), jego siły jonowej (0.01; 0.1; 1) i pH roztworu (3; 6; 9) na adsorpcję kwasu poliakrylowego (PAA 2 000 i 60 000) na powierzchni ditlenku manganu (MnO_2). Otrzymane wyniki dowodzą, że adsorpcja PAA jest największa w obecności chlorku sodu w porównaniu z adsorpcją PAA w obecności innych elektrolitów. Adsorpcja kwasu poliakrylowego wzrasta również wraz ze wzrostem siły jonowej elektrolitu podstawowego lecz maleje ze wzrostem

pH roztworu. Wyniki te pozostają w zgodzie z przewidywaniami teoretycznymi dotyczącymi adsorpcji anionowych polielektrolitów na powierzchni tlenków metali. Mierzono również wpływ rodzaju elektrolitu i siły jonowej na potencjał dzeta w obecności kwasu poliakrylowego. Zostało udowodnione, że potencjał dzeta MnO_2 przyjmuje najwyższe wartości w obecności chlorku wapnia jako elektrolitu podstawowego. Co więcej, wartość ta wzrasta wraz ze wzrostem siły jonowej w każdym z badanych układów.

słowa kluczowe: kwas poliakrylowy, ditlenek manganu, adsorpcja polimerów, konformacja polimerów, potencjał dzeta

M. Krzan* and K. Małysa*

INFLUENCE OF SOLUTION pH AND ELECTROLYTE PRESENCE ON BUBBLE VELOCITY IN ANIONIC SURFACTANT SOLUTIONS

Influence of sodium n-dodecyl sulfate (SDDS) concentration, presence of electrolytes (NaCl and KCl) and the solution pH variation on profiles of the bubble local velocity and values of the bubble terminal velocity were studied. It was found that in SDDS solutions the bubble accelerated rapidly after the detachment and either a maximum was observed (low SDDS solution concentrations) followed by a period of monotonic decrease or the terminal velocity was attained immediately after the acceleration stage (high SDDS concentrations). Addition of the electrolyte and/or the pH variation caused significant diminishing the local velocity in low concentrations solutions and lowering the bubble terminal velocity to a value characteristic for SDDS solutions of high concentrations. This effect of electrolyte and pH on the bubble velocity variations was attributed to lowering surface tension of the SDDS solutions.

keywords: sodium n-dodecyl sulfate, SDDS, bubble; surface tension, adsorption coverage;velocity; fluidity of interface; adsorption kinetics; dynamic structure of adsorption layer.

INTRODUCTION

Bubble motion is an important issue in many industrial applications. As Kulkarni and Joshi (2005) underlined in their review, the gas bubbles and gas-liquid contacting are the most important and very common operations in the chemical process industry, petrochemical industry, and mineral processing. In applications such as absorption, distillation, and froth flotation, the interaction of two phases occurs through dispersing the gas into bubbles and their subsequent rise in the liquid pool. In froth flotation

* Institute of Catalysis and Surface Chemistry, Polish Academy of Sciences, ul. Niezapominajek 8, 30-239 Krakow, Poland, nckrzan@cyfronet.pl

the bubble acts as a carrier of the attached particles having density greater than the continuous liquid medium (pulp). Probability of formation of the stable bubble-particle aggregate is considered (Derjaguin and Dukhin, 1960; Schimmoler et. al., 1993; Ralston and Dukhin, 1999) to be a product of the probabilities of collision and attachment (formation of the three-phase contact) and the probability that detachment would not subsequently occur. The probability of the collision is determined mainly by hydrodynamic conditions of the bubbles and particles motion. As surfactant adsorption at the interface of the rising bubble can lower its terminal velocity over two-fold (Clift et al., 1978; Krzan and Malysa, 2002ab; Krzan et al., 2007), so an addition of the surfactant (frother) can affect significantly not only the collision probability but also the probability of the particle attachment due to prolongation of the contact time between the colliding bubble and particle. Various reagents are employed in mineral industry as frothers (Laskowski, 1998) to modify properties of the liquid/gas interfaces and to facilitate the flotation aggregate formation (Leja, 1982). The frother addition assures formation of the froth layer, facilitates the gas dispersion and increases the gas/liquid interfacial area, as a result of diminishing sizes of the bubbles formed, and lowers significantly velocity of the bubbles formed. The size of bubbles formed and their velocity are considered (Azgomi et al., 2007) to be the main factors determining the gas holdup in flotation column and the bubble velocity is related to its size. As smaller bubble size and velocity leads to a larger the gas holdup, so Azgomi et al. (2007) attempted to find a unique relationship among gas holdup, gas rate and bubble size, which would be independent of frother (surfactant) type. However, the attempt was unsuccessful and they found in their analysis of the bubble size and gas holdup vs. frothers concentration that for the same gas holdup, the bubble sizes for different frothers were different. A failure of this analysis is most probably related to the fact that the size of the bubbles formed and the bubble rising velocity is determined by the state of adsorption layer at the bubble surface. Identical bulk concentration does not mean that the adsorption coverage is similar.

The presence of adsorption layer and time of formation of the dynamic adsorption layer (DAL) are the parameters which affect, to a great extent, values of the local and terminal velocities of the rising bubbles (Clift et al., 1978; Sam et al., 1996; Krzan and Malysa, 2002ab; Krzan et al., 2007). In water devoid of surfactants, the bubble surface is fully mobile, and therefore, the bubble velocity is higher than that of solid sphere of identical diameter and density (Levich, 1962). Adsorption layer of surfactant molecules at the bubble surface retards fluidity of the gas/liquid interface and lowers the bubble rising velocity. Simultaneously, as a result of the viscous drag exerted by continuous medium on the bubble surface, an uneven distribution of the adsorbed surfactant molecules along the interface of the rising bubble is devel-

oped. Such adsorption layer, called the dynamic adsorption layer (DAL) (Dukhin et al., 1998), determines values of the bubble terminal velocity and profiles of the bubble local velocity (Krzan et al, 2007). Formation of the DAL means that the adsorption coverage (surface concentration) is at minimum at the upstream pole of the moving bubble, while at the rear pole is higher than the equilibrium coverage (Dukhin et al., 1995, 1998). This gradient of the surface concentration (surface tension) retards mobility of the bubble surface and consequently the bubble velocity is lowered.

Bubble formation is a dynamic process and in surfactant solutions is interrelated with adsorption of surfactant molecules at the expanding bubble surface. A degree of the adsorption coverage at the surface of the bubble formed is determined by the rate of bubble formation and kinetics of the surfactant molecules adsorption of at the expanding bubble surface (Warszynski et al., 1998b; Jachimska et al., 2001). The equilibrium adsorption coverage is attained at surface of the bubble formed and starting to rise only in the case when the adsorption is faster than the bubble surface expansion. The bubble formed accelerates immediately and at some distance from the point of its formation reaches the terminal velocity which is determined by the balance between all acting forces.

The paper presents results of studies on local and terminal velocities of the bubbles rising in n-dodecyl sulfate solutions of different concentrations, and on influence of solution pH and presence of various electrolytes on the bubble motion.

EXPERIMENTAL

A square glass column (40×40 mm) having at the bottom a capillary of inner diameter 0.075 mm was used. Bubbles were formed at the capillary orifice with the help of Cole-Parmer syringe pump enabling high precision control of the gas flow. Figure 1 presents schematically the set-up used in measurements of the bubble dimensions and velocities. A Moticam 2000 digital camera (with Nikkor f=60 objective and rings for magnification) was used to monitor and record the bubbles motion. The picture recorded was magnified approximately twenty-fold as a result of applying the rings between the objective and the camera body. To determine local velocities of the bubble at various distances from the capillary orifice a stroboscope lamp (Drelloscope) illumination with 100 flashes per second was applied. The data were next analyzed by the image analysis software SigmaScan Pro 5.0.

Sodium n-dodecyl sulfate and sodium and potassium hydroxides were used as received from Fluka and Merck. Sodium and potassium chlorides used were heated up to $550^{\circ}C$ in order to get rid of any surfactant contaminations. The surfactant solutions were carefully prepared immediately before experiment to avoid any a long term hy-

drolysis. Distilled water (Millipore) was used for the solution preparation. The measurements were carried out at room temperature, 22±1 ºC.
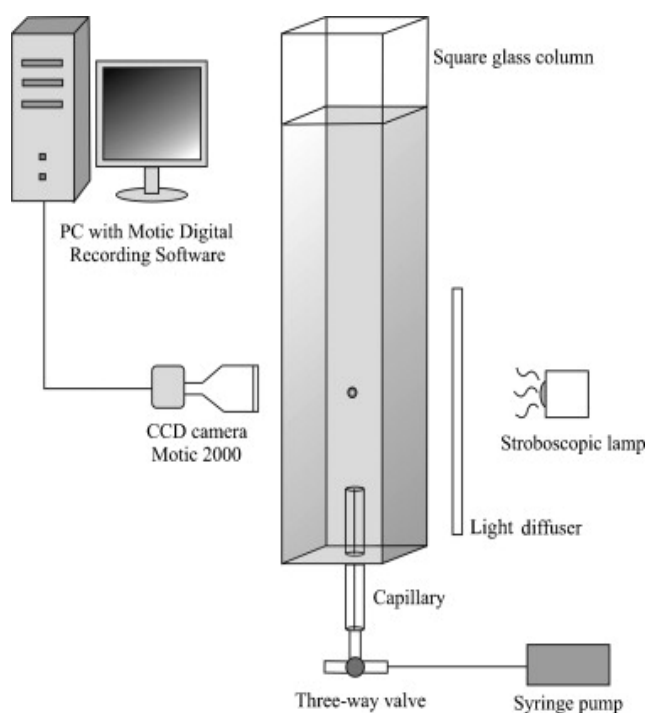
Fig. 1. The experimental set-up

RESULTS AND DISCUSSION

Local velocity profiles, i.e. variations of the bubble local velocity with distance from the point of the bubble formation, are different for pure water and surfactant solutions. Generally, in clean water there can be distinguished two stages: i) acceleration, and ii) steady state motion, when the terminal velocity is attained. In surfactant solutions an additional stage can be observed, i.e. a maximum followed by a deceleration until the terminal velocity is established (Krzan and Malysa, 2002ab; Krzan et al., 2004, Malysa et al., 2005, Krzan et al., 2007ab). The bubble terminal velocity in surfactant solutions is lower than that in clean water. The presence and the position of the maximum is a function of the surfactant concentration and both of them depend on type of the surfactant used.

Figure 2 present the images of bubbles departing from the capillary orifice at various concentrations of sodium n-dodecyl sulfate solutions. From the left, there are images showing the bubble detachment and acceleration in $1 \cdot 10^{-5}$ M, $1 \cdot 10^{-4}$ M and $3 \cdot 10^{-3}$ M SDDS solutions, respectively. As these experiments were carried out under identical stroboscopic illumination (100 flashes per second) so it can be noted immediately that the bubbles velocity was increasing with distance from the capillary and decreasing with increasing the SDDS concentration. It is seen also that the bubbles, which were spherical at the capillary orifice, underwent deformation immediately after departure and the deformation was the largest in lowest concentration. There were also observed differences in the bubble path motion at different concentrations. At concentration of $1 \cdot 10^{-5}$ M the bubbles moved up along a straight line. In $1 \cdot 10^{-4}$ M the presence of the zig-zag and later helical path of the rising bubble was observed from a distance of ca. 10 cm above the capillary. At high SDDS concentration ($3 \cdot 10^{-3}$ M) the path of the bubbles rise was again linear. These differences in the bubble path motion are related – in our opinion – to degree of immobilization of the bubble surface. The bubble interface in $1 \cdot 10^{-5}$ M SDDS solution is practically fully mobile, in $1 \cdot 10^{-4}$ M the surface is partially immobilized, and in $3 \cdot 10^{-3}$ M the bubble surface is fully immobilized – fluidity of the solution/gas interface is completely retarded.
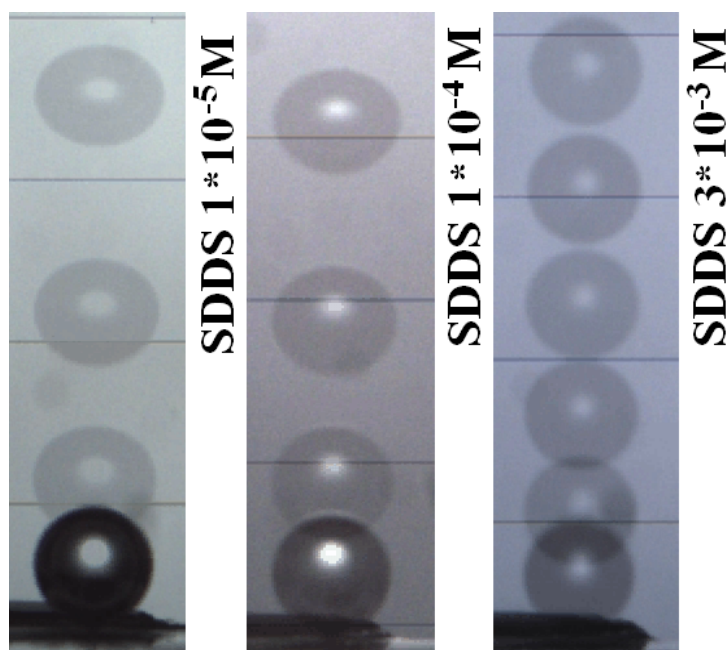
Fig. 2. Examples of images of the bubbles departing from the capillary orifice at SDDS solutions of concentration $1*10^{-5}$, $1*10^{-4}$ and $3*10^{-3}$ mol dm^{-3}. Strobe frequency-100 flashes per second

Figure 3 presents the results of the measurements of bubbles' local velocity as a function of the distance from the capillary in SDDS solutions. As a reference the values of bubbles' local velocities in distilled water are also presented. Generally, the variations (profiles) of the local velocities with distance show a similar feature like in the case of previously studied nonionic and cationic surfactants. Immediately after detachment, the bubble velocity increases rapidly in all the SDDS studied solutions and in distilled water. Having passed the period of rapid acceleration either a maximum was observed (low SDDS solution concentrations) followed by a period of monotonic decrease, which ended up (in the majority of cases) as a plateau (a constant value of the terminal velocity), or the terminal velocity was attained immediately after the acceleration stage (high SDDS concentrations). The height and the width of the maximum diminished with increasing concentration of the surfactants. The distance from the capillary at which the maximum velocity was observed, for a definite concentration of the surfactants, shifted closer to bubble's starting point with increasing solution concentration. As can be observed in Figure 3, bubbles' terminal velocity was decreasing steadily with increasing solution concentration, from 34.8 ± 0.3 cm/s in distilled water, down to a level of ca. 15 cm/s, which is almost identical like for all surfactants studied at their highest solution concentrations (Krzan and Malysa, 2002ab; Krzan et al., 2004, Malysa et al., 2005, Krzan et al., 2007ab).

Fig. 3. Bubble local velocities in water and SDDS solutions of various concentrations

The degree of adsorption coverage and distribution of the adsorbed surfactants over surface of the rising bubble are of crucial importance for the bubble motion be-

cause there exist minimum adsorption coverage necessary for a complete immobilization of the bubble interface. The values of these minimum adsorption coverage needed to 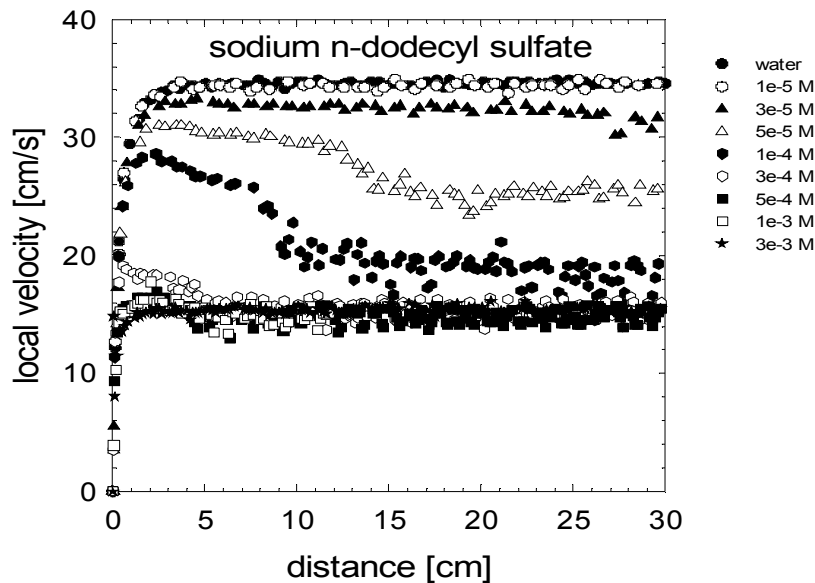immobilize the bubble interface can be quite different and, as shown by Krzan et al. (2002ab; 2004, 2007ab), can vary from ca. 2% up to 25%, depending on the surfactant type. Figure 4 presents the dependence of the bubble terminal velocity on the degree of adsorption coverage at surface of the bubble detaching from the capillary in solutions of sodium n-dodecyl sulfate. The degree of adsorption was calculated using the adsorption kinetics model for the expanding bubble surface elaborated by Warszynski et al., (1998b) and described in details in (Jachimska et al., 2001). The model assumptions are as follows: (i) bubble grows uniformly with constant (velocity) up to its detachment from the capillary orifice, (ii) surfactant molecules are transferred to the interface by the convective-diffusion mechanism, and (iii) adsorption kinetics is described by the Frumkin-Hinshelwood model, which at equilibrium is consistent with the Frumkin adsorption isotherm. Values of parameters of the Frumkin adsorption isotherm used in the calculations were taken from the paper by Warszynski et al., (1998b). Knowing that in our experiments the time of the bubble surface expansion, i.e. the time available for the surfactant adsorption, was 1.6 s we could evaluate the degree of adsorption coverage. It was found that that the adsorption coverage at the surface of the detaching bubble was closed to the equilibrium adsorption coverage in all SDDS solutions - only in lowest SDDS concentrations the coverage's at the surface of the detaching bubble were lower, but still over 80% of the equilibrium ones. As seen in Figure 4, the minimum adsorption coverage needed for a complete retardation of fluidity of the rising bubble interface was equal to ca. 10%.

The SDDS solution of concentration $1 \cdot 10^{-4}$ mole/dm^3 was chosen for studies of the influence of the solution pH and the electrolyte presence on the bubble motion. At this concentration (see Figure 2) there was a distinct maximum, i.e. three different stages of the bubble motion, indicating that dynamic structure of the adsorption layer (DAL) was not established at the stage of the bubble acceleration. Moreover, at the adsorption coverage at surface of the detached bubble (ca. 2%) still did not assure a complete retardation of the bubble surface fluidity. Thus, in this solution an influence of pH and electrolyte presence on various stages of the bubble motion can be observed.

Figure 5 presents images of bubbles departing from the capillary orifice for the $1 \cdot 10^{-4}$ M SDDS solutions of different pH's; not adjusted (ca. 7), pH 2 (HCl added) and pH 11 (NaOH added), respectively. As these experiments were carried out under stroboscopic illumination of 100 flashes per second, it can be clearly seen that the pH variation had a strong impact on the bubble acceleration and velocity immediately after its detachment from the capillary – the bubble acceleration was much smaller. An addition of the electrolyte had a similar effect on the bubble acceleration and initial velocity.
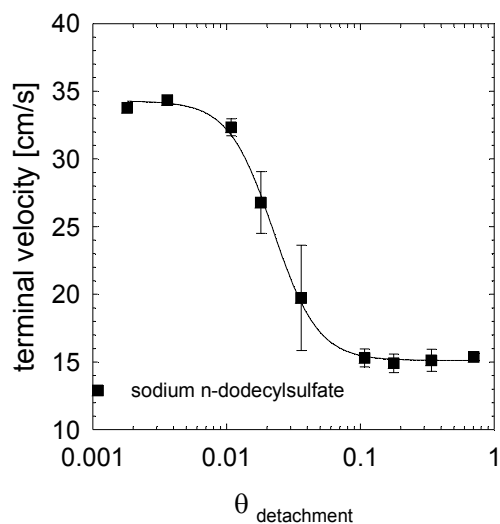
Fig. 4. Bubble terminal velocity as a function of the adsorption coverage degree over surface of the bubbles detaching from the capillary in sodium n-dodecyl sulfate solutions (adsorption time = 1.6 s)
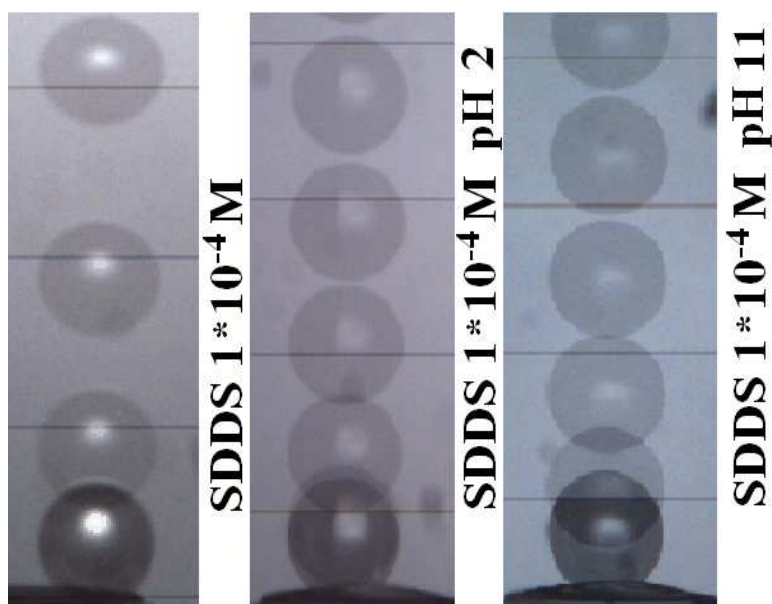
Fig. 5. Images of bubbles departing from the capillary orifice in $1 \cdot 10^{-4}$ mole/dm^3 SDDS solutions of different pH's; not adjusted (ca. 7), pH 2 (HCl added) and pH 11 (NaOH added), respectively. Strobe frequency-100 flashes per second

Figures 6A–D present the quantitative data on influence of electrolyte (NaCl or KCl) and solution pH on profiles of the bubble local velocity and the terminal velocity values. To check if there is any specific effect of the type of the electrolyte cation, the potassium and sodium chlorides were used and the alkaline pH of the solutions was adjusted by applying either NaOH or KOH. As seen in Figures 6A–D, without any additives in $1 \cdot 10^{-4}$ M SDDS solutions, the period of rapid acceleration is followed by a stage of velocity decrease, preceding an attainment of the terminal velocity equal to 17–18 cm/s. An addition of the electrolyte and/or the pH variation had a drastic influence on the bubble velocity profiles. As can be observed in Figures 6A–D, the maxima disappeared and the terminal velocity stage was achieved immediately after the acceleration period. Moreover, the terminal velocity was lowered to ca. 14–15 cm/s and was attained already at distance of 2–3 cm from the capillary orifice. A small maximum can be noted only in solutions at pH=11 (Figures 6A and 6B) without any electrolyte added.

Fig. 6A. Profiles of the bubble local velocity in $1 \cdot 10^{-4}$ M SDDS solutions of pH=11 (NaOH adjusted), without and with 0.05 M NaCl added. The velocity profile in $1 \cdot 10^{-4}$ M SDDS solutions without any additives is given as the reference

In our opinion the influence of electrolyte and pH on the bubble velocity variations is related to the effect of electrolytes on surface tension of ionic surfactant solutions. When the ionic surfactant molecules are adsorbed, the electrical double layer is built and, as a result, an energetic barrier of electrostatic origin appears. It is known that

adsorption of ionic surfactants is strongly influenced by the electrical double layer arising due to surfactants ion adsorption and repulsive interactions between the adsorbed ionic molecules within the adsorption layer. Warszynski et al., (1998a) showed and developed a theoretical model to describe the influence of electrolyte on the surface tension of ionic surfactants. There are presented experimental data for a broad range of NaCl concentrations (0–1M NaCl) showing that addition of NaCl can shift the SDDS surface tension isotherm by more than order of magnitude towards lower concentrations. This effect of lowering of surface tension of ionic surfactant solutions is due to neutralization of the surface charge of adsorbed ionic surfactant molecules by counterions adsorbed in the Stern layer (Warszynski et al., 1998a). The counterion adsorption causes that interface is almost "neutral" for the adsorbing surfactant, and thus, the surface activity of the ionic surfactant almost approaches the surface activity of nonionic surfactant with the same carbon chain length. In other words the electrolyte presence means that at identical bulk concentration the SDDS solution surface tension is lowered. Lower surface tension means higher SDDS adsorption coverage over interface of the rising bubble and higher retardation of the bubble surface fluidity. As a result the bubble local and terminal velocities are lowered in electrolyte presence.

Fig. 6B. Profiles of the bubble local velocity in $1 \cdot 10^{-4}$ M SDDS solutions of pH=11 (KOH adjusted), without and with 0.05 M KCl added. The velocity profile in $1 \cdot 10^{-4}$ M SDDS solutions without any additives is given as reference

Fig. 6C. Profiles of the bubble local velocity in $1 \cdot 10^{-4}$M SDDS with 0.05 M NaCl or 0.05 M KOH added. The velocity profile in $1 \cdot 10^{-4}$M SDDS solutions without any additives is given as the reference
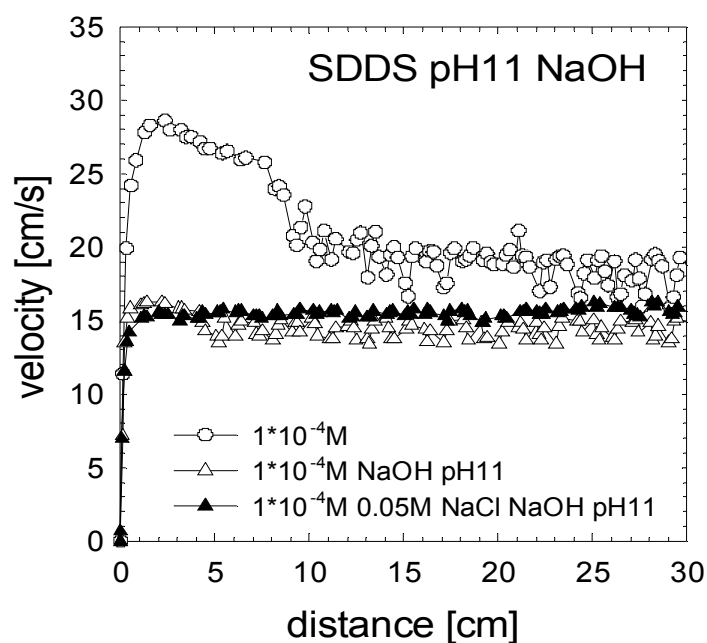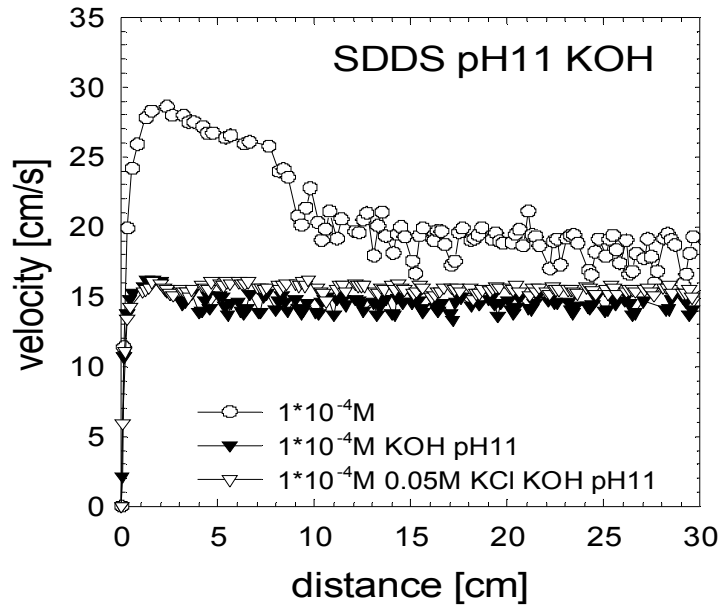

Fig. 6D. Profiles of the bubble local velocity in $1 \cdot 10^{-4}$ M SDDS solutions of pH=2 (HCl adjusted), without and with 0.05 M NaCl added. The velocity profile in $1 \cdot 10^{-4}$ M SDDS solutions without any additives is given as the reference
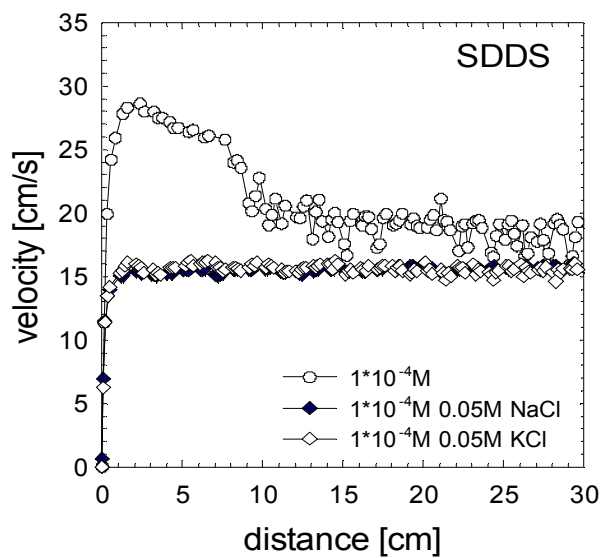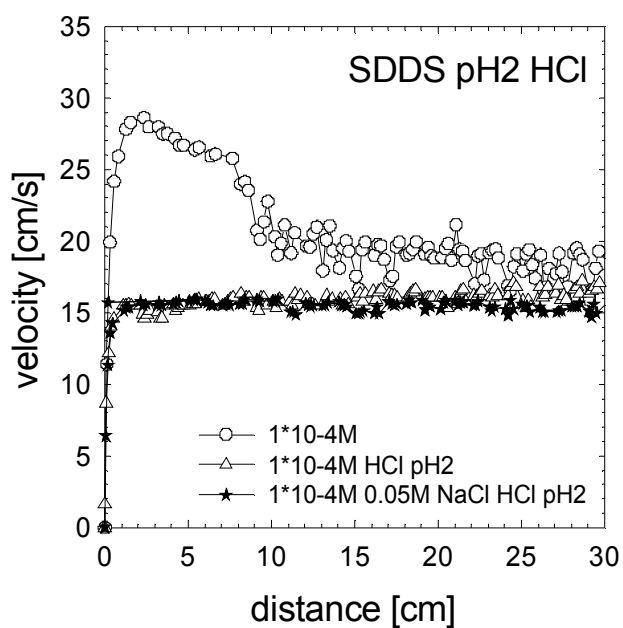
    To confirm that the influence of pH and electrolyte on the bubble motion is due to lowering surface tension of the SDDS solutions, the sizes of bubbles formed were measured and collected in Table 1. Size of the bubble formed at the capillary orifice under equilibrium or quasi-equilibrium conditions is given by Tate law (Adamson, 1990):

$$r_b = \sqrt[3]{\frac{3}{2} \frac{\sigma r_k}{\Delta \rho g}}$$

where r_b is the bubble radius, d_0 is the capillary orifice diameter, σ is the solution surface tension, $\Delta \rho$ is the density difference between air and water and g is the gravity acceleration. As showed elsewhere (Krzan et al. 2002a) the sizes of the detaching bubbles were in good agreement with that calculated from the Tate law. Thus, from the measured size of the detaching bubbles the solution surface tension can be evaluated. As can be clearly seen in Table 1, the bubble diameter decreased from 1.45 mm in the SDDS solution without any additives, down to ca. 1.39–1.40 mm in the presence of NaCl, NaCl/NaOH, KCl, KCl/KOH or HCl, NaCl/HCl, KCl/HCl. In the case of experiments with addition of NaOH or KOH, the bubble diameters were 1.42–1.43 mm. Using the Tate law the surface tension values reflecting these variations of the bubble diameter were calculated and are listed in Table 1. When in $1 \cdot 10^{-4}$ M SDDS solution without any electrolyte the surface tension was 72 mN/m, then it decreased to ca. 62.5 mN/m for the bubble diameter of 1.39mm (solution pH=2). An addition of 0.05 M of NaCl or KCl caused the bubble diameter to diminished from 1.45 to 1.40 mm and its is equivalent to the surface tension decrease from 72 to ca. 64.5 mN/m. It is worthy to add here that these evaluations of the surface tension variations with electrolyte addition are in reasonable agreement with data published by Warszynski et al. (1998a).

Table 1. Variations of the bubble diameter in $1 \cdot 10^{-4}$ M SDDS solutions without and with electrolyte addition and at different pH's. Diameter of the capillary orifice – 0.075mm

SDDS $1 \cdot 10^{-4}$ M with addition of:	bubble diameter [mm]	surface tension [mN/m] (calculated from theTate law)
-	1.45 ± 0.01	72.0 ± 0.5
0.05 M NaCl	1.40 ± 0.01	64.5 ± 1.0
0.05 M NaCl NaOH pH 11	1.41 ± 0.01	65.5 ± 1.0
0.05 M NaCl HCl pH 2	1.40 ± 0.01	64.5 ± 1.0
NaOH pH 11	1.43 ± 0.01	68.5 ± 0.8
HCl pH 2	1.39 ± 0.01	62.5 ± 1.0
0.05M KCl	1.40 ± 0.01	64.5 ± 1.0
0.05 M KCl KOH pH 11	1.40 ± 0.01	64.5 ± 1.0
0.05 M KCl HCl pH 2	1.40 ± 0.01	64.5 ± 1.0
NaOH pH 11	1.43 ± 0.01	68.5 ± 0.8

CONCLUSIONS

Concentration of sodium n-dodecyl sulfate (SDDS), presence of electrolyte and the solution pH variation affect significantly bubble motion parameters. The bubble terminal velocity was decreasing with increasing SDDS concentration, from 34.8 ± 0.3 cm/s in distilled water to ca. 15 cm/s at high SDDS concentrations. Lowering the bubble terminal velocity to 15 cm/s means that fluidity of the bubble surface is completely retarded due to formation of the SDDS dynamic adsorption layer. It was found that the minimum SDDS adsorption coverage needed for a complete retardation of fluidity of the rising bubble interface was equal to ca. 10%.

The bubbles detached from the capillary accelerated rapidly in the SDDS solutions and either a maximum was observed (at low SDDS solution concentrations) followed by a period of monotonic decrease or the terminal velocity was attained immediately after the acceleration stage (at high SDDS concentrations). The height and the width of the maximum diminished with increasing SDDS concentration.

An addition of the electrolyte and/or the pH variation caused significant diminishing of the bubble velocity in the SDDS solutions. It was shown that the influence of electrolyte and pH on the bubble velocity variation was caused by lowering the surface tension of the SDDS solutions. The electrolyte presence means that at an identical SDDS bulk concentration the solution surface tension is lowered. A lower surface tension means a greater SDDS adsorption coverage over the interface of rising bubble and a greater retardation of the bubble surface fluidity. Therefore, the bubble local and terminal velocities were lowered in the electrolyte presence.

ACKNOWLEDGMENTS

REFERENCES

ADAMSON A.W., *Physical chemistry of surface*, A Wiley-Interscience Publication, New York, 1990.
AZGOMI F., GOMEZ C.O., FINCH J.A., 2007, *Correspondence of gas holdup and bubble size in presence of different frothers,* Int. J. Miner. Process*.,* 83, 1–11.
CLIFT R., GRACE J.R.,. WEBER M.E, 1978, *Bubbles, Drops and Particles*, Academic Press, 1978
DERJAGUIN B. V., DUKHIN S. S., 1961, *Theory of flotation of small and medium size particles,* Trans. Inst. Mining Metal., **70**, 221–246.
DUKHIN, S.S. KRETZSCHMAR, G. AND MILLER, R., 1995, *Dynamics of adsorption at liquid interfaces*. Theory, Experiments, Application*,* Elsevier, 1995
DUKHIN, S.S. MILLER, R., LOGIO G.(1998), *Physico-chemical hydrodynamics of rising bubble in Drop and Bubbles Interfacial Research* (D. Mobius and R. Miller - Eds.), Elsevier, New York

JACHIMSKA, B. WARSZYNSKI, P., MALYSA K., 2001, *Influence of adsorption kinetics and bubble motion on stability of the foam films formed at n-octanol, n-hexanol and n-butanol solution surface*, Colloids & Surfaces A:, 192, 177–193.

KRZAN M., LUNKENHEIMER K., MALYSA K., 2004, *On the influence of the surfactant's polar group on the local and terminal velocities of bubbles*, Colloid & Surfaces A:, 250, 431–441.

KRZAN M., MALYSA K., 2002a, *Profiles of local velocities of bubbles in n-butanol, n-hexanol and n-nonanol solutions*,Colloids & Surfaces A:, 207, 279–291.

KRZAN M., MALYSA K., *2002b, Influence of frother concentration on bubble dimension and rising velocities*, Physicochem. Problems Mineral Process., 36, 65–76.

KRZAN M.,. ZAWALA J,. MALYSA K., 2007a, *Development of steady state adsorption distribution over interface of a bubble rising in solutions of n-alkanols (C$_5$, C$_8$) and n-alcyltrimethylammonium bromides (C$_8$, C$_{12}$, C$_{16}$)*, Colloids & Surfaces A:, 298, 42–51.

KRZAN M., ZAWALA J., MALYSA K., 2007b, *Dynamic structure of adsorption layer over interface of bubble rising in protein solutions I*nternational Scientific Conference SURUZ *Surfactants and Dispersed Systems in Theory and Practice,* Książe k/Wałbrzycha, May 22–25, *2007*, ISBN 83-7076-125-9, p. 91–95.

KULKARNI, A.A., JOSHI, J.B. 2005, *Bubble Formation and Bubble Rise Velocity in Gas-Liquid Systems: A Review,* Ind. Eng. Chem. Res., 44, 5873–5931.

LASKOWSKI J., 1998, *Frothers and Frothing in Frothing in Flotation - II.* (J.Laskowski and E.T.Woodburn - Eds.), Gordon and Breach Publishers, chap.1

LEJA J., (1982), *Chemistry of Froth Flotation.*, Plenum Press, New York and London

LEVICH, V.G., 1962, *Hydrodymanics,* Prentice-Hall, Englewood Clifts

MALYSA K., KRASOWSKA M., KRZAN M., 2005, *Influence of surface active substances on bubble motion and collision with various interfaces*, Advances in Colloid and Interface Science, 114–115C: 205–225.

RALSTON J., DUKHIN S.S., 1999, *The interaction between particles and bubble*s, Colloids & Surfaces A:, 151**,** 3–14.

SAM A., GOMEZ C.O., FINCH J.A., 1996, *Axial velocity profiles of single bubbles in water/frother solutions*, Int. J. Miner. Processing*,* 47, 177–196.

SCHIMMOLER B.K., LUTRELL G.H., YOON R-H., 1993, *A combined hydrodynamic-surface force model for bubble- particle collection,* XVIII Int. Miner. Process. Congress., **3**, 751–756.

WARSZYNSKI, P., BARZYK W., Lunkenheimer K., Fruhner, H., 1998a, *Surface tension and surface potential of Na n-Dodecyl Sulfate at the air-solution interface: Model and experiment*, J. Phys. Chem. B., 102, 10948–10957.

WARSZYNSKI, P., LUNKENHEIMER K., CICHOCKI G., 2002, *Effect of counterions on the adsorption of ionic surfactants at fluid-fluid interfaces,* Langmuir, 18, 2506–2514.

WARSZYNSKI, P., WANTKE, K.-D., FRUHNER, H., 1998b, *Surface elasticity of oscillating spherical interfaces*, Colloids & Surfaces A:, 139, 137–153.

Krzan M., Małysa K., *Wpływ pH roztworu oraz obecności elektrolitów na prędkości pęcherzyków gazowych w roztworach wodnych anionowych związków powierzchniowo aktywnych* Physicochemical Problems of Mineral Processing, 43 (2009), 43–58 (w jęz. ang)

Wyznaczono profile prędkości lokalnych oraz zmiany prędkości granicznych pęcherzyków powietrza w roztworach n-dodecylosiarczanu sodu (SDDS) o różnych stężeniach, w obecności różnych elektrolitów (NaCl i KCl) oraz przy różnych pH roztworów. Stwierdzono, że przy niskich stężeniach SDDS pęcherzyki po oderwaniu od kapilary zaczynają wypływać z dużym przyspieszeniem początkowym i osiągają maksimum, po którym występuje etap zmniejszenia prędkości, aż do osiągnięcia stałej wartości granicznej. W

wysokich stężeniach przyspieszenie było niższe, a prędkości graniczne ustalały się bezpośrednio po etapie przyspieszenia – nie występowało maksimum. Stwierdzono, że dodatek elektrolitów do badanych roztworów oraz zmiany pH roztworów powodują drastyczne zmniejszenie prędkości lokalnych przy niskich stężeniach SDDS i obniżenie prędkości granicznej aż do wartości charakterystycznej dla wysokich stężeń SDDS. Zjawisko to związane było jest ze znacznym obniżeniem napięcia powierzchniowego w roztworach po dodaniu elektrolitu oraz po zmianie pH.

słowa kluczowe: n-dodecylosiarczan sodowy SDDS, pęcherzyk gazowy, napięcie powierzchniowe, pokrycie adsorpcyjne, prędkość, ruchliwość powierzchni, kinetyka adsorpcji, dynamiczna struktura warstwy adsorpcyjnej.

L. Kushakova*, A. Muszer**

OPTIMISATION OF ROASTING OF ARSENIC-CARBON REFRACTORY GOLD ORES FOR CYANIDE LEACHING

To optimize the technology for Bakyrchik deposit gold ore processing according to roasting - cyanidation pattern, the researches on sorption properties and the influence of carbon-bearing minerals content in calcine on gold recovery have been carried out. The results of conducted investigations showed that sorption properties of coal - Au concentrate during roasting process change even at relatively high residual carbon content in the calcine. Chemical sorption, dominating in gold-bearing solutions contact with coal concentrate, changes into physical sorption after its roasting. Roasting was applied in order to liberate noble metals, to produce the calcine with porous structure, unaffected by processes of surface melting and sintering.

key words: carbon-bearing minerals, sorption, gold recovery, roasting-cyanidation process, carbon in pulp, arsenic-carbon gold-bearing ores

INTRODUCTION

Bakyrchik deposit located in East Kazakhstan is one of the largest in the world gold ore deposits (Komarov, Tomson 2007; Yakubchuk 2004). Difficulties in processing of Bakyrchik ores are caused by extremely fine dissemination of gold in arsenopyrite and pyrite and by the presence of active carbon agent having high sorption capacity with respect to gold-cyanide complex.

---

* The Eastern Mining and Metallurgical Research Institute for Non-ferrous Metals, Ust-Kamenogorsk, Kazakhstan

** University of Wrocław, Institute of Geological Sciences, Pl. Maksa Borna 9, 50-204 Wrocław, Poland, antoni.muszer@ing.uni.wroc.pl

Decomposition of iron sulphides (arsenopyrite and pyrite) can be effectively carried out using either pressure and bacterial leaching or different types of roasting. However, in most cases it does not always provide high gold recovery in the following cyanide leaching of solid residues or calcines because of high content of sorption-active (pregg - robbing) carbon agent (Fridman, Savari 1985; Ibrado, Fuerstenau 1992: Sobel et al. 1995; Lodeischikov 1999; Tretbar 2004, Lars et al. 2007). Carbon removal at the step of enrichment is usually connected with considerable decrease in gold recovery (from 88–90 to 70%).

The highest gold recovery was observed during pilot plant tests to process Bakyrchik gold-bearing concentrates. Bacterial leaching (with recovery of 68–80%) and oxidizing roasting (with recovery of 78–84%) were used in the tests.

Gold recovery might be increased without gold losses at the enrichment step. To process finely ground ore directly, the use of oxidizing roasting process might be recommended as an alternative.

EXPERIMENTAL

Laboratory investigations for development of roasting technology for carbon, arsenic and sulfur removal, were initially carried out in Kazakhstan (VNIItsvetmet). Subsequently, pilot plant tests were performed by "FFE Minerals" company (USA) using Waelz kiln with the length of 4.5 m and the diameter of 0.3 m (Trancoso et al., 2006).

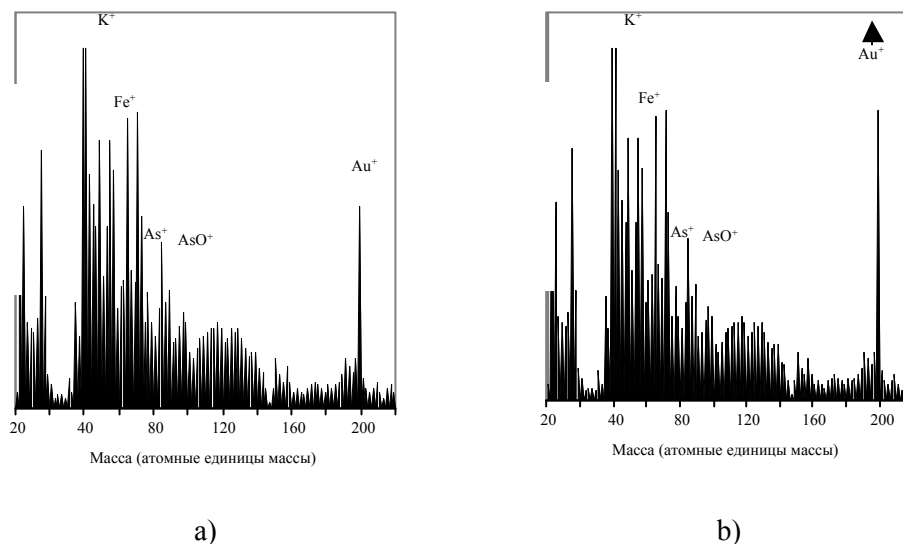a)   b)

Fig. 1. Surface spectrum of calcine carbon agent (a) and calcine leaching residue (b).

In the course of pilot tests, the process parameters were changed, in which there was the variation of material retention time in the kiln (1–4 hours), ore grain size (1, 2, 5 mm), temperature (650–790°C), oxygen partial pressure in different areas of the kiln, carbon residual content in calcine was from 0.2 to 0.99%.

It was found that carbon‑bearing agent, not removed during roasting, was impregnated into quartz. Subsequent grinding of calcine before leaching exposed the surface of carbon agent. Consequently, the calcined material sorbed gold from cyanide solutions. To determine gold concentration directly on carbon agent particles the method of TOF-RIMS was used. Figure 1 exhibits the results of analysis.

From data presented in Figure 1 it can be found that gold concentration in surface layer (thickness – 7 nm) of calcine carbon agent was 14.8 ppm before cyanide leaching and increased to 100 ppm – after gold leaching. Examinations of cyanide leaching of calcines indicated that decrease in carbon content in calcine not always results in increase of gold recovery into the cyanide solution.

RESULTS AND DISCUSSION

To determine the effect of carbon content in calcine on gold recovery in leaching and for technology parameters optimization, the series of experiments were carried out. Experiments on differential thermal analysis (TGA/DTA) of ore samples and ore coal concentrate were conducted on thermoanalyzer "Rigaku Denki" in air atmosphere with heating rate of 20 °C/min (Figure 2, 3). Maximum heating temperature was 1000 °C.

Temperature interval, accompanied by DTA effect, was 430 – 770 °C. In the established temperature interval DTA has two maximum exothermic effects overlaid on each other at 496 and 615 °C. Loss of a portion of weight was found to be 7.4 %. It is supposed that heat release is connected with oxidation of pyrite and arsenopyrite sulfur in a sample. The second significant exothermic effect begins at the temperature of 550 °C and continues up to approximately 800 °C. This second peak is probably appearing as a result of carbon oxidation.

Temperature range, accompanied by DTA effect, while analyzing coal concentrate is 430–830°C. In the examined temperature interval there is one big exothermic effect detected with the maximum at 540°C. Loss of portion weight was determined to be 21.0%.

Therefore, TGA/DTA data show that for complete carbon burning-out from the ore the rise of ore roasting temperature is necessary. It was found, that maximum porous calcines were formed at temperatures 600–700°C. Taking into account that during roasting phase changes of carbon precede its burning-out and different carbon modifications possess markedly various sorption properties. There were conducted examinations of gold sorption using unroasted and roasted coal flotation concentrate of Ba-

kyrchik ore. Chemical analysis results of examined samples are presented in the Tab. 1.
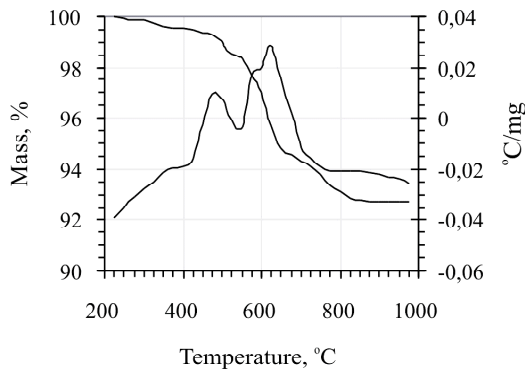
Fig. 2. TGA/DTA analysis of gold-bearing ore.
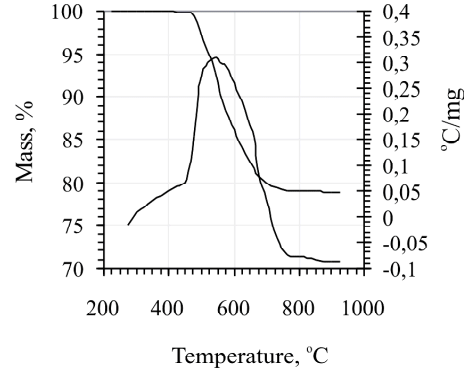
Fig. 3. TGA/DTA analysis of coal concentrate of gold-bearing ore enrichment.

Table 1. Chemical analyses of gold-bearing coal concentrate.

Sample	Content					
	Au, g/Mg	As, %	Fe, %	S, %	C, %	Ca, %
Coal concentrate, raw	42.3	4.30	10.5	7.87	14.70	1.10
Coal concentrate, calcine (650 °C, 3.5 hours)	58.0	1.26	12.3	0.92	2.05	1.35

Sorption capacity and samples sorption isotherms at different temperatures were determined using artificially prepared gold-cyanide solutions (20–150 mg/dm^3 Au, 0.03 % NaCN). Samples of coal concentrate and coal concentrate calcine were agitated in closed bottles for 24 hours in gold-cyanide solutions of different gold concentration.

After analysis of both solutions and solid products on gold content in experiments with coal concentrate sorption isotherms were determined (Figure 4). Moreover, the process activation energy was calculated to be 124 kJ/mole. Coal concentrate sorption capacity increased with the rise of temperature and at the temperature of 75 °C it achieved 2380 g/Mg.

The experiments performed with calcine coal concentrate showed that concentrate calcine contact with gold-bearing solutions resulted in decrease of gold content in solids from 58 g/Mg (initial content) up to 45–11 g/Mg and practically was not dependent on gold initial concentration in solutions (10–150 mg/dm^3). At temperature rise the content of gold in solid products was reduced (Figure 5). It was connected with the decrease of their sorption capacity and the increase of leaching rate, that evidently

took place in spite of cyanide low concentration (0.03 %). Calculated activation energy of the process amounted to 47 kJ/mole.
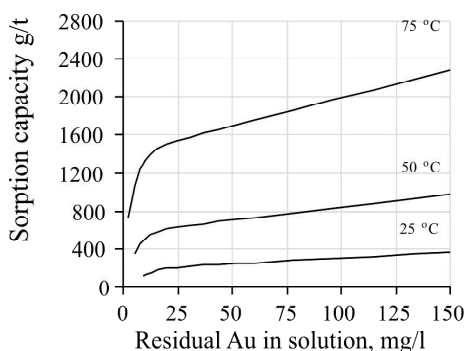
Fig. 4. Isothermal curves of gold sorption using coal concentrate.
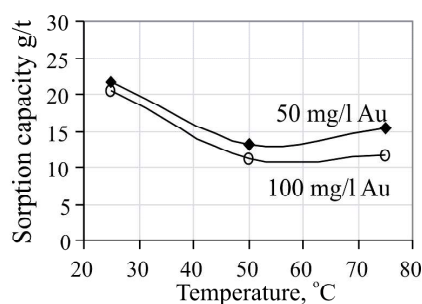
Fig. 5. Temperature dependence of coal concentrate sorption capacity.

CONCLUSIONS

The results of conducted investigations showed that sorption properties of coal - Au concentrate during roasting process change even at relatively high residual carbon content in the calcine. Chemical sorption, dominating in gold-bearing solutions contact with coal concentrate, changes into physical sorption after its roasting. As far as physical sorption, in contrast to chemical sorption, is a reversible process, in order to reduce gold sorption property on calcine carbon agent, the consumption of absorbent coal into cyanidation pulp might be increased, that was confirmed by pilot test processing results.

Roasting was applied to provide maximum liberation of noble metals, production of calcine with porous structure, unaffected by processes of surface melting and sintering. Optimum burning - out ratio of carbon for every batch of ore shall be determined by results of calcine testing on gold recovery in the process of cyanide leaching by "coal in pulp" technology.

REFERENCES

FRIDMAN I.D., SAVARI Y.Y., 1985. *Study of sorption properties of carbon-bearing components of gold-arsenic ores.* Non-ferrous metals, 4. 99–101.

IBRADO A. S., FUERSTENAU D. W., 1992. *Effect of the Structure of Carbon Adsorbents on the Adsorption of Gold Cyanide*, Hydrometallurgy, 30, 243–256, Elsevier Science Publishers.

KOMAROV P.V,. TOMSON I.N., 2007. *Plumes and their influence on the formation of noble metal mineralization in carbonaceous rocks*. Doklady Earth Sciences. V. 415, 6. 779–781.

LARS D. HYLANDER L.D., PLATH D., MIRANDA C.R., LÜCKE S., ÖHLANDER J.,. RIVERA
    A.T.F., 2007. *Comparison of Different Gold Recovery Methods with Regard to Pollution Control
    and Efficiency*. Clean 2007, 35 (1), 52 – 61

LODEISCHIKOV V.V., 1999. *Technology to recover gold and silver from hard-to-dress ores. 2 Volumes*.- Irkutsk. V.1 - 342 p., V.2 – 452p.

SOBEL, K.E.; BOLINSKI, L., FOO, K.A., 1995. *Pilot plant evaluation of the redox process for bakyrchik gold p*lc. Minerals Engineering. V. 8, Issue: 4–5, 431–440.

TRETBAR D., 2004. *Preg-robbing carbon in processing of gold-bearing ores: Definitions, analytical
    methodology and characterization.* Rocky Mountain (56th Annual) and Cordilleran (100th Annual)
    Joint Meeting.

TRANCOSO H., USHAKOV N.N., SAPRYGIN A.F., KUSHAKOVA L.B., 2006. *Causes and ways to
    decrease gold losses during cyanidation of arsenic-carbon gold-bearing ores roasting products.*
    Non-ferrous metals. 5. 29–31.

YAKUBCHUK A., 2004. *Architecture and mineral deposit settings of the Altaid orogenic collage: a
    revised model*. Journal of Asian Earth Sciences 23. 761–779.

Kushakova L., Muszer A., *Optymalizacja przeróbki złotonośnych rud arsenowo-węglowych na drodze
prażenia i cyjankowania.* Physicochemical Problems of Mineral Processing, 43 (2009), 59–64 (w jęz.
ang)

Złoże Bakyrchik, leżące we Wschodnim Kazachstanie, jest jednym z największych złóż złotonośnych
w świecie. Ruda złota charakteryzuje się występowaniem bardzo drobno rozproszonego złota w arsenopi-
rycie i pirycie wraz z substancją węglistą, posiadającą wysoką zdolność sorpcyjną w odniesieniu do kom-
pleksów cyjankowych złota. Głównym celem badań było określenie możliwości pozbycia się z rudy sub-
stancji nieużytecznych, tj. węgla oraz związków arsenu w celu uwolnienia złota, a następnie jego wyłu-
gowania. Przeprowadzone badania DTA wykazały, że najkorzystniejszy ubytek masy w trakcie prażenia
materiału poddanego eksperymentom zachodzi przy temperaturze 540°C (najlepszy efekt egzotermiczny).
Po analizie roztworów i produktów stałych w eksperymentach z węglowym koncentratem wykreślono
izotermy sorpcji i obliczono energię aktywacji procesu, która wynosi 124 kJ/mol. Sorpcyjna pojemność
analizowanego węglowego koncentratu powiększała się wraz ze wzrostem temperatury procesu i osiągnę-
ła 2380 g/Mg w temperaturze 75°C. Rezultaty przeprowadzonych badań pokazały, że sorpcyjne właści-
wości rudy złotonośnej, zawierającej znaczne ilości substancji węglistej, zmieniają się w trakcie procesu
jej wypalania. Chemiczna sorpcja przeważająca w procesie eksperymentu, po wypaleniu rudy zmienia się
na fizyczną. Ponieważ fizyczna sorpcja, w odróżnieniu od chemicznej, jest procesem odwracalnym, moż-
na obniżyć sorpcyjność złota na węglowej substancji powiększając aktywność węgla w procesie cyjan-
kowania. Prażenie rudy złota powinno spowodować jak najlepsze uwolnienie metali szlachetnych, po-
wstanie porowatej struktury, nie zniszczonej w wyniku topienia i spiekania. Optymalny stopień wypalenia
węgla dla każdej partii rudy powinien być poprzedzony eksperymentami, których celem musi być mak-
symalne odzyskanie złota w procesie ługowania cyjankowego "coal in pulp".

*słowa kluczowe: rudy Au trudnowzbogacalne, rudy złota, arsenki Au-nośne, sorpcja, złoto drobnody-
spersyjne, procesy cyjanowania, złoże Bakyrchik,*

P. Maciejewski*, M. Żuber*, M. Ulewicz**, K. Sobianowska***

REMOVAL OF RADIOISOTOPES FROM WASTE WATER AFTER "DIRTY BOMB" DECONTAMINATION

An adequate response to terrorist event of any magnitude requires the effective coordination of many organizations. A terrorist event involves the release and dispersion of radioactive material among civilian population or over vital area causes a permanent radioactive contamination, which should be removed in decontamination process. Finally, after this procedure, a large amount of radioactive waste water is made, which should be collected and stored in a special nuclear waste stockpile. We present results of experimental work, which was focused on removal of radioactive substances from waste water from decontamination process after using "dirty bomb". The ion flotation process was used to remove radioisotopes from slightly salty ($<1.0 \cdot 10^{-3}$ mol/dm^3) aqueous solutions. Multistage ion flotation and fractionation of concentrate from the ion flotation process using appropriate lariat ethers as collectors allowed separation of radioisotopes, which might have a practical usage for the decontamination of radioactive waste aqueous solutions.

key words: ions flotation, Cs-137, Sr-85, Ba-133, Co-60,Pb-212, proton-ionizable crown ether

INTRODUCTION

The threat of radiation event as a result of terrorist activity has recently arisen, and a "dirty bomb" seems to be excellent "psychological" weapon to cause the ensuing panic and psychological distress. In the "dirty bomb" conventional explosives are linked to a radioactive source with the intention of dispersing radioactive particles.

----

   * The Tadeusz Kosciuszko Land Forces Military Academy, ul. Czajkowskiego 109, 51-150 Wrocław, Pawel.Maciejewski@tedc.nato.int

  ** Czestochowa University of Techology, ul. J.H. Dąbrowskiego 69, 42-200 Częstochowa

*** Wrocław University of Techology, Wyb. Wyspiańskiego 27, 50-370 Wrocław

Sealed medical and industrial sources, such as cobalt-60, cesium-137, strontium-90, and iridium-192, could be targets for terrorists (Tintinalli, 2004). A terrorist event involves the release and dispersion of radioactive material among civilian population or over vital area causes a permanent radioactive contamination, which should be removed in decontamination process. Finally, after this procedure, a large amount of radioactive waste water is made, which should be collected and stored in a special nuclear waste stockpile. The ion flotation process seems to be excellent for this task as that it is a simple and effective method for removal and separation of metals ions from dilute aqueous solutions ($c < 1.0 \ 10^{-4}$ mol/dm^3). In this process, an ionic surface active compound (collector) is introduced to the aqueous solution to transport non-surface active colligent of the opposite charge from a bulk aqueous solution to the interface of solution and vapour. Counter ions must be co-adsorbed to neutralize the charge. If a sufficiently large aqueous solution/gas interface is provided by sparging gas through the solution, the colligend ions can be concentrated and removed along with the collector in a foam phase. The most important fact is that the radioactive substances are collected in a separate container.

We now present results of experimental work, which was focused on removal of radioactive substances from waste water from decontamination process after using "dirty bomb" in the ion flotation process.
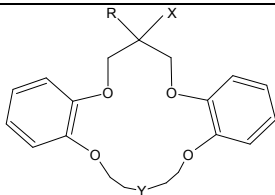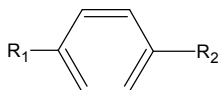

MACROCYCLIC COMPOUNDS IN ION FLOTATION

Since the discovery of the first crown ether in 1967 by Pedersen the, i.e. dibenzo-18-crown-6, the macrocyclic compounds hold great interest and potential. They have applied successfully for many metal ion separations in solvent extraction, transport across liquid membranes, and ion-exchange systems (Bond et al., 1999; Bartsch, Way, 1996; Nghiem et al., 2006; Ulewicz et al., 2006). The recent advances of the crown ethers chemistry have been reviewed (Ludwig; 2000; Alexandratos, Stine, 2004; Robak et al., 2006; Maciejewski et al., 2008). There are only few papers which deal with application of macrocycles in the ion flotation process. Koide et al. (1996) used phosphate ethers of C-undecylcalix(4)resorcinarenes for uranium flotation from seawater and calyx(4)arenes derivatives for alkali metal cations flotation (1993). Schulz and Warr (1998) applied cryptand 222, and 18-crown-6 together with anionic surfactant, i.e. bis (2,2')-ethylhexylsulfosuccinate (AOT) for alkali metal cations separation. Another approach to application of macrocycles for flotation of metal cations was done by Charewicz et al. (2001). They used the macrocycles proton-ionizable lariat ethers with sulphonic, phosphate and carboxylic acid groups for flotation of Sr^{2+} and Cs^+ cations. Ulewicz et al. (2003, 2006) used proton-ionizable lariat ethers with foaming agent for flotation of Zn(II) and Cd(II) ions from aqueous solutions. Maciejewski and Walkowiak (2004) studied selective removal of Cs(I), Sr(II) and Ba(II) cations with proton-ionizable lariat ethers in the ion flotation process.

EXPERIMENTAL SECTION

Reagents. The aqueous solutions were prepared with doubly distilled water of 5 μS/m conductivity at 25 °C. Analytical grade inorganic compounds: $NaNO_3$, HNO_3, $NH_3 \cdot H_2O$, were obtained from POCh (Gliwice, Poland). The nonionic foaming agent - octylphenylodecyl (ethylene glycol) ether (Triton X-100) was from Merck. As the collectors 6 lariat ethers possessing cavities from DB-16-C-5 to DB-22-C-7 and different acidic groups, i.e. sulphonamide and sulfonic were used (from prof. Bartsch, R.A., Department of Chemistry and Biochemistry, Texas Tech University, Lubbock, USA, see Tab.1). The lariat ethers were added as ethanol solutions. The gamma-radioactive isotopes, i.e. Cs-137, Sr-85 and Co-60 were purchased from the Atomic Energy Institute (Swierk/Otwock, Poland), Ba-133 and Pb-212 from Institute of Nuclear Chemistry and Technology (Warsaw, Poland). They were of sufficiently high specific activity to neglect the effect of carrier concentration.

Table 1. List of lariat ethers and nonionic foaming agent

Structure	Crown	R	X	No. ether
R, X structure (DB crown ether)	DB16C5	$-C_{10}H_{21}$	$-OCH_2CONHSO_2CF_3$	1
			$-O(CH_2)_3SO_3Na$	2
	DB19C6	$-C_{10}H_{21}$	$-OCH_2CONHSO_2CF_3$	3
	DB22C7	$-C_7H_{15}$	$-O(CH_2)_3SO_3Na$	4
		$-C_4H_9$	$-OCH_2CONHSO_2CF_3$	5
		$-C_{10}H_{21}$		6
R_1 — benzene — R_2	$R_1 = -C_8H_{17}$ $R_2 = -O(CH_2CH_2O)_{10}H$	Triton X-100 (eter oktylofenylodekaetylenoglikolowy)		7

Ion Flotation Procedure. The flotation experiments have been carried out in ambient temperature (20 ± 2°C) in a glass column 45.7 cm in height and 2.4 cm in diameter. The argon gas was saturated with water, and the flow rate was maintained at 12 mL/min through a sintered glass sparger of 20–30 μm nominal porosity. The initial volume of each feed solution was 100 mL and contained aqueous solutions of Cs-137, Sr-90, Ba-133, Co-60 and Pb-212 radioisotopes (at $1.0 \cdot 10^{-8}$ mol/dm³ concentration), and $NaNO_3$ as the source of foreign cations (at $1.0 \cdot 10^{-3}$ mol/dm³ concentration). The single and multi channel, gamma radiation spectrometers were used as the detectors of radiation intensity of specific energy.

The percent of decontamination was calculated by the equation:

$$D = (1 - A_r / A_i) \cdot 100\% \tag{1}$$

where A_i, A_r – initial and residual gamma radiation intensity of solution, Bq/dm^3.
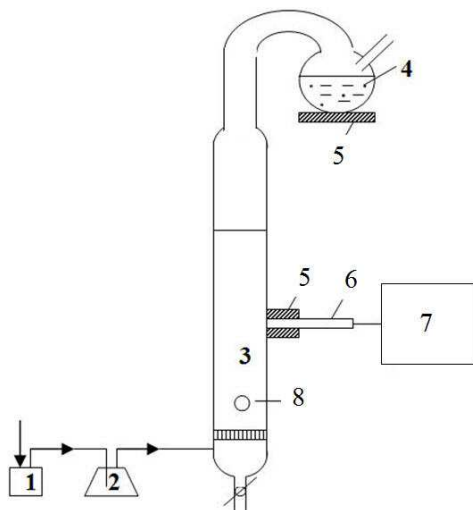
Fig. 1. Scheme of ion flotation apparatus
1 – gas flow and pressure meter,
2 – humidifier,
3 – flotation column,
4 – foam receiver,
5 – lead screen,
6 – spectrometric scintillation probe,
7 – gamma radiation spectrometer with computer,
8 – injection capable valve (for collector).

RESULTS AND DISCUSSION

RADIATION RESISTANCE OF LARIAT ETHERS

An important parameter for flotation of metal ions from radioactive waste aqueous solutions is a radiation resistance of lariat ethers. The radiation resistance of two lariat ethers (1, 2) using Cs-137 source was measured. The lariat ethers after exposition (dose from 0.1 to 10 Gy) were examined for Cs-137 ($1.0 \cdot 10^{-8}$ mol/dm^3). The percent decontamination of Cs-137 for 1 and 2 after exposition is at the same level as before radiation, so the lariat ethers have enough radiation resistance and can be used for ion flotation of radioactive cations.

SELECTIVE FLOTATION OF CS-137, SR-90, BA-133, CO-60 AND PB-212 RADIOISOTOPES

The ion flotation process was applied for selective removal of Cs-137, Sr-90, Ba-133, Co-60 and Pb-212 radioisotopes, which could be consider as radioactive waste water from decontamination. The aqueous solutions contained Cs-137, Sr-90, Ba-133, Co-60 and Pb-212 radioisotopes (at $1.0 \cdot 10^{-8}$ mol/dm^3 concentration) and NaNO$_3$ as the source of foreign cations (at $1.0 \cdot 10^{-3}$ mol/dm^3 concentration).

The preliminary flotation experiments with the addition of $NaNO_3$ as the source of foreign cations indicated reduction of all radioisotopes removal. When the concentration of $NaNO_3$ was higher than $1.0 \cdot 10^{-3}$ mol/dm³, the removal of radioisotopes was very low. The experiments were performed also at the various initial concentrations of lariat ethers and pH values.
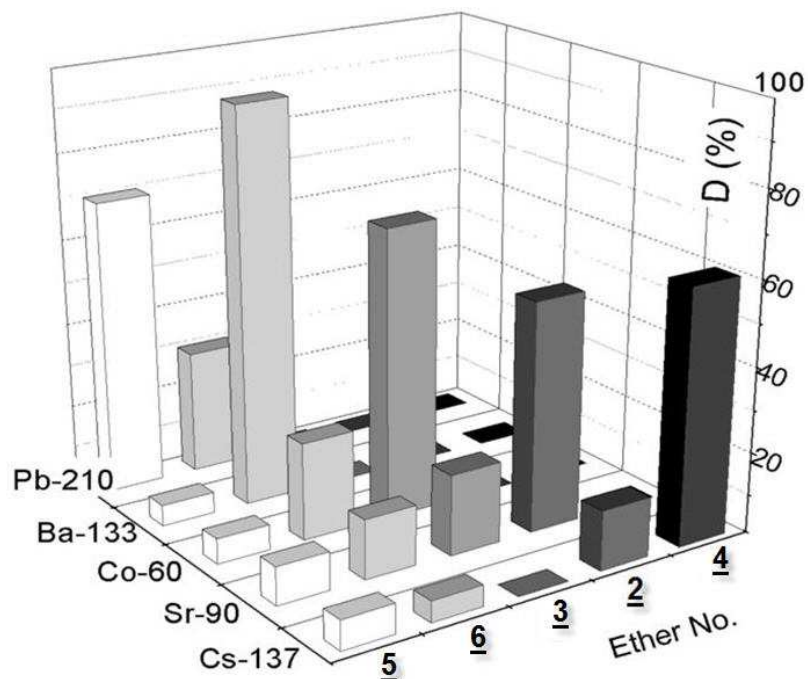
Fig. 2. The selective flotation of Cs-137, Sr-90, Ba-133, Co-60 and Pb-212 with lariat ethers: **5**, **6**, **3**, **2** and **4** at $1.0 \cdot 10^{-8}$ mol/dm³ initial concentration and in the presence of nonionic foaming agent **7** from aqueous solutions containing $NaNO_3$ ($1.0 \cdot 10^{-3}$ mol/dm³), [Lariat ether] = [**7**] = $1.0 \cdot 10^{-5}$ mol/dm³

In the Figure 2, there are results for competitive flotation of Cs-137, Sr-90, Ba-133, Co-60 and Pb-212 radioisotopes with appropriate proton-ionizable lariat ethers from dilute, slightly salty ([$NaNO_3$] = $1.0 \cdot 10^{-3}$ mol/dm³) aqueous solutions. The studied cations have different ionic radius and ionic potential, which allow separation of mentioned cations from dilute aqueous solutions with using 5 lariat ethers possessing DB-16-C-5 cavity and different liphofilic (from butyl to decyl) and acidic groups, i.e. sulfonamide (i.e. **1**, **3**, **5**, **6**) and sulfonic (**2**, **4**) (Ulewicz et. al., 2006a). As it can be seen in this Figure, five stages of ion flotation and concentrate fractionation of the ion flotation process with appropriate lariat ethers as collectors (i.e. **5**, **6**, **3**, **2**, **4**) allow separation of radioisotopes in the order: Pb-212 > Ba-133 > Sr-85 > Co-60 > Cs-137. A multistage ion flotation means that in one experiment the same feed solution is floated with using a proper collector in a correct sequence. Each stage was started with injec-

tion of a new portion of collector ($<1.0 \cdot 10^{-5}$ mol/dm^3) which was injected through valve 8 (see Figure 1) and the stage was finished when it was stopped floating. One stage took about 5 minutes and there was a small amount of foam ($< 0,5$ g), which means that the enrichment ratio of radioisotope in foam is high. The competitive ion flotation of radioisotopes was fast and after 30 minutes final removal was reached, which might have a practical usage for the decontamination of radioactive, slightly salty ($<1.0 \cdot 10^{-3}$ mol/dm^3), waste aqueous solutions.

CONCLUSIONS

Proton-ionizable crown ethers with sufficient surface activity and water solubility seem to be the new generation of collectors for flotation of Cs^+, Sr^{2+}, Ba^{2+} and Pb^{2+} cations from dilute aqueous solutions.

The lariat ethers have enough radiation resistance so they can be used for ion flotation of radioactive isotopes.

The ion flotation process allows the efficient decontamination of slightly salty ($<1.0 \cdot 10^{-3}$ mol/dm^3) aqueous solutions containing Co-60, Sr-85, Ba-133, Cs-137 and Pb-212 isotopes. Multistage ion flotation and fractionation of concentrate from the ion flotation process using appropriate lariat ethers as collectors allowed us to separate radioisotopes with selectivity decreasing in the order: Pb-212 > Ba-133 > Sr-85 > Co-60 > Cs-137. The competitive ion flotation of radioisotopes is fast, with final removal reached in just 30 minutes, which might have a practical usage for the decontamination of radioactive waste aqueous solutions.

REFERENCES

ALEXANDRATOS, S.D., STINE, CH.L. (2004) *Synthesis of ion-selective polymer-supported crown ethers: a review,* Reactive & Functional Polymers, Vol. 60, pp.3–16.

BARTSCH, R. A., WAY, J. D., (eds.) (1996) *Chemical Separations with Liquid Membranes*, ACS Symposium Series 642, Washington, DC.

BOND, H., DIETZ, M.L., ROGERS, R.D. (eds.) (1999) *Metal-Ion Separation and Preconcentration*, Progress and Opportunities, ACS Symposium Series 716, Washington, DC.

CHAREWICZ, W., GRABOWSKA J., BARTSCH, R.A. (2001) *Flotation of Co(II), Sr(II), and Cs(I) cations with proton-ionizable lariat ethers*, Sep. Sci. Technol., Vol. 36, pp.1479–1494.

KOIDE, Y., OKA, T., IMAMURA, A., SHOSENJI, H., YAMADA, K. (1993) *The selective flotation of cesium ion with resorcinol type calyx(4)arenes with alkyl side chains*, Bull. Chem. Soc. Jpn., Vol. 66, pp. 2137–2132.

KOIDE, Y., TERASAKI, H., SATO, S., SHOSENJI, H., YAMADA, K. (1996) *Flotation of uranium from sea water with phosphate ethers of C-undecylcalix(4)resorcinaren'e,* Bull. Chem. Soc. Jpn., Vol. 69, pp. 785–790.

LUDWIG, R. (2000) *Foam separation*, Fresenius J. Anal. Chem., Vol. 367, pp. 103–128.

MACIEJEWSKI, P., WALKOWIAK, W. (2004) *Selective removal of cesium(I), strontium(II) and barium(II) cations with proton-ionizable lariat ethers in the ion flotation process,* Physicochemical

Problems of Mineral Processing, 38, 139–146.

MACIEJEWSKI, P., ROBAK, W., ULEWICZ, M., SOBIANOWSKA, K. (2008) *Zastosowanie związków makrocyklicznych do usuwania toksycznych kationów metali z roztworów wodnych w procesie flotacji jonowej*, Zeszyty naukowe WSOWLąd, 1(147), 113–125.

NGHIEM, L.D., MORNANE, P., POTTER, I.D., PERERA, J.M., CATTALL, R.W., KOLEV, S.D. (2006) *Extraction and transport of metal ions and small organic compounds using polymer inclusion membranes (PIMs), J. Membrane Sci*., Vol. 281, pp.7–41.

PEDERSEN, C.J., 1967, *Cyclic polyethers and their complex with metal salts*, J. Am. Chem. Soc., Vol. 89, pp. 7017–7036.

ROBAK, W., APOSTOLUK, W., MACIEJEWSKI, P. (2006), *Analysis of liquid-liquid distribution constans of nonionizable crown ethers and their derivetives*, Anal. Chim. Acta, Vol. 569, pp.119–131.

SCHULZ, C., WARR, G.G. (1998) *Comparison of variables in ion and precipitate flotation*, Ind. Eng. Chem. Res., Vol. 37, pp.2807–2809.

TINTINALLI, J.E. (2004) *Emergency medicine*, 6. Edition McGraw-Hill, New York.

ULEWICZ, M., WALKOWIAK, W., BARTSCH, R.A. (2006a) *Ion flotation of zinc(II) and cadmium(II) with proton-ionizable lariat ethers. Effect of cavity size,* Sep. Purif. Technol., Vol. 48, pp. 264–269.

ULEWICZ, M., LESINSKA, U., BOCHENSKA, M., WALKOWIAK, W. (2006b) *Facilitated transport of Zn(II), Cd(II) and Pb(II) ions through polymer inclusion membranes with calyx(4)-crown-6 derivatives,* Sep. Purif. Technol.

ULEWICZ, M., WALKOWIAK, W., JANG, Y., KIM, J.S., BARTSCH, R.A. (2003) *Ion flotation of cadmium(II) and zinc(II) in the presence of proton–ionizable lariat ethers,* Anal.Chem., Vol. 75, pp. 2276–2279.

Zbadano selektywne wydzielanie radioizotopów: Pb-212, Ba-133, Sr-85, Co-60 i Cs-137, z rozcieńczonych, zasolonych $NaNO_3$ $(1.0 \cdot 10^{-3}$ M) roztworów wodnych z użyciem nowej grupy związków makrocyklicznych, tj. jonizowanych eterów lariatowych o stężeniu $1 \cdot 10^{-5}$ M w obecności spieniacza niejonowego Tritonu X-100 $(1 \cdot 10^{-5}$ M). Stężenie każdego radioizotopu w mieszaninie wynosiło $1 \cdot 10^{-8}$ M i założenia odpowiadało składem radioaktywnym ściekom po dekontaminacji obiektów po ataku bombą radiologiczną. Zastosowanie frakcjonowania koncentratu podczas flotacji radioaktywnych, zasolonych $NaNO_3$ $(1.0 \cdot 10^{-3}$ M) roztworów wodnych z użyciem odpowiedniej sekwencji jonizowalnych eterów lariatowych $(1 \cdot 10^{-5}$ M) umożliwiła efektywne i selektywne usunięcie radioizotopów z roztworu wodnego. Zbadano również odporność radiacyjną kolektorów, która okazała się wysoka (< 10 Gy), co pozwala na wielokrotne użycie kolektora w procesie flotacji jonowej. Omawiana metoda może być użyta do dekontaminacji toksycznych (radioaktywnych) roztworów wodnych.

słowa kluczowe: flotacja jonowa, Cs-137, Sr-85, Ba-133, Co-60, Pb-212, jonizowalny eter lariatowy

M. Markiewicz*, J. Hupka*, M. Joskowska*, Ch. Jungnickel*

POTENTIAL APPLICATION OF IONIC LIQUIDS IN ALUMINIUM PRODUCTION – ECONOMICAL AND ECOLOGICAL ASSESSMENT

Aluminium is one of the most popular materials in the automotive, plane, ship, food and packaging industries mainly due to its light weight and corrosion resistance. The annual production of this metal is growing by 2 % every year. The aluminium production technology applied in an industry is based on electrodeposition in cryolite in so called Hall–Héroult process. This process is considered very energy consuming and was proven to have considerably high negative environmental impact. However an alternative technology has been suggested in the literature since aluminium deposition has been successfully demonstrated with room temperature ionic liquids (RTILs) based on imidazolium, pyridinium and quaternary ammonium cations with $AlCl_3$ with an efficiency reaching almost 100%. The aim of this paper is to perform a comparison of conventional Hall–Héroult process with new ionic liquid technology taking into account mainly the environmental and economical impact.

As the result of our studies we came to the conclusion that ionic liquid's application in aluminium production presents a very interesting alternative for technologies applied so far in the industry. However care must be taken when introducing ionic liquids to wide-scale use as their environmental impact is not fully acknowledged. In the process of industrial utilization of chemical substances a risk of unintentional release is always present and should be taken into account. Therefore, prior to the implementation of this new technology a full risk assessment, including potential adverse effects determination and estimation of mobility in all possible environmental compartments, is required.

key words: ionic liquids, aluminium production, global warming potential

* Department of Chemical Technology, Chemical Faculty, Gdansk University of Technology, ul. Narutowicza 11/12, 80-952 Gdansk, Poland Corresponding author, email: cahj@chem.pg.gda.pl, tel: +48583472334, fax: +48583472065

INTRODUCTION

The natural resource for primary aluminium production is bauxite ore. Production involves two main stages: refining of alumina (aluminium oxide) form the ore in the Bayer's process and then reduction of the oxide to metallic aluminium in the Hall-Héroult process. Due to its light weight and corrosion resistance, aluminium is one of the most popular materials in the automotive, plane, ship, food and packaging industries. Worldwide production has been growing continuously by 2% annually for the last 25 years to reach 28.9 kt in 2005 (Gielen 1998; Norgate, Jahanshahi and Rankin 2007). Generally, in the Hall-Héroult process alumina is dissolved in a molten cryolite (Na_3AlF_6) bath at 1000°C from which it is deposited by applying low voltage high electric current across carbon electrodes. In crude aluminium production energy costs is the key factor, as the Hall-Héroult process is known to be highly energy consuming (Gielen 1998). Moreover there are additional costs connected with aluminium production coming from a necessity to comply with environment protection regulations. They can be separated into two streams: first is a gaseous hydrofluoric acid (HF) and volatilized fluorides emission due to a hydrolysis reaction during the electrodeposition process. This can be almost completely prevented by either exchanging moisture bearing oxides for anhydrous ones or removing fluoride containing solvents. Otherwise it can also be decreased by constructing more efficient gas trapping devices. Another environmental issue is the emission of carbon dioxide during the production process. It has been calculated that more CO_2 than aluminium is produced from a mass unit of ore (Welch 1999). Due to these facts, extensive research for a better electrolyte which will allow for aluminium deposition at ambient temperatures and without formation of harmful substances is being conducted by a number of research groups (Yuguang and VanderNoot 1997; Jiang, Brym, Dubé, Lasia and Brisard 2006; Jiang, Brym, Dubé, Lasia and Brisard 2006). Electrodeposition from aqueous solutions is known to be inapplicable due to the aluminium reduction potential and hydrogen formation during the process (Abbott, Eardley, Farley, Griffith and Pratt 2001; Jiang, Brym, Dubé, Lasia and Brisard 2006). Organic solvents such as aromatic hydrocarbons or ethers were introduced as replacements of cryolite but were not considered superior due to their low conductivity, relatively narrow electrochemical window and the risk of self-combustion and potential explosion. Furthermore there are environmental issues connected with volatile organic compounds (VOC's) application in industry as it is estimated that 20 billion kg of VOC's are released to the atmosphere every year (Jiang, et al., 2006; Liu, Abedin and Endres 2006; Beaulieu, Tank and Kopacz 2008). In the 1980s, the application of a new type of solvents – ionic liquids (ILs) in aluminium production industry has been suggested and is continuously investigated up to date (Liu, Abedin and Endres 2006).

IONIC LIQUID'S POTENTIAL APPLICATION IN ALUMINIUM ELECTRODEPOSITION

Ionic liquids have melting points usually below 100ºC due to large non-symmetrical organic cations. If they are substituted in place of cryolite they have a significant potential to reduce the energy consumption of the aluminium production process. Additionally ILs have a remarkably wide electrochemical potential window, often up to 5V. This property makes them particularly suitable for electrodeposition of metals and semiconductors as they do not undergo either oxidation or reduction within the respective potential range (Baker, Baker, Pandey and Bright 2005; Frank. and El. 2006). Other advantages of IL application in aluminium production include: good solvent properties that allow for high concentrations of metals in the electrolyte, low vapour pressure limiting losses and air contamination, and good thermal and chemical stability (Moustafa, Abedin, Shkurankov, Zschippang, Saad, Bund and Endres 2007).

First aluminium electrodeposition from ILs to be reported in literature was the utilization of so-called first generation ILs which are a combination of $AlCl_3$ and organic chlorides (e.g. substituted pyridinium and imidazolium chlorides). The major drawback of those solvents was their hygroscopic nature due to which the whole process had to be conducted under an inert gas atmosphere. Additionally, the pyridinium cation is susceptible to reduction, and thereby it is narrowing electrochemical window of pyridinium based ILs (Jiang, Brym, Dubé, Lasia and Brisard 2006). Research groups attempted to change the anion to a more stable one such as: tetrafluoroborate (BF_4^-) or hexafluorophosphate (PF_6^-). Unfortunately these were proven to release HF after being exposed to the moisture. Third generation ILs – containing more hydrophobic anions, for example: trifluoromethanesulfonate ($CF_3SO_3^-$), bis(trifluoromethylsulfonyl)amide [$(CF_3SO_2)_2N^-$], or tris(trifluoromethanesulfonyl) methide [$(CF_3SO_2)_3C^-$], yield good quality aluminium deposits with no simultaneous solvent decomposition or toxic/dangerous side products evolving during the reaction (Abedin, Moustafa, Hempelmann, Natter and Endres 2005). In addition the conductivity of ILs that can be applied in the Al industry is an order of magnitude lower than that of cryolite, but still higher than that of tetrahydrofuran or toluene (Liu, Yang and Zhang 2004). Albeit the low conductivity the temperature of the process would be two orders of magnitude lower that with cryolite. The electrodeposition of Al from $AlCl_3$ has a cell voltage of 3–3.4V (distance between plates of 10mm). The $AlCl_3$ required for this process is obtained from the chlorination of bauxite in the presence of carbon. The chlorine gas can be recycled from the electrolysis reaction of $AlCl_3$ to metallic Al and Cl_2 (Wu, Reddy and Rogers 2008).

It is commonly believed that ILs, mostly imidazolium and pyridinium based, are promising solvents for aluminium and other metals production on a wide scale. Nevertheless there are still a few problems that need to be solved before their implementation in the industry. Those challenges are mainly: high cost of ILs

tion in the industry. Those challenges are mainly: high cost of ILs production, lower conductivity in comparison to cryolite (Edwards, Taylor, Russell and Maranville 1952) as well as lack of information about their environmental impact and chemical fate (Abbott, Eardley, Farley, Griffith and Pratt 2001; Abedin, Moustafa, Hempelmann, Natter and Endres 2005; Jiang, Brym, Dubé, Lasia and Brisard 2006). A broad range of international programs already exist which aim to protect humans health and the surrounding environment by introducing regulations concerning safe usage and management of chemical substances. The European Commission REACH system (Registration, Evaluation and Authorisation of Chemicals system) and United Nations Agenda 21, are two of the more significant ones, that attempt to gather information about the environmental impact and mobility, toxicity and contamination potential of chemicals used in industrial processes prior to their implementation. This knowledge is needed to provide defined set of information of the properties of chemical substances used and potential risk management strategies (United Nations Department of Economic and Social Affairs 2004; REACH 2007).

ENVIRONMENTAL IMPACT OF CONVENTIONAL ALUMINIUM PRODUCTION

The most significant disadvantage of the conventional Hall-Héroult process is its high energy demand. The theoretical minimum amount of energy required for the reduction of alumina to aluminium based on reaction enthalpy is 29.9 GJ/Mg of Al. However in real industrial aluminium refining processes, depending on the technology applied, 46 – 60 GJ/Mg is required. The high temperatures necessary to keep the cryolite molten is responsible for this large electricity demand. Although since the introduction of the process in 1886 significant improvements in energy efficiency have been made, the continually increasing prices of electricity have not allowed for major cost reductions of the production process (Gielen 1998).

The other important concern is environment pollution. Main air contaminants from aluminium production that might enter the atmosphere are: fluorides, perflourocarbons (PFC), tars, polycyclic aromatic hydrocarbons, sulphur dioxide and other sulphur containing compounds, dust, metal containing compounds, nitrous oxides, and carbon mono- and dioxide. To decrease the melting temperature of a bath the fluoride compound, most often AlF_3, is added in a stoichiometric excess. The higher is the excess of AlF_3 the higher is the emission of fluoride to the atmosphere. Total fluoride formation from electrodeposition processes range from 20 kg to 40 kg of F/Mg of Al, after purification of effluent gases this values decreases to 0.4 kg – 1.0 kg of F/Mg of Al. Another dangerous substances evolved during electrodeposition process are perflourocarbons, mainly tertafluoromethane and hexafluoroethane produced in a 10:1 ratio. Once produced, they cannot be removed from the gas stream by available tech-

nologies and their estimated atmospheric lifetime is approximately 50000 and 10000 years respectively. The so called "anodic phenomena", responsible for their formation, are caused by a decrease of the amount of alumina in the bath below 1–2%. As the result voltage rises to reach the value that is high enough to cause the oxidation of fluoride components present in the bath on the anode and form PFC. The ILs that are suitable for aluminium production, based on the literature, are those containing halide alkylimidazolium and chloroaluminate mixture. During the electrodeposition of aluminium in these ILs the occurrence of PFC by anodic phenomena is not expected at all since there are no fluoride bearing compounds to be oxidised (Marks, Tabereaux, Pape, Bakshi and Dolin 2001), however chlorine is still be produced. Due to the low temperatures the aluminium is electrodeposited on the cathode.

Technologically advanced production lines use semi-continuous automatic alumina feeding the bath which can significantly reduce PFC emissions to 0.02–0.1 kg PFC/Mg of Al (EU 2001). Technological modification of the arrangement of an electrodeposition cell for example by applying a Vertical Electrode Cell has the potential of cutting down energy demand by 15% and global warming potential by 35%, however other far more beneficial possibilities exist (Norgate, Jahanshahi and Rankin 2007).

In addition, the solid wastes generated during aluminium production in Hall-Héroult process present an environmental threat. Spent Pot Lining (SPL) is produced when the carbon refractory lining of an aluminium smelting pot reaches the end of its serviceable life. During its lifetime the cathode will crack and adsorb a high level of fluorides and cyanides. The contaminated pot lining has been classified as a hazardous waste material. Throughout decades, the amount of fluoride bearing waste generated is significant, considering that an average aluminium plant may have an annual production of 670 000 tons of aluminium (201 tons/year of fluoride bearing waste). Worldwide, quantities exceeding 500 000 tonnes a year of SPL are produced. A large majority of SPL is unprocessed, stockpiled or buried using licensed landfill sites. This type of disposal can have the potential of impacting on the environment. The leachate of such waste stockpiles can enter the ground and aquifers.

A variety of technologies exist which allow for safer disposal of SPL waste after aluminium production. These include utilising ion exchange to remove fluoride from the leachate (Singh, Kumar, Sen and Majumdar 1999), by integration into cement (Silveira, Dantas, Blasques and Santos 2002), or by oxidation of the graphite (Mazumder 2003). The inclusion of IL into the electrolytic mixture might influence the effectiveness of any or all of these waste disposal methods for the SPL waste. However a number of these methods, for example, the immobilisation by cementing, have been shown to be effective also with some organic compounds. It is therefore not unfeasible that IL can be included in the electrolytic mixture, and the resultant SPL waste, containing IL, may still be disposed of safely.

ENVIRONMENTAL IMPACT OF IONIC LIQUIDS

ILs are known to be non-volatile and thus to have low potential for atmospheric contamination or intoxication of humans by inhalation. However ILs posses the potential of soil and water contamination as they might be water soluble and can be sorbed onto solids. Their unintentional release to the environment can create a threat to human and animal life or health and as such should be by all possible means prevented. Limited research has been done in the field of ILs environmental fate assessment and more knowledge is urgently required (Jastorff et al., 2003). One of the most crucial issues in ecological risk assessment of ILs is the determination of their bioavailability and mobility in aquatic and terrestrial ecosystems. Due to the hydrophobicity of alkyl substituents and the positive charge (e.g. as a delocalised charge on the imidazole ring), ILs can be sorbed to organic matter and minerals by van der Waals forces and electrostatic interaction respectively; moreover there is the possibility of hydrogen bond formation between hydrogen atoms of ILs and polar moieties of soil organic matter. Finally the given three mechanisms combine together resulting in higher net sorption (Beaulieu, Tank and Kopacz 2008). The strength of sorption will determine the potential of soil and water contamination. Strong bonding to soil particles or organic matter can prevent leaching to groundwater which can further cause drinking water contamination. It can also decrease toxicity for flora and fauna since bound chemicals are not available for uptake. Similarly partitioning between sediments and water bodies will decrease toxicity towards aquatic organisms (Matzke, Stolte, Arning, Uebersa and Filser 2008)

Several research groups investigated the phenomenon of sorption of ILs onto soils and minerals. The overall conclusion was that dialkylimidazolium ILs are unlikely to be retarded in most geological systems to a large extent, taking into account also bacterial community, unless significant amount of clay or organic matter is present. Consequently they possess a potential to enter ground water systems and to act as contaminants. It was also confirmed that sorption can be altered by pH of soil since the more acidic the soil solution the less negatively charged active sites are available, and the lower is the cation exchange capacity (CEC). Thus decreasing the pH of soil/solution can cause desorption of ILs already immobilized by soil and their leaching. Furthermore ionic strength of solution was proven to influence sorption due to the competition of ILs cations and salt cations for negatively charged active sites of solids (Stepnowski, Mrozik and Nichthauser 2007). Data obtained independently by Stepnowski and Matzke stated that more hydrophilic ILs (with shorter alkyl side chain) would be more mobile in the environment than hydrophobic ones due to a reduced amount of possible interactions with soil/organic matter system since organic substances present in soil were proven to be responsible for ILs retention, however interaction by ion exchange is also playing a role in the sorption process (Stepnowski 2005; Matzke, Stolte, Arning, Uebersa and Filser 2008). Exact sorption

mechanisms have not been described yet since there are discrepancies in the result of sorption experiments by a number of researchers (Markiewicz, Biedrzycka and Bielecka 2006). It is also not possible to unequivocally state what parameter of the system are influencing sorption of ILs in the environment (Gorman-Lewis and Fein 2004; Stepnowski 2005; Stepnowski, Mrozik and Nichthauser 2007; Beaulieu, Tank and Kopacz 2008)

FROM AN ECONOMICAL POINT OF VIEW

Total energy demand for primary aluminium production is approximately 170 GJ/Mg, 16–20% of this energy is required for Bayer's bauxite ore refining whereas as much as 65% is needed for aluminium electrodeposition in Hall–Héroult process (Gagnea and Nappi 2000). About 60% of electricity used in aluminium production comes from hydroelectric power (Moors, Mulder and Vergragt 2005). The source of energy powering the electrolytic bath is an important factor from an environmental point of view since the carbon dioxide emission can vary by a factor of five depending on whether coal or hydroelectricity was used. Substitution of cryolite with ionic liquids not only has a potential of decreasing energy demand but could also prevent the emission of greenhouse gases to the atmosphere. Common enterprise of industry and academia in Australia, which is one of the biggest aluminium producers, revealed that application of ionic liquids might cut down the electricity cost of Hall–Héroult process by 30% as well as reduce atmospheric emission (Nogrady 2006)

The substitution of cryolite with ILs is beneficial form the economical and environmental point of view. To obtain a clear comparison of environmental and economical parameters of aluminium production in standard Hall-Héroult and ionic liquids utilizing processes we prepared Figure 1.

Significant energy demand reduction is possible due to lower temperature required during electrolysis in IL. Since electricity costs are a key factor for aluminium production, energy input reduction can provide significant savings. Energy demand is also influencing global warming potential (GWP) of the process since energy needed for heating the electrolytic bath can also result in CO_2 production. Taking into account that almost 40% of energy for smelting comes from coal burning power plants the possibility of IL's application in aluminium industry offers a GWP as well as costs reduction potential (Moors, Mulder and Vergragt 2005). Additionally a considerable decrease in harmful gas emission might be achieved when fluoride bearing electrolyte is excluded from the process. As shown on Figure 1, their evolution to the atmosphere can be avoided by performing electrolysis in a non-fluoride IL. The influence of aluminium production technology on global warming potential was divided into two parameters: GWP of smelting process and total GWP. The first one is describing reduction of possible adverse effects due to mainly PFCs emission elimination. Knowing that greenhouse impact of those pollutants is exceeding CO_2 global

warming potential by a factor of 6500 and 9200 respectively and mass released per kg of Al we calculated the GWP due to PFCs formation as CO_2 mass equivalents. The greenhouse impact of other gases is negligible in comparison to PFCs thus taking only those entities into account provides a good estimation of GWP (EU 2001). The total GWP includes emission of greenhouse gases during aluminium production, starting from extraction of alumina from bauxite ore to electrolytic separation of aluminium (Norgate, Jahanshahi and Rankin 2007). Air emission presented on the graph is taking into account amount of PFCs released in a form of CF_4 and C_2F_6. IL's toxicity measured as a LD_{50} value in acute toxicity test of *Daphnia sp.* is lower than cryolite's which allows for safer handling.
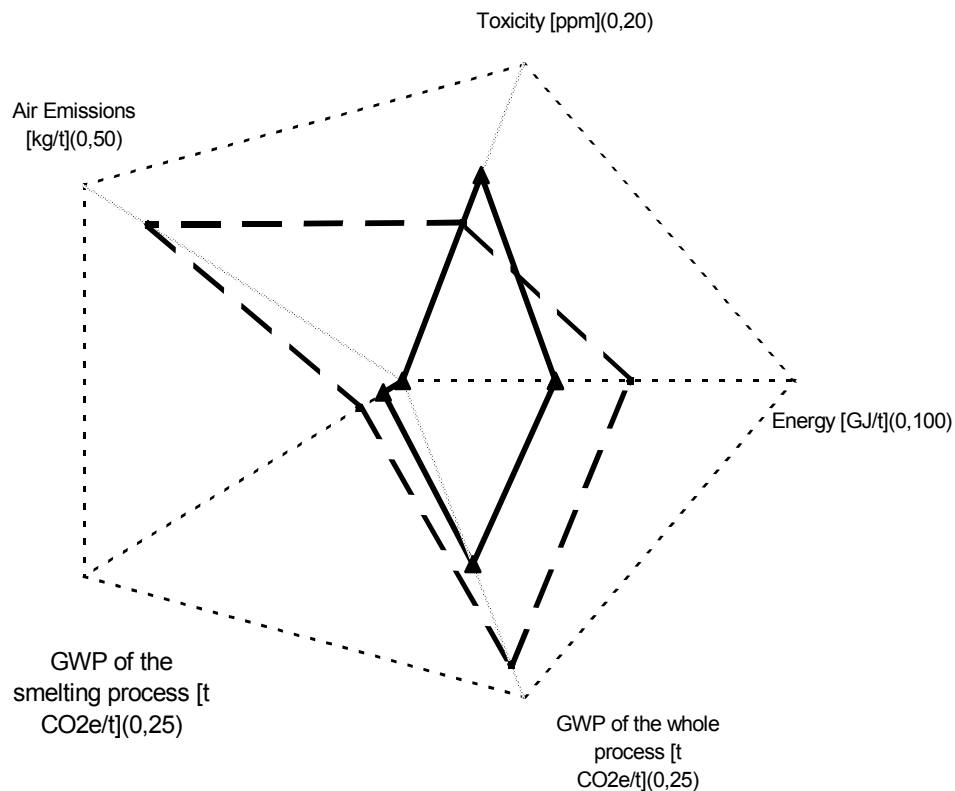

Fig. 1. Comparison of economical and environmental factors in aluminium production by Hall-Herault process (− − −), and ILs utilizing process (———)

CONCLUSIONS

Electrodeposition of aluminium from ionic liquids was proven, presenting a promising alternative to the high cost and high environmental impact production by standard Hall-Héroult process. From present analysis it can be seen that introduction of ionic liquids to aluminium smelting can be beneficial for environmental and economical point of view.

Current research conducted into the phenomenon of ILs sorption to soils gives different, sometimes contradictory results. Even in simplified, artificial systems like one applied by Gorman – Lewis and Fein no clear answer for the question: "What is the mechanism of ILs sorption?" could been obtained. Together with complicating the matrix, in order to simulate environmental conditions, more sorption mechanisms have to be taken into account and results become even more ambiguous.

Regardless of the level of uncertainty considering sorption strength one have to bear in mind that all the benefits connected with its application joined with the proper handling and usage management can introduce a significant improvement in economy and ecology of aluminium production. Additionally, according to predictions available up to date, ILs are not much more dangerous that cryolite although they are definitely less recognised.

REFERENCES

ABBOTT, A. P., C. A. EARDLEY, N. R. S. FARLEY, G. A. GRIFFITH AND A. PRATT (2001). *Electrodeposition of aluminium and aluminium/platinum alloys from AlCl3/benzyltrimethylammonium chloride room temperature ionic liquids.* Journal of Applied Electrochemistry 31: 1345–1350.

ABEDIN, S. Z. E., E. M. MOUSTAFA, R. HEMPELMANN, H. NATTER AND F. ENDRES (2005). *Additive free electrodeposition of nanocrystalline aluminium in a water and air stable ionic liquid.* Electrochemistry Communications 7: 1111–1116.

BAKER, A. G., S. N. BAKER, S. PANDEY AND F. V. BRIGHT (2005). *An analytical view of ionic liquids.* Analyst 130: 800–808.

BEAULIEU, J. J., J. L. TANK AND M. KOPACZ (2008). *Sorption of imidazolium-based ionic liquids to aquatic sediments.* Chemosphere 70 1320–1328.

EDWARDS, J. D., C. S. TAYLOR, A. S. RUSSELL AND L. F. MARANVILLE (1952). *Electrical Conductivity of Molten Cryolite and Potassium, Sodium, and Lithium Chlorides.* Journal of The Electrochemical Society 99(12): 527–535.

EU (2001). *Reference Document on Best Available Techniques in the Non Ferrous Metals Industries.* I. P. P. a. C. (IPPC), European Commission: 275–335.

FRANK., E. and A. S. Z. EL. (2006). *Air and water stable ionic liquids in physical chemistry.* Physical Chemistry Chemical Physics 8: 2101–2116.

GAGNEA, R. and C. NAPPI (2000). *The cost and technological structure of aluminium smelters worldwide.* Journal of Applied Econometrics 15: 417–432.

GIELEN, D. J. (1998). *Methodological Aspects of Resource-Oriented Analysis of Material Flows,workshop.* The Future of the European Aluminium Industry: a MARKAL Energy and Material Flow Analysis.

GORMAN-LEWIS, D. J. and J. B. FEIN (2004). *Experimental Study of the Adsorption of an Ionic Liquid onto Bacterial and Mineral Surfaces*. Environmental Science and Technology 38: 2491–2495.

JASTORFF, B., R. STÖRMANN, J. RANKE, K. MÖLTER, F. STOCK, B. OBERHEITMANN, W. HOFFMANN, J. HOFFMANN, M. NÜCHTER, B. ONDRUSCHKA AND J. FILSER (2003). *How hazardous are ionic liquids? Structure–activity relationships and biological testing as important elements for sustainability evaluatio*n. Green Chemistry 5: 136–142.

JIANG, T., M. J. C. BRYM, G. DUBÉ, A. LASIA AND G. M. BRISARD (2006). *Electrodeposition of aluminium from ionic liquids: Part I—electrodeposition and surface morphology of aluminium from aluminium chloride (AlCl3)–1-ethyl-3-methylimidazolium chloride ([EMIm]Cl) ionic liquids*. Surface & Coatings Technology (201): 1–9.

JIANG, T., M. J. C. BRYM, G. DUBÉ, A. LASIA AND G. M. BRISARD (2006). *Electrodeposition of aluminium from ionic liquids: Part II - studies on the electrodeposition of aluminum from aluminum chloride (AlCl$_3$) - trimethylphenylammonium chloride (TMPAC) ionic liquids*. Surface & Coatings Technology (201): 10–18.

LIU, L., Y. YANG AND Y. ZHANG (2004). *A study on the electrical conductivity of multi-walled carbon nanotube aqueous solution* Physica E: Low-dimensional Systems and Nanostructures 24(3–4): 343–348

LIU, Q. X., S. Z. E. ABEDIN AND F. ENDRES (2006). *Electroplating of mild steel by aluminium in a first generation ionic liquid: A green alternative to commercial Al-plating in organic solvents*. Surface & Coatings Technology 201: 1352–1356.

MARKIEWICZ, L., E. BIEDRZYCKA AND M. BIELECKA (2006). *Różnicowanie mleczarskich szczepów lactobacillus metodą PFGE*. Żywność. Nauka. Technologia. Jakość. 47(2): 216–222.

MARKS, J., A. TABEREAUX, D. PAPE, V. BAKSHI, E. J. DOLIN (2001*). Factors affecting PFC emission from commercial aluminium reduction cells*. Light Metals(295–302).

MATZKE, M., S. STOLTE, J. U. ARNING, U. UEBERSA J. FILSER (2008). *Imidazolium based ionic liquids in soils: effects of the side chain length on wheat (Triticum aestivum) and cress (Lepidium sativum) as affected by different clays and organic matter*. Green Chemistry 10: 584–591.

MAZUMDER, B. (2003). *Chemical oxidation of spent cathode carbon blocks of aluminium smelter plants for removal of contaminants and recovery of graphite value*. Journal of Scientific & Industrial Research 62(12): 1181–1183

MOORS, E. H. M., K. F. MULDER AND P. J. VERGRAGT (2005). *Towards cleaner production: barriers and strategies in the base metals producing industry*. Journal of Cleaner Production 13: 657–668.

MOUSTAFA, E. M., S. Z. E. ABEDIN, A. SHKURANKOV, E. ZSCHIPPANG, A. Y. SAAD, A. BUND AND F. ENDRES (2007). *Electrodeposition of Al in 1-Butyl-1-methylpyrrolidinium Bis(trifluoromethylsulfonyl)amide and 1-Ethyl-3-methylimidazolium Bi (trifluoromethylsulfonyl)-amide Ionic Liquids: In Situ STM and EQCM Studies*. Journal of Physical Chemistry B 111: 4693–4704.

NOGRADY, B. (2006). *Ionic liquids - cutting aluminium energy bills: designer solvents*. Process. Clayton South. 6: 6–7.

NORGATE, T. E., S. JAHANSHAHI AND W. J. RAnkin (2007). *Assessing the environmental impact of metal production processes*. Journal of Cleaner Production 15(8–9): 838–848.

REACH (2007). European Commission Environment Directorate General - REACH system.

SILVEIRA, B. I., A. E. M. DANTAS, J. E. M. BLASQUES AND R. K. P. SANTOS (2002*). Effectiveness of cement-based systems for stabilization and solidification of spent pot liner inorganic fraction* Journal of Hazardous Materials 98(1–3): 183–190

SINGH, G., B. KUMAR, P. K. SEN AND J. MAJUMDAR (1999). *Removal of Fluoride from Spent Pot Liner Leachate Using Ion Exchange*. Water Environment Research 71(1): 36–42(7).

STEPNOWSKI, P. (2005). *Preliminary Assessment of the Sorption of some Alkyl Imidazolium Cations as*

used in Ionic Liquids to Soils and Sediments. Australian Journal of Chemistry 58: 170–173.

STEPNOWSKI, P., W. MROZIK AND J. NICHTHAUSer (2007). *Adsorption of Alkylimidazolium and Alkylpyridinium Ionic Liquids onto Natural Soils*. Environmental Science and Technology 41: 511–516.

United Nations Department of Economic and Social Affairs, D. f. S. D. (2004). Agenda 21: *Environmantally sound management of toxic chemicals, including prevention of illegal international tarffic in toxic and dangerous products.* Chapter 19.

WELCH, B. J. (1999). *Aluminium production paths in a new millennium*. Journal of the Minerals, Metals and Materials Society 51: 24–28.

WU, B., R. G. REDDY AND R. D. ROGERS (2008). *Production, refining and recycling of lightweight and reactive metals in ionic liquids*. U. S. Patent, The Board of Trustees of the University of Alabama. US 7,347,920 B2.

YUGUANG, Z. AND T. J. VANDERNOOT (1997). *Electrodeposition of aluminium from room temperature $AlCl_3$-TMPAC molten salts*. Electrochimica Acta 42(I I): 1639–1643.

Markiewicz M., Hupka J., Joskowska M., Jungnickel Ch., *Wykorzystanie cieczy jonowych w procesie produkcji aluminium – ocena ekonomiczna i ekologiczna,* Physicochemical Problems of Mineral Processing, 43 (2009), 73–84 (w jęz. ang)

Ze względu na swój niewielki ciężar właściwy oraz odporność na korozję aluminium jest jednym z najczęściej wkorzystywanych materiałów w przemyśle samochodowym, lotniczym, stoczniowym, spożywczym i w produkcji opakowań. Produkcja tego metalu rośnie o 2% w skali roku. Technologia wytwarzania aluminium stosowana na skalę przemysłową oparta jest na elektrodepozycji w ciekłym kriolicie i nosi nazwę procesu Hall-Heroult'a. Technologia ta wymaga wysokich nakładów energii elektrycznej, charakteryzuje się ponadto, szeroko udokumentowanym, negatywnym wpływem na środowisko naturalne. Produkcja aluminium możliwa jest również z wykorzystaniem innych technologii, jako że istnieją doniesienia literaturowe na temat elektrodepozycji aluminium z mieszaniny cieczy jonowych zawierających w rdzeniu imidazol, pirymidynę lub czwartorzędową sól amoniową oraz $AlCl_3$, w temperaturze zbliżonej do pokojowej z efektywnością sięgającą niemal 100%. Celem niniejszej publikacji jest dokonanie porównania obu wspomnianych technologii pod względem wpływu na środowisko oraz ekonomii produkcji.

W wyniku przeprowadzonych studiów doszliśmy do wniosku, iż zastosowanie cieczy jonowych w produkcji aluminium stanowi inetersującą alternatywę dla dotychczas stosowanego procesu Hall-Heroult'a. Niemniej jednak wprowadzeniu tych nowych mediów do produkcji na szeroką skale towarzyszyć powinna nadzwyczajna ostrożność jako że wpływ tycz związków na środowisko nie został w pełni poznany. W procesie przemysłowego użytkowania związków chemicznych ryzyko ich niezamierzonego uwolnienia musi być brane pod uwagę. Z tego względu przed wprowadzeniem tej technologii produkcji aluminium należy dokonać pełnej analizy ryzyka, uwzględniając ewentualny negatywny wpływ na środowisko jak również oraz zidentyfikować potencjalne rozmieszenie w różnych elementach ekosystemów

słowa kluczowe: ciecze jonowe, produkcja aluminium, potancjał tworzenia efektu cieplarnianego

E. Zarudzka*

PRE-FLOTATION LEACHING OF POLISH CARBONATE COPPER ORE

The copper ore deposit of LGOM (Legnica-Glogow Copper Basin) is located in the Foresudetic Monocline (SW Poland) and has a polymetallic character because of content of silver, lead, copper and accompanying metals such as cobalt, zinc, nickel, rhenium and gold. Over 110 metalliferous minerals were identified in the deposit. A sedimentary nature of the deposit results in necessity of fine grinding for effective liberation of sulfide particles prior to flotation. Fine dissemination of metalliferous minerals, particularly in the carbonate type ore, considerably reduces the susceptibility to effective liberation. A beneficial effect of non-oxidative leaching of carbonate gangue with sulfuric acid on copper ore flotation was presented in the paper. It was shown that the non-oxidative leaching of the flotation feed is a selective process leading to liberation of sulfide minerals disseminated in the gangue carbonate matrix. Acid leaching causes chemical decomposition of carbonate matter and releases fine grains of copper minerals. Kinetics of leaching of the investigated ore sample with various amounts of sulfuric acid were presented. It was shown that after decomposition of 70% of carbonates in the flotation feed, metal recovery and concentrate grade increased remarkable in comparison to the results observed for the unleached feed. The products of leaching contain solid hydrated calcium sulfate (gypsum), soluble magnesium sulfate and gaseous carbon dioxide. Carbon dioxide evolving during the reaction creates a non-oxidizing atmosphere in the pulp during leaching and therefore effectively prevents digestion of metals from sulfide minerals. The liberation of copper minerals due to leaching provides better separation of metallic ore components by flotation.

key words: leaching, flotation, carbonate copper

INTRODUCTION

The Polish copper ore deposit of the Foresudetic Monocline is rather difficult-to-process due to a specific mineralogical composition, presence of three different
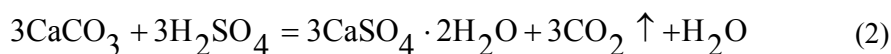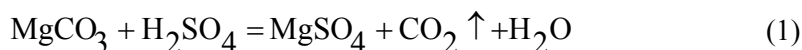
---

* Wroclaw University of Technology, Faculty of Geoengineering, Mining and Geology, Pl. Teatralny , 50-051 Wroclaw, Poland, emilia.zarudzka@pwr.wroc.pl

lithological layers and fine size of sulfide minerals. In the mined ores of the Legnica-Glogow Copper Basin, the copper-bearing sulfide minerals are present in three layers: dolomitic, sandstone and shale (Piestrzynski and Zalewska-Kuczmierczyk, 1996). Principal carriers of copper minerals are chalcocite (Cu_2S), bornite (Cu_5FeS_4), chalcopyrite ($CuFeS_2$), and covellite (CuS). Chalcocite is the major copper sulfide mineral that dominates in the deposit. Some ores require very fine grinding for efficient liberation of sulfide minerals prior to flotation because of fine sulfide grains which are disseminated in carbonate matrix mainly as complicated intergrowths.

The efficiency of the flotation process of copper-bearing minerals depends on the degree of liberation of sulfide minerals from gangue, which is most often accomplished during comminution. One of the concepts of treatment of copper ores, especially their carbonate fraction, suggests selective decomposition of gangue using sulfuric acid. Non-oxidative leaching of copper ore in an oxygen-free atmosphere seems to be a very efficient process for enhancement of the metal recovery.

NON-OXIDATIVE LEACHING

Selective leaching of the copper ore is based on chemical reactions between sulfuric acid and calcium as well as magnesium carbonate minerals (dolomite). Dolomite is a dominating gangue component of the Polish copper ores. This process, called either acid leaching or non-oxidative leaching, relies on treatment of the ore with less-than-stoichiometric amount of H_2SO_4 required for a total decomposition of carbonates. The amount of sulfuric acid applied in the leaching corresponds to the content of carbonates in the ore and must be controlled to maintain the final pH of the suspension on a proper level. Products of the decomposition of dolomite are solid hydrated calcium sulfate (gypsum $CaSO_4 \cdot 2H_2O$), soluble magnesium sulfate ($MgSO_4$), and gaseous carbon dioxide (CO_2). The following chemical reactions describe the non-oxidative leaching:

$$MgCO_3 + H_2SO_4 = MgSO_4 + CO_2 \uparrow + H_2O \tag{1}$$

$$3CaCO_3 + 3H_2SO_4 = 3CaSO_4 \cdot 2H_2O + 3CO_2 \uparrow + H_2O \tag{2}$$

Carbon dioxide evolving during the reaction creates a non-oxidizing atmosphere in the slurry during leaching, and therefore effectively prevents the leaching of metals from the sulfide minerals (Chmielewski, 2007). Saturation of the slurry with CO_2 assures selective leaching of only carbonates. Liberation of sulfide minerals from the gangue minerals, when applying sulfuric acid, is rapid, mainly at the first stage of the process and it can be performed at ambient temperature in a standard reactor equipped with mechanical stirring.

A selective chemical digestion of dolomite is shown schematically on Figure 1.
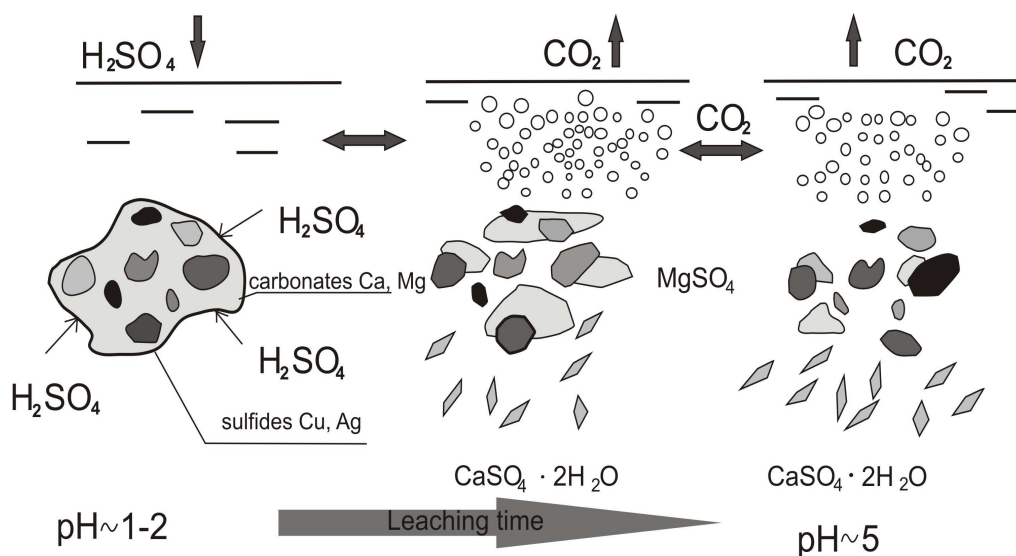
Fig. 1. A selective chemical decomposition of carbonate-sulfide intergrowths during non-oxidative leaching with sulphuric acid (Luszczkiewicz and Chmielewski, 2006)

Leaching of the flotation feed with H_2SO_4 reduces the size of particles due to liberation of the gangue minerals from the copper-bearing minerals. A low energy-consumption of the size reduction process is an important feature of this process in comparison to conventional methods of mechanical grinding. Traditional methods of grinding are not able to liberate fine minerals without overgrinding of already liberated copper sulfide minerals because overgrinding makes the flotation nonselective.

The amount of sulfuric acid required for leaching of dolomite is determined by the mass of sulfuric acid necessary for the total decomposition of carbonates present in 1 kg of the dry solid feed ($z_{H_2SO_4}^{max}$). The content of carbonates in the investigated feed was determined analytically utilizing a laboratory procedure. I was calculated that 154 g H_2SO_4/kg of dry solid feed is needed for their decomposition. A 70–80 % decomposition of carbonates by leaching was found to be satisfactory for subsequent flotation. The final pH of the slurry should be was maintained at about 5 (Chmielewski, 2007).

MATERIALS AND METHODS

The material used in laboratory investigations during the acid non-oxidative leaching was a copper ore from the Rudna Concentrator. The feed for all experiments contained about 90 % of particles below 75 μm in size. The material prepared in such a way was subjected to acidic leaching and subsequently to flotation. The flotation

experiments were carried in the "Mekhanobr" mechanical laboratory flotation machine which was equipped with a 1 dm^3 cell. Standard flotation reagents were applied. The laboratory investigations were performed under constant conditions during flotation. The acid leaching with concentrated acid (95 % H$_2$SO$_4$) was performed in a glass reactor applying intensive mechanical stirring of the suspension. Total time of decomposing 70 % of carbonates in sulfide concentrate was 60 minutes. The scheme of laboratory experiments of unleached and leached materials is shown in Figure 2. The pH and redox potential were measured during flotation tests using a combination electrode. Under controlled conditions of the E potential it is possible to reach maximum recovery of copper at E about 0.2V (NEW) (Lekki, 1996). For the unleached material the pH varied from 7.1 to 7.6 and for leached material from 6.1 to 6.8.
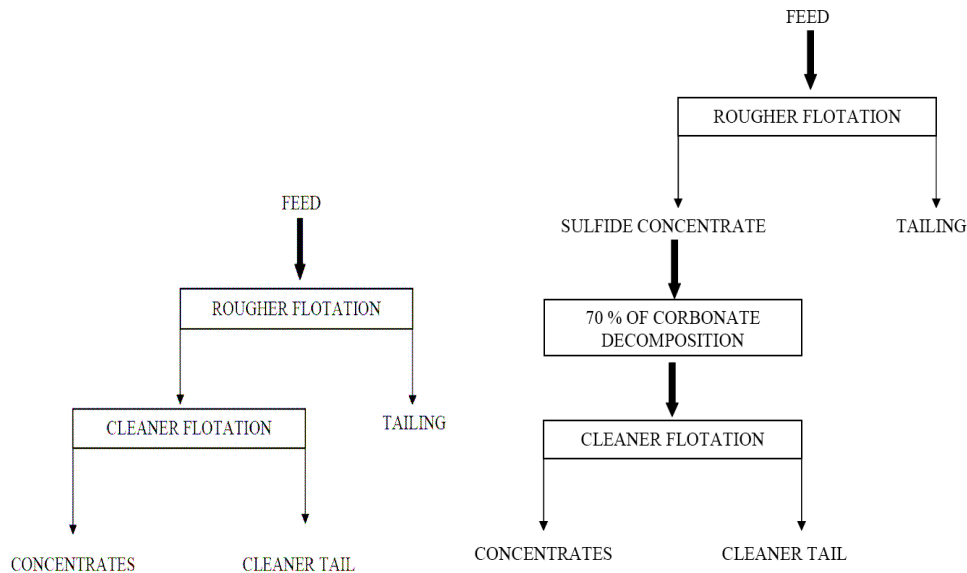
Fig. 2. Scheme of laboratory investigations

RESULTS

The kinetics of non-oxidative leaching of the feed was investigated by measuring the pH and redox potential as a function of reaction time. The redox potential and pH-time curves depended on the used amount of sulphuric acid. The leaching kinetics of the feed were investigated at various degrees, from 30 to 100 %, of carbonates decomposition. Figure 3 illustrates a relationships between the pH and leaching time of the investigated ore.
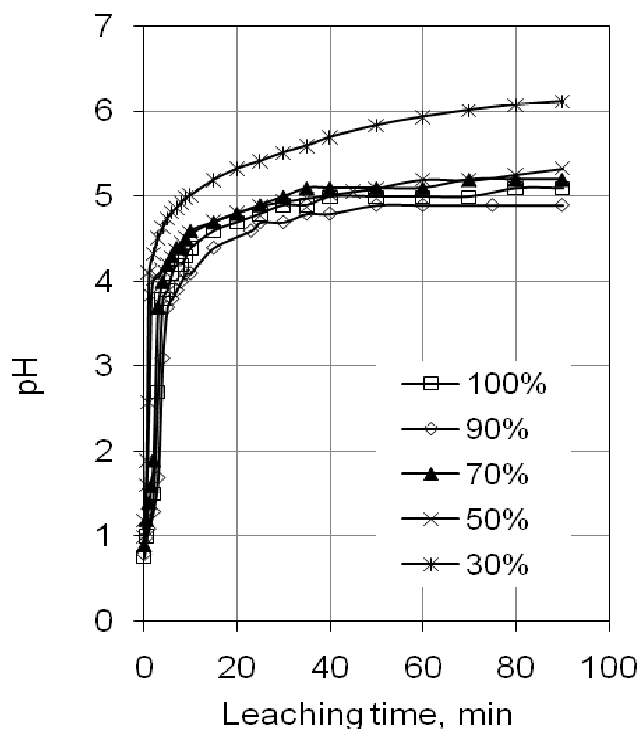
Fig. 3. pH-time relationship for non-oxidative leaching. Copper ore at various degrees of carbonate decomposition (from 30 to 100 %) was investigated

The leaching process appeared to be very rapid. After 5–10 minutes the pH of the slurry was equal to 4. It can be assume that further increase of the pH was caused by CO_2 removal from the slurry.

It can be seen from Figure 4 that pH-time carbonate decomposition kinetics can be well related to the redox potential at the initial stage of the process. A significant decrease of the redox potential from about 360 mV to about 140 mV was observed after introduction of H_2SO_4 to the feed slurry. The leaching was completed when the acid was used up. At that point the suspension's pH was around 5. The constant values of the pH and redox potential were resulted from the saturation of the solution with CO_2. They permit to determine the direction of reaction and control of the non-oxidative leaching. The potential of the combination electrode, valid for Ag/AgCl reference system, during non-oxidative leaching at 100 % carbonate decoposition is shown in Figure 4.

Undoubtedly, the presence of carbon dioxide in the leaching suspension caused the red-ox potential to drop.

Flotation of the unleached material was performed to compare reference results for the outcome achieved by flotation after acid leaching. The results of flotation experiments are given in tables 1 and 2 and in Figure 5.

A relationship between separation parameters, recovery of copper in the concentrate and recovery of remaining (non-copper) components, also called ~~as~~ the Fuerstenau upgrading curve (Drzymala and Ahmed, 2005) is shown in Figure 5. Fuerstenau's curves can be plotted in one graph for different recoveries of various ores, which metal contents in the feed are at different levels.
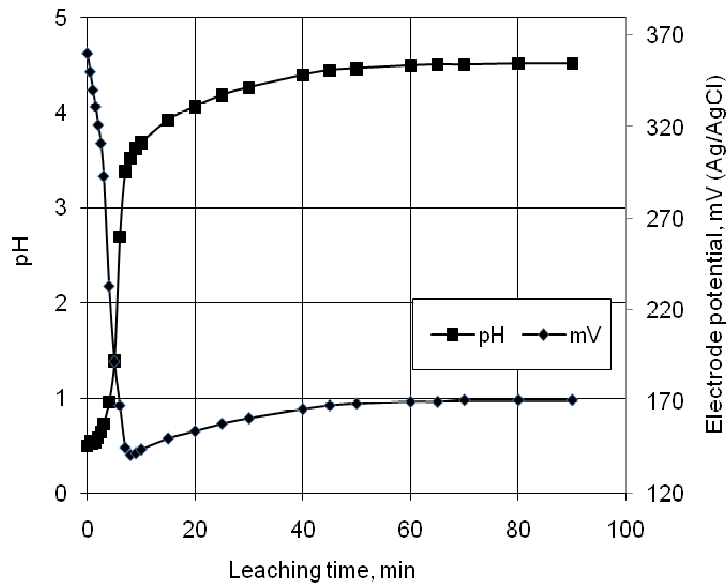

Fig. 4. Potential of combination electrode, valid for Ag/AgCl reference system, during non-oxidative leaching

Table 1. Results of reference flotation

Product	Yield, %	Copper content, %	Copper recovery, %
C-1	1.27	15.54	12.03
C-2	1.66	15.87	16.05
C-3	4.31	12.95	33.95
Cleaning tail	10.44	4.16	26.45
Tailing	82.32	0.23	11.53
Feed (calculated)	100.00	1.64	
Feed assay		1.47	

During comparing leached and unleached materials, it was noticed that both copper content in the concentrate and copper recovery of leached material were higher by 1.5% and 0.9% in the leach feed, respectively. All comparisons were performed for a constant recovery of 88% and a constant yield of 16%.

Table 2. Flotation results of feed after acid leaching

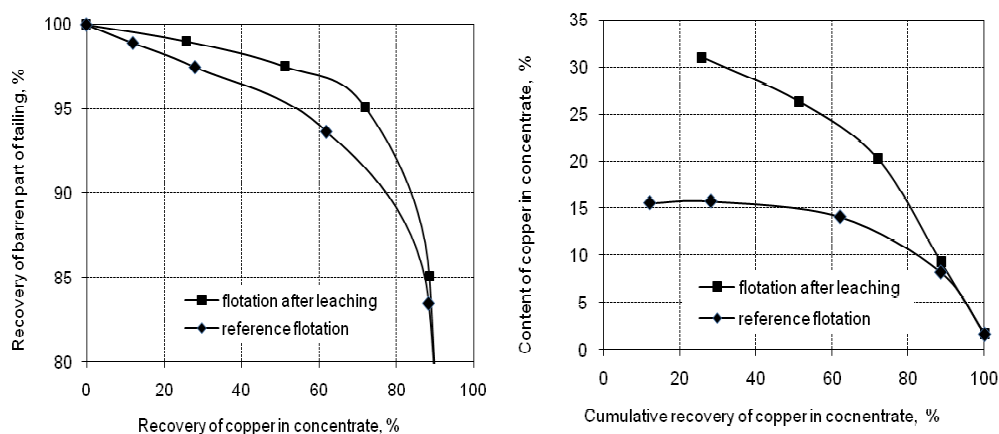| Product	Yield, %	Copper content, %	Copper recovery, %
C-1	1.41	31.04	25.85
C-2	1.89	22.84	25.44
C-3	2.72	12.90	20.71
Cleaning tail	10.13	2.78	16.62
Tailing	83.85	0.23	11.38
Feed calculate	100.00	1.69	
Feed assay		1.47	

Fig. 5. A section of upgrading curves of copper ore flotation for unleached and leached feeds. Based on date from Table 1 and 2

CONCLUSSION

A beneficial influence of acid leaching on the enrichment of Polish copper ore in comparison with the unleached material was noticed. A 70% decomposition of carbonate of the flotation feed leads to an enhanced recovery and content of copper in the concentrate. The leaching of the flotation feed with H_2SO_4 can be used as an effective operation for selective liberation of sulfide minerals. Carbon dioxide evolving during the reaction of sulfuric acid with carbonate gangue creates beneficially non-oxidative conditions, preventing the digestion of metals from sulfide minerals.

The pH and redox potential permit to determine the direction of reaction and control the non-oxidative leaching.

REFERENCES

PIESTRZYŃSKI A.; ZALEWSKA-KUCZMIERCZYK M; 1996; *Okruszcowanie*; In: Monografia KGHM Polska Miedź SA; (Piestrzyński A.); 200–201; CBPM CUPRUM; Wrocław

CHMIELEWSKI T.; 2007; *Non-oxidative leaching of black shale copper ore from Lubin Mine;* Physico-chemical Problems of Mineral Processing; Vol. 41; 323–335

ŁUSZCZKIEWICZ A.; CHMIELEWSKI T.; 2006; *Technology of chemical modification of by-products in copper sulphide ore flotation systems;* Rudy i Metale Nieżelazne; 51/1; 2–10 (in Polish)

LEKKI J.; 1996; *Thermodynamical interpretation of collectorless and xanthate flotation of copper ore with controlled redox potential*; Zeszyty Naukowe Politechniki Śląskiej; Vol. 231; 315–331 KGHM CUPRUM; Wrocław (in Polish)

DRZYMALA J.; AHMED H.A.M.; 2005; *Mathematical equations for approximation of separation results using the Fuerstenau upgrading curves;* International Journal of Mineral Processing; Vol. 76; 55–65

Przedstawiono wpływ kwaśnego ługowania krajowej rudy węglanowej za pomocą kwasu siarkowego. Głównym celem procesu jest uwolnienie minerałów miedzionośnych, które są rozproszone i zamknięte w skale węglanowej w postaci drobnych wpryśnięć i zrostów. Dolomit w złożach Legnicko-Głogowskiego Okręgu Miedziowego stanowi główny składnik skały płonnej. Kwaśne ługowanie zapewnia rozkład minerałów węglanowych i gwarantuje skuteczne uwalnianie ziarn kruszcowych. W wyniku rozkładu skały węglanowej powstaje krystaliczny gips ($CaSO_4 \cdot 2H_2O$), rozpuszczalny siarczan magnezu ($MgSO_4$) oraz ditlenek węgla (CO_2). Wydzielający się podczas ługowania CO_2 tworzy w zawiesinie warunki nieutleniające i zabezpiecza mieszaninę przed dostępem tlenu, utleniaczem minerałów siarczkowych. Dzięki selektywnemu rozkładowi minerałów węglanowych następuje podwyższenie wskaźników flotacji w porównaniu z nadawą nieługowaną. Zaleta tego procesu jest również wykorzystanie stężonego kwasu siarkowego do chemicznej obróbki. Pozwala to na zagospodarowanie dużych ilości tego kwasu, co jest istotne w okresie malejącego popytu na ten produkt.

słowa kluczowe: ługowanie, flotacja, ruda węglanowa

Physicochemical Problems of Mineral Processing, 43 (2008)